INTENSIFICATION OF BIOCONVERSION PROCESSES: DESIGN AND DEVELOPMENT OF REACTORS WITH HIGH BIOCATALYST LOADING

Maria Elena Russo

Dottorato in Scienze Biotecnologiche – XX ciclo
Indirizzo Biotecnologie Industriali
Università di Napoli Federico II

Dottorato in Scienze Biotecnologiche – XX ciclo
Indirizzo Biotecnologie Industriali
Università di Napoli Federico II

INTENSIFICATION OF BIOCONVERSION PROCESSES: DESIGN AND DEVELOPMENT OF REACTORS WITH HIGH BIOCATALYST LOADING

Maria Elena Russo

Dottoranda: Maria Elena Russo

Relatori: Antonio Marzocchella
Piero Salatino
Giovanni Sannia

Coordinatore: Prof. Giovanni Sannia

Index

Abstract

The present research program addressed some open issues related to immobilization of biological systems (enzymes, microrganisms) for bioprocess applications. The research pathway is ultimately targetted at the development of novel and effective tools for bioprocess intensification based on the use of immobilized biocatalysts. The attention has been specifically focused on two processes: an enzymatic and a microbial process.

Conversion of the synthetic dye Remazol Brilliant Blue R (RBBR) by means of crude laccase mixtures from *Pleurotus ostreatus*.

The study aimed at the optimization of the enzymes immobilization protocol and at the characterization of the RBBR conversion by means of free and immobilized enzymes. The immobilization process was optimized with reference to the covalent binding on granular supports - EUPERGIT C 250L©. In particular, operating conditions were selected so as to maximize the immobilization yield. A reactor for the activity assay of the immobilised enzymes was designed and set-up. The kinetics of RBBR conversion by means of immobilized laccase mixtures was characterised using a purposely designed fixed bed reactor. A kinetic model has been best-fitted against experimental data relative to conversion degree and reactor space-time to assess kinetic parameters. The role of mass transport phenomena between the phases and of adsorption during heterogeneous enzymatic conversion of the dye were investigated.

Based on data collected in the experimental campaign and on kinetic models developed, two alternative processes for remediation of dye-bearing wastewaters have been assessed: i) a batch Stirred Tank Reactor (STR) operated with a homogeneous liquid phase containing both the crude laccase mixture and the dye; ii) a Continuous Fixed Bed Reactor (CFBR) loaded with laccases immobilised on EUPERGIT© and continuously fed with the dye-bearing liquid stream. The results highlighted the role played by biocatalyst stability and immobilisation yield on the selection of the best option in terms of the volume of wastewater cumulatively treated in either option.

Conversion of the phenol by means of *Pseudomonas sp. OX1* biofilm in three-phase bioreactors.

The study has addressed both experimental and theoretical aspects of the problem. The experimental study has been directed to the assessment of the growth of *P. sp OX1* biofilm on silica-based granular supports. Two bench-scale reactor typologies were investigated: a three Phase Circulating (3PC) reactor and an Internal Loop Airlift (ILA) reactor. Tests with the 3PC reactor were directed to optimize the conditions for biofilm growth. Tests with the ILA reactor were aimed at investigating the effect of dilution rate on the performance of the system operated with a mature biofilm that had been previously partly grown up on the solid carrier.

The theoretical work has addressed the analysis of the bifurcational and dynamic patterns of an ILA reactor operated with biofilm of *P. sp. OX1* attached on granular solids. The role of the growth rate of suspended and immobilised cells using phenol as carbon source, the adhesion rate of suspended cells on carrier surface and the detachment rate of biofilm from the solids carrier were investigated. The dependence of bifurcational patterns on detachment coefficient and dilution rate has been analysed. Results from the theoretical study and from tests carried out with the ILA reactor were compared: the model properly reproduces the functional dependence of the steady state behaviour of the biofilm on the dilution rate observed during the tests.

List of Related Publications

M. E. Russo, P. Giardina, A. Marzocchella, P. Salatino, G. Sannia.
“Assessment of antraquinone-dye conversion by free and immobilized crude laccase mixtures”. Submitted for publication on Enzyme and Microbial Technology.

M. E. Russo, P. L. Maffettone, A. Marzocchella, P. Salatino. “Bifurcational and dynamical analysis of a continuous biofilm reactor”. Submitted for publication on Journal of Biotechnology.

Acknowledgements

The work has been carried out at the Department of Chemical Engineering at University of Naples 'Federico II', parts of the work has been carried out with the contribution of the Department of Organic Chemistry and Biochemistry and the Department of Functional and Structural Biology at the same University. The European Commission, Sixth Framework Program (SOPHIED contract NMP2-CT2004-505899), and the Centro Regionale di Competenza BioTekNet have financed this work.

I wish to express my gratitude towards my supervisors Professors Antonio Marzocchella, Piero Salatino and Giovanni Sannia. I am also grateful to Dr. Giuseppe Olivieri, Dr. Francesco Di Natale, Dr. Fabiana Alfieri and Cinzia Pezzella for helpful discussions and to co-authors of the papers Professors Paola Giardina and Pier Luca Maffettone. Finally, I would like to thank my family and friends for their support and encouragement.

Riassunto del lavoro di tesi

Introduzione. L'interesse del mondo scientifico nei confronti dei processi biotecnologici riflette la crescente consapevolezza del mondo sociale-industriale di ricercare soluzioni economicamente ed ambientalmente sostenibili per la produzione di specie chimiche di bulk e lo smaltimento dei reflui civili ed industriali [Soetaert e Vandamme, 2006; Verstraete, 2007]. Con riferimento al biocatalizzatore adottato i processi possono essere suddivisi in processi basati sull'impiego di microrganismi e processi enzimatici. In entrambe le tipologie si ritrovano i processi di biorisanamento, volti alla valorizzazione delle sostanze di scarto oppure all'abbattimento della tossicità nei reflui.

Tra i requisiti fondamentali dei processi per la produzione di specie chimiche di bulk e per il biorisanamento dei reflui il contenimento dei costi riveste un ruolo primario. Una soluzione per soddisfare questo vincolo è rappresentata dalla "intensificazione" di processo, intesa come incremento di potenzialità per unità di volume delle apparecchiature. Le strategie adottate sono incentrate su soluzioni che permettono di ovviare ai limiti imposti dalla bassa attività biocatalitica degli enzimi/microrganismi riscontrabile verso substrati/nutrienti meno affini rispetto alla specie naturalmente convertite/metabolizzate.

Di seguito si riportano gli aspetti rilevanti nello sviluppo di processi enzimatici e microbici.

Processi enzimatici: caratterizzazione della cinetica enzimatica in fase liquida verso i substrati di interesse in ambienti controllati e in ambienti prossimi a quelli caratteristici dell'applicazione industriale; sviluppo di sistemi biocatalitici caratterizzati da elevata attività per unità di volume (sconfinamento mediante membrane, immobilizzazione dell'enzima, ecc.); caratterizzazione delle cinetiche di conversioni (di composti di interesse) condotte con i sistemi biocatalitici sviluppati; progettazione di sistemi reattoristici per l'utilizzo degli enzimi in processi continui; caratterizzazione dell'efficienza del processo di conversione mediante i sistemi biocatalitici sviluppati anche con riferimento ai fenomeni chimico-fisici caratteristici dei processi in fase eterogenea (trasporto di materia tra le fasi, adsorbimento, precipitazione di composti polimerici, ecc.).

Processi basati su microrganismi: caratterizzazione delle cinetiche di crescita dei microrganismi selezionati (consumo di substrato/i, respirazione, *manteinance*, produzione di metaboliti, rese ecc.) in sistemi discontinui e continui; selezione di tecniche per sviluppo di colture microbiche ad alta densità cellulare (reattori a membrana, *solid state fermentation*, reattori a biofilm); progettazione di reattori bi- o tri-fasici per la conduzione del processo di bioconversione; ottimizzazione delle condizioni operative (alimentazione dei substrati, ossigenazione, tempi di permanenza, miscelazione, *wall-growth* ecc.); sviluppo di modelli teorici di supporto alla progettazione e conduzione di processi industriali (*pathway* metabolici, analisi dinamica, analisi biforcazionale, ecc.).

Lo studio finalizzato alla caratterizzazione di valide soluzioni reattoristiche per i processi produttivi di specie chimiche di bulk e per il biorisanamento di reflui è inoltre di supporto alla valutazione della fattibilità economica dei processi stessi. Infatti, particolare interesse è rivolto all'analisi – tecnica ed economica – delle operazioni di *up-stream* e *down-stream* complementari per il processo investigato. Tale analisi è volta all'ottimizzazione delle prestazioni del processo (produttività, volumi trattati,

dimensionamento dei reattori, costi, …) con individuazione delle variabili di maggior influenza (ad es. stabilità del biocatalizzatore).

Scopo della tesi*.* Il lavoro di tesi ha riguardato le tecniche di intensificazione di processi biotecnologici. L'attività è stata articolata in due linee di ricerca:

A) Processo di conversione di coloranti sintetici mediante miscele di laccasi da *Pleurotus ostreatus*. È stata studiata la conversione catalizzata da laccasi libere ed immobilizzate su supporti solidi.

Gli obiettivi della ricerca sono stati: i) selezione di una tecnica di immobilizzazione di miscele di laccasi prodotte da *P. ostreatus*; ii) verifica dell'efficacia delle laccasi immobilizzate come catalizzatore per la conversione del colorante antrachinonico Remazol Brilliant Blue R (RBBR) e caratterizzazione della cinetica di conversione; iii) sviluppo di un modello teorico per il confronto delle prestazioni - espresse in termini di volumi di soluzione di RBBR trattata - tra un reattore agitato discontinuo (STR), esercito con miscela di laccasi in fase libera, e un reattore bifasico (CFBR), esercito in continuo rispetto alla fase liquida e in modalità discontinua rispetto al biocatalizzatore (letto fisso di particelle con laccasi immobilizzate).

B) Processo di conversione di fenolo mediante biofilm di *Pseudomonas sp.* OX1 in reattori trifasici a letto fluidizzato. Sono state condotte indagini sperimentali e teoriche.

L'attività sperimentale ha riguardato: i) la crescita di biofilm di *P. sp.* OX1 su pomici granulari in un reattore trifasico discontinuo (3PC); ii) la caratterizzazione dell'effetto delle condizioni operative sul biofilm in un reattore *airlift* a circolazione interna (ILA).

L'attività teorica ha riguardato lo sviluppo di un modello del reattore ILA finalizzato allo studio della dinamica e del comportamento biforcazionale. Le variabili considerate sono: le concentrazioni volumetriche delle cellule libere e del substrato nella fase liquida, la concentrazione volumetrica del biofilm (cellule adese). Le previsioni del modello sono state confrontate con i risultati sperimentali.

La presentazione del lavoro di tesi rispecchia l'articolazione dell'attività svolta. Con riferimento a ciascuna linea, i manoscritti in corso di pubblicazione costituiscono parte integrante della tesi. I risultati non inseriti nei manoscritti sono riportati in sezioni separate.

Processo di conversione di coloranti sintetici mediante miscele di laccasi da *Pleurotus ostreatus*. Una prima fase del lavoro è stata finalizzata alla caratterizzazione della cinetica di conversione di RBBR mediante una miscela di laccasi [Palmieri et al., 2005 a-b]. Gli esperimenti sono stati condotti in modalità *fed-batch* (successive aggiunte di RBBR al campione contenente le laccasi). I risultati hanno evidenziato che la velocità di decolorazione (da misure spettrofotometriche) diminuisce passando dal primo all'ultimo ciclo di decolorazione, a fronte di una disattivazione dell'enzima indifferente alla presenza di RBBR in soluzione (trascurabile effetto del RBBR sulla stabilità delle laccasi). Poiché l'entità della riduzione della velocità di decolorazione è maggiore dell'entità della disattivazione dell'enzima, si è ritenuto che il processo è influenzato dall'accumulo dei prodotti di decolorazione. Una conferma del ruolo dei prodotti sulla capacità catalitica dell'enzima è stata ottenuta da misure della velocità di conversione dell'ABTS in presenza di tali prodotti. Si è riscontrata una diminuzione del 9% nella velocità di conversione dell'ABTS rispetto alla velocità in assenza di prodotti di conversione

dell'RBBR. La conversione enzimatica del RBBR è stata caratterizzata mediante il seguente modello cinetico

$$r(C) = \frac{v_{max} C}{k_m + C + (C_0 - C) \cdot \frac{1}{k_p}} \quad (1)$$

Poiché la miscela di laccasi è costituita prevalentemente da POXC [Palmieri et al. 2005 b], il valore di k_m assunto per la miscela si è ritenuto coincidente con quello stimato per l'isoforma più abbondante (16.5 mg/L). In tale ipotesi, i parametri ottenuti dalla regressione dei dati sperimentali (miscela laccasi 12±2 IU/mL) risultano:

v_{max}=2.43±0.19 mg/L·min k_p= 0.35±0.12 (2)

La miscela di laccasi è stata immobilizzata su granuli di EUPERGIT C 250L© del diametro di 180μm. L'enzima è immobilizzato per via covalente reagendo con i gruppi epossidici presenti sulla superficie del supporto. Le condizioni ottimali per l'immobilizzazione sono state selezionate con riferimento alla resa in attività immobilizzata definita come il rapporto tra l'attività espressa dall'enzima immobilizzato e quella inizialmente presente nella fase liquida. L'attività delle laccasi immobilizzate su EUPERGIT© è stata misurata mediante un sistema reattoristico specificamente progettato costituito da un reattore a letto fisso (volume=1mL) esercito con ricircolo della corrente di liquido contenente il substrato (ABTS). L'operazione condotta in condizioni di regime cinetico permette di misurare l'attività fenolossidasica della miscela di laccasi immobilizzata.

Le seguenti condizioni sono state identificate come ottimali per la massimizzazione della resa di immobilizzazione: incubazione per 4 h a temperatura ambiente in tampone sodio fosfato 0.1M pH 6.5 di una miscela di laccasi con attività di circa 90 IU/g di resina secca. La concentrazione di proteine totali dovrebbe essere superiore a circa 2 g/L. Quest'ultimo vincolo emerge dall'esigenza di controllare i fenomeni di *multipoint-attachment* che caratterizzano l'immobilizzazione di proteine su supporti con alta densità di siti attivi [Katchalsky-Katzir et al., 2000].

La caratterizzazione della conversione di RBBR mediante laccasi immobilizzate su EUPERGIT è stata condotta in un reattore a letto fisso (ID 1.5 cm, volume ≥4mL). La corrente di liquido contenente il colorante è stata alimentata inizialmente a portata elevata (circa 30 mL/min) per raggiungere rapidamente le condizioni di equilibrio con riferimento all'adsorbimento del colorante sulla resina. L'operazione si è resa necessaria poiché la capacità di adsorbimento del supporto legato alla miscela di laccasi è risultata particolarmente elevata (circa 10mg RBBR/g resina secca). Stabilizzate le condizioni di equilibrio del colorante in fase liquida ed in fase adsorbita, la portata di soluzione di RBBR alimentata al reattore è stata diminuita per consentire conversione apprezzabili di colorante. Quindi, i valori di tempo-spazio (rapporto volume/portata volumetrica) e di concentrazione di RBBR all'uscita del reattore (τ, C_{out}) sono stati registrati in condizioni di regime stazionario. Le misure (τ, C_{out}) sono state interpretate alla luce del bilancio di materia riferito al colorante in condizioni di regime stazionario esteso ad un reattore caratterizzato da flusso a pistone. Ipotizzando una cinetica con inibizione da prodotto (eq. 1) la regressione ha fornito i parametri riportati in tabella 1 per due campioni di laccasi immobilizzate.

Attività laccasi immobilizzate per unità di volume di letto fisso IU/L	V_{max} mg/L min	K_p -
8000	43±9	0.08±0.02
10000	47±11	0.02±0.004

Tabella 1: Parametri cinetici per laccasi immobilizzate su EUPERGIT©.

Si è ipotizzato che K_m coincide con il valore stimato per POXC in fase liquida.

Al fine di stimare i vantaggi connessi all'immobilizzazione di miscele di laccasi da *P. ostreatus* per la conversione di coloranti presenti in reflui industriali si è proceduto alla stima delle prestazioni di due sistemi reattoristici. In particolare le prestazioni dei due sistemi sono state espresse in termini di volume di liquido trattato. I sistemi reattoristici sono:

STR: reattore discontinuo esercito con miscela di laccasi libere nella soluzione di colorante trattata.

CFBR: reattore a letto fisso (particelle di biocatalizzatore) esercito in continuo rispetto alla fase liquida contenente il colorante.

Nei modelli sviluppati sono stati adottati i parametri cinetici precedentemente riportati. Per entrambi i sistemi si è ipotizzato che: i) la conversione del colorante (alimentato alla concentrazione di 100 mg/L) è del 99%; ii) la miscela di laccasi si disattivi, fino al 10% dell'attività iniziale, in accordo alle cinetiche osservate durante i test svolti con enzimi liberi (decadimento esponenziale). L'attività iniziale è stata fissata a 7IU (immobilizzate) per il CFBR e 45IU (libere) per il STR. Tali valori sono stati assunti considerando che: per 100 IU disponibili come miscela di laccasi si ottengono 7IU immobilizzate su EUPERGIT C 250L© (massima resa 7%) a valle di una diminuzione di attività in fase libera del 45%. Il confronto delle prestazioni dei due sistemi reattoristici ha mostrato che il volume complessivamente trattato dal CFBR è superiore a quello trattato dal STR. Tale vantaggio dipende dalla maggiore stabilità delle laccasi immobilizzate rispetto alle libere che bilancia la perdita di attività conseguente all'immobilizzazione.

Processo di conversione di fenolo mediante biofilm di *Pseudomonas sp.* OX1 in reattori trifasici a letto fluidizzato. Le prove sono state condotte utilizzando un reattore 3PC per lo studio della crescita di biofilm di *P. sp.* OX1 su pomici granulari e il reattore ILA per la conversione di fenolo tramite biofilm maturi di *P. sp.* OX1 adesi alle pomici. In Figura 1 si riporta lo schema dei due impianti le cui caratteristiche sono riportate in tabella 2.

Il reattore 3PC (Fig. 1) è stato esercito in modalità discontinua rispetto alla fase liquida circolante tra il serbatoio e la colonna inoculata con una precolutura di cellule di *P. sp.* OX1. Durante il corso dell'esperimento si è proceduto: i) alla misura della concentrazione di fenolo (fonte di carbonio) e della concentrazione cellulare in fase libera; ii) al campionamento del solido (particelle di pomice 212÷300μm) e alla sua caratterizzazione mediante microscopia a scansione elettronica (SEM) ed analisi elementare (frazione in peso di carbonio). I risultati hanno evidenziato che dopo circa 14 giorni la frazione in peso di carbonio misurata sui campioni di solido è circa 0.9% (0.1% per le pomici sterili). Le immagini ottenute dal SEM mostrano che il biofilm occupa lo spazio dei pori nelle particelle di pomici e porzioni della superficie esterna. Confrontando tali risultati con quelli ottenuti da Alfieri [2006] durante la crescita di biofilm di *P. sp.* OX1 su pomici in beute agitate e in reattore airlift, si è potuto affermare che il reattore 3PC costituisce una valida alternativa per l'ottimizzazione della crescita di tale biofilm su scala da laboratorio in tempi brevi.

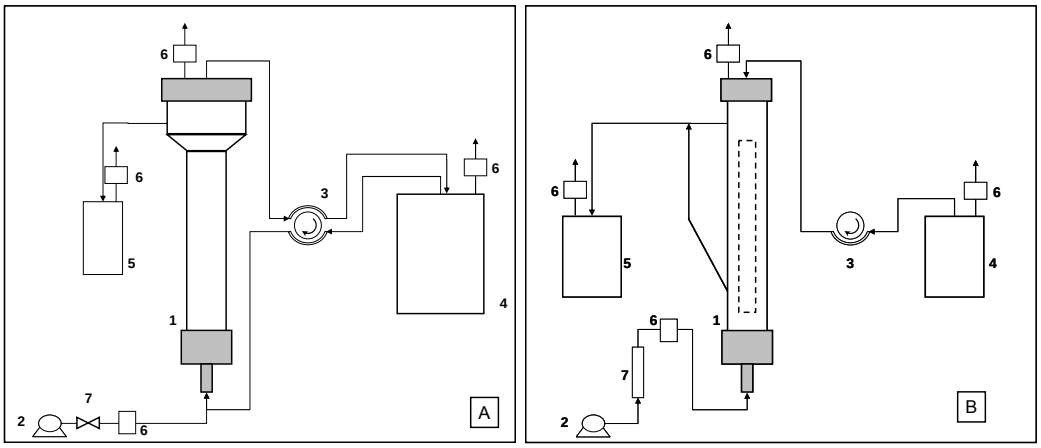

Figura 1: A) Reattore trifasico a ricircolo (3PC). 1 colonna in vetro, 2 unità di pompaggio aria, 3 unità di pompaggio liquido (peristaltica), 4 serbatoio, 5 serbatoio di raccolta, 6 unità di filtrazione gas, 7 valvola. B) Reattore *airlift* a circolazione interna (ILA). 1 reattore *airlift* (*draft-tube* linea tratteggiata), 2 unità di pompaggio aria, 3 unità di pompaggio liquido (peristaltica), 4 serbatoio alimentazione, 5 serbatoio scarico, 6 unità di filtrazione gas, 7 flussimetro aria.

Reattore ILA		**Reattore 3PC**	
Volume totale	0.15 L	Volume totale	0.25 L
Volume di controllo	0.13 L	Volume di controllo	0.15 L
Altezza totale	20 cm	Altezza totale	32 cm
Diametro interno *Downcomer*	4 cm	Diametro interno colonna	3 cm
Altezza *Draft-tube*	10 cm	Diametro interno sezione di testa colonna	4 cm
Diametro interno *Draft-tube*	2 cm	Volume serbatoio	2.25 L
Luce di passaggio al fondo	1 cm	Volume totale	0.25 L

Tabella 2: Caratteristiche degli apparati sperimentali.

Gli esperimenti condotti con il reattore ILA hanno permesso di analizzare l'effetto della velocità di diluizione sulla crescita del biofilm. Il reattore è stato esercito in modalità continua rispetto alla fase liquida e alla fase gassosa. Durante il corso delle indagini sono state effettuate le stesse misure condotte per il reattore 3PC. Le pomici adottate sono state preventivamente trattate nel reattore 3PC cosicché le operazioni del reattore ILA fossero avviate con una quantità non nulla di biofilm (frazione di carbonio dell'inoculo variabile tra 0.42 e 0.96%). La portata di liquido è stata fissata nell'intervallo 0.03-0.09L/h corrispondente a velocità di diluizione variabili tra 0.23 e 0.69h^{-1}, valori sono superiori alla massima velocità specifica di crescita stimata per le cellule sospese di *P. sp.* OX1 (0.17h^{-1}) [Alfieri, 2006]. Il reattore è quindi stato esercito in condizioni di *wash-out* rispetto alle cellule in fase libera, favorendo la crescita del biofilm come suggerito da Heijnen [1984] e da Tang e Fan [1987]. Durante le prove si è proceduto alla caratterizzazione del biofilm in corrispondenza dei regimi stazionari stabilizzatisi alle diverse velocità di diluizione investigate. La frazione di carbonio associata alla presenza di biofilm batterico sulla superficie interna ed esterna delle pomici cresce all'aumentare della velocità di diluizione fino al valore massimo registrato (circa 1.4% dopo 18 giorni di esercizio). Osservando le immagini prodotte dall'analisi SEM si può dedurre che la crescita del biofilm interno ai pori è limitata dal volume disponibile mentre il biofilm esterno è limitato dal raggiungimento dell'equilibrio tra crescita e distacco di frammenti dipendente dalle condizioni operative adottate.

Analisi dinamica e biforcazionale del reattore ILA. Il modello è stato sviluppato considerando: cinetica di crescita con inibizione da substrato per le cellule libere ed immobilizzate [Alfieri 2006]; cinetica di adesione delle cellule, ad un supporto granulare

impervio, lineare con la concentrazione di cellule libere; cinetica di distacco del biofilm lineare con la concentrazione di cellule immobilizzate. Il comportamento del sistema è stato studiato in termini di: analisi biforcazionale rispetto alla velocità di diluizione (numero di Damköhler, Da), coefficiente di distacco (G), concentrazione di substrato alimentata (S_{in}), analisi dinamica. L'elaborazione numerica è stata eseguita con l'algoritmo di continuazione fornito dal software Matlab®. I diagrammi delle biforcazioni per il parametro G (Da<4.01, S_{in}=0.6 g/L) hanno mostrato che: i) il sistema prevede molteplicità delle soluzioni stazionarie e non sono ammesse soluzioni periodiche; ii) il campo di valori di G per cui sono ammesse soluzioni stabili diverse da quella banale (conversione nulla) è limitato superiormente come conseguenza dell'equilibrio tra velocità di crescita e velocità di distacco; iii) la soluzione stabile di alta conversione prevede la presenza di biomassa sospesa anche esercendo il reattore in condizioni di *wash-out* (Da<4.1) come conseguenza del distacco di frammenti di biofilm; iii) il raggiungimento del regime stazionario stabile è subordinato alla presenza di una quantità non nulla di biofilm all'inizio dell'operazione.

I dati sperimentali relativi alla crescita di biofilm ottenuta nel reattore ILA per diversi valori della velocità di diluizione sono stati confrontati con le previsioni del modello teorico. IL confronto conferma che: i) in condizioni di *wash-out* (secondo la cinetica di crescita adottata) la concentrazione stazionaria di biofilm cresce al crescere della velocità di diluizione (Da→0); ii) la biomassa sospesa permane anche operando in condizioni di *wash-out* per effetto del distacco della biomassa immobilizzata. La crescita prevista dal modello risulta sovrastimata rispetto ai dati sperimentali. Tra le spiegazioni della differenza maggior contributo dovrebbe essere dovuto a: i) presenza del biofilm sviluppato nei pori interni delle particelle, non preso in considerazione nel modello; ii) cinetica di crescita delle cellule immobilizzate differente da quella delle cellule sospese adottata nella modellazione teorica.

1 INTRODUCTION

The development of the “white” biotechnologies [Soetaert and Vandamme, 2006; Verstraete, 2007] have been driven by the increasing demand for processes for the production of chemicals and the remediation of waste streams from industrial, agricultural and civil plants. As regards bioremediation, several applications have been envisaged. A broad distinction can be made between bioprocesses whose main goal if to produce added-value products from conversion of waste and bioprocesses whose main goal is the decrease of the toxicity of waste streams by converting pollutants. These goals may be achieved using either microrganisms or enzymes as biocatalysts. Together with the constraints posed by specific bioprocesses, some distinctive advantages and drawbacks of each of these two classes of processes must be taken into account in a feasibility analysis.

Microrganism-based processes are widely used in white biotechnologies. With specific reference to treatment of waste, two main advantages can be recognized: exploitation of microbial consortia for the concurrent removal of different toxic compounds and the relative easiness of up-stream processes required to made biocatalytic activity available, as compared with that required by enzyme based processes. On the other hand, well known drawbacks are those related with the (often severe) constraints associated with microrganism management: the disposal of spent biomass and the need of complex down-stream processes for the recovery of value-added products when necessary.

Enzyme-based processes have been the subject of an extensive literature and have stimulated several industrial applications for the production of fine chemicals. Successful results [Nierstrasz and Warmoeskerken, 2003] have encouraged further efforts to fully exploit enzyme-based processes also in the field of bioconversion of pollutants or organic compounds contained in waste-stuffs [Gianfreda and Rao, 2004; Nicell, 1996]. The main advantages associated with these remediation processes are: continuous waste conversion by immobilized enzyme or membrane reactors, overcoming of problems related with disposal of spent biomass and sterile environment. Drawbacks are related to the costs of enzyme production and other upstream processes (purification, immobilisation, etc.) and to the variable environmental conditions provided by the waste streams that can negatively affect activity of the enzyme.

The industrial success of many bioprocesses is often constrained by the inherent low productivity. In the last decade the productivity enhancement has been pursued by acting on different aspects of the process. Microbiology, biochemistry and genetic engineering have provided effective tools to select and design novel and more performant biocatalysts. Process “intensification” is pursued by biochemical engineers with different strategies that include increase of biocatalyst loading in the reactor, optimization of mass transfer phenomena in multiphase systems and enhancement of biocatalysts stability under actual process conditions. Increasing biocatalyst loading in the reactor is crucial to most industrial bioprocesses because of the limited catalytic/metabolic activity of enzymes/microrganisms as they are active in unusual and harsh environment (e.g. waste water) or when they are forced to act/grow on unusual substrates.

1.1 Enzymatic conversion of dyes: the case of laccases

Polyphenols oxidases are active in the presence of oxygen without any interaction with mediators or coenzymes. Two subclasses can be identified: tyrosinases and laccases. Laccase (EC 1.10.3.2) is able to oxidize phenolic compounds to their corresponding free radicals. The nature of end products is influenced by reactivity of these free radicals and is strongly dependent on the particular compound oxidized as well as on the source of laccases and environmental factors [Bollag, 1998]. Laccase activity toward several aromatic compound has been extensively characterized. Typically phenolic compounds have been investigated in presence of mediators (ABTS, HBT, etc.). Published studies on this subject have been based on laccases extracted from a variety of sources, mainly fungi and plants [Duran and Esposito, 2000]. The interest on laccases applications has been further stimulated by results obtained by Bourbonnais et al. [1990] who were among the first to report successful conversion of non-phenolic compounds by laccase.

Among the aromatic compounds tested, synthetic dyes have been used as substrates for laccase catalyzed oxidations [McMullan et al., 2001; Claus et al., 2002; Correira, 1994]. Experimental evidence encouraged the development of bioremediation processes based on laccases in order to remove colour and reduce toxicity of wastewaters. Conversion of dyes based on both enzyme and microrganism activity have been explored [Rodriguez et al., 1999; Claus et al., 2002; Wesenberg et al., 2003; Swami and Ramsay, 1999]. Tests carried out with different basidiomycetes and ascomycetes strains, showed successful colour removal in solutions containing the most common commercial dyes (reactive, acid and direct). Among the commercial dyes, anthraquinonic sulfonic dyes have been used in several studies as substrates of laccases. Recently, Palmieri et al. [2005a] tested decolourization of Remazol Brilliant Blue R solution by means of laccases extracted form *Pleurotus ostreatus* (type Florida) culture broth. They observed a decolourization extent up to 70÷80%. It is likely that the extent of decolourization is improved by the concerted action of POXC and POXA3 [Palmieri et al., 1997] isoforms when compared with the decolourization carried out with single purified POXC or POXA3 at equal activity concentration. They also provided the Michaelis constant and catalytic efficiency for both the purified isoforms. This study led to the formulation of an optimal growth medium for *P. ostreatus* in order to maximize phenol oxidases activity (about 100 IU/mL) in a mixture composed mainly by POXC and POXA3 [2005 b].

Remediation of dye-bearing wastewaters, particularly from the textile and leather industries, may be conveniently accomplished by enzyme-based instead of microrganism-based processes. The last process could be affected by growth inhibition in presence of waste waters that, among other harsh conditions, cannot provide a sterile environment. Moreover, the growth of a complex microrganism such as filamentous fungi deserves attention in design and operation of a full scale bioreactor. The formation of three-dimensional structures must be carefully controlled: their expansion can prevent adequate oxygenation of the medium and mass transfer of substrates to the less exposed cells [Moreira et al., 2004; Robinson et al., 2001, Michel et al., 1992]. Applications of free enzymes are less demanding when based on single-phase batch operation. However, this advantage is often counterbalanced by a number of drawbacks: high activity requirement, non-

reusability of enzymes dissolved in the liquid phase at the end of the discontinuous operation.

An increase of process throughput could be achieved through enzyme confinement in continuously operated bioreactors. Two main classes of bioreactors have been developed in this field of application: membrane enzymatic reactors [Rios et al., 2004] and immobilised enzyme reactors. In any case, the lack of added-value associated with bioremediation processes poses tight constraints to the confinement methods which should be cheap and reliable and should not interfere significantly with enzyme activity. For this reason, referring to immobilisation of enzymes as process intensification strategy, a detailed analysis for the selection of the proper technique is required.

Process intensification calls for immobilisation techniques that are both effective in stabilizing enzymes and provide biocatalysts that are able to whitstand the (typically harsh) physico-chemical characteristics of waste waters. The simplest techniques for enzyme immobilization are based on the adsorption of enzymes on solid carriers [Lalonde and Margolin, 2002; Tisher and Volker, 1999]. These techniques, however, are based on phenomena that are strongly affected by ionic strength and pH of the liquid phase. Accordingly, the amount of enzyme retained by the solid support is quite stable if the environmental conditions are optimized whereas the enzyme can be released as changes in pH and/or ionic strength occur. For this reason, these immobilization techniques fall short if the biocatalyst is to be used for waste water remediation since, depending on the variability of the upstream industrial process, the liquid phase is generally not characterized by a stable physico-chemical environment. A more effective immobilisation technique is based on covalent immobilization on active solid supports or by entrapping the enzyme into a matrix [Mateo et al., 2007; Cao, 2005]. These techniques should be optimized in order to obtain the maximum increase in enzyme stability with respect to the free status and the lowest loss of activity due to covalent immobilisation. Referring to inert supports, the immobilisation process requires preliminary activation of the solid surface (e.g. derivatization of siliceous supports and subsequent activation with glutaraldehyde) and then the optimization of the immobilisation procedure (activity and protein content per unit mass of supports, environmental conditions). If a commercially available activated support is selected, immobilization may significantly contribute to the optimization of operating conditions. In any case, the effect of covalent binding on enzyme activity should be analysed considering, among the other factors, the difference between activity loss in the original liquid phase and the actual activity expressed by the immobilized biocatalyst. Finally, it is advisable to take into account not only the stability of the immobilised enzyme under storage conditions but also enzyme stability under conditions holding during conversion. A comprehensive survey on the application of immobilised phenoloxidases has been given by Duran et al. [2002].

A few fundamental aspects are typically addressed in studies of bioconversion by immobilised enzymes: biocatalytic activity of the immobilized enzyme; mass transfer phenomena in the bioreactor; adsorption phenomena between liquid and solid phase; influence of flow pattern established into the reactor on performance of the biocatalyst. These issues have been widely investigated with reference to the case of a single substrate converted by a purified immobilised enzyme forming a single product [Kobayashi and Moo-Young, 1971; Swanson et al., 1978, Al-Muftah and Abu-Reesh, 2005]. As regards enzymatic kinetics several models can be adopted (Michaelis and Menten, substrate inhibition, competitive product inhibition,

etc.). The knowledge of the kinetic rate and mechanism characteristic of free enzyme usually represents the starting point. If porous supports are used for enzyme immobilization, internal and external mass transfer take place in close association with heterogeneous reaction, and may strongly affect apparent conversion rate observed during reactor operation. For this reason an assessment of mass transfer rate is necessary to define which regime (kinetic or mass transfer limited) is established in the reactor.

Among the other issues, the effect of reactor configuration and operating conditions on flow pattern within the reactor deserve consideration. Kobayashi and Moo-Young [1971] provided a general theoretical study in which the effects of flow patterns on reactor performances have been highlighted. They investigated the ideal cases of perfectly mixed and plug flow reactors as well as in the general case of a steadily operated reactor characterized by finite dispersion coefficient.

Some authors have highlighted that an enzymatic heterogeneous reaction can be coupled with adsorption of substrates (desorption of products) on the solid carrier supporting the enzyme [Kandelbauer et al., 2004; Peralta-Zamora et al., 2003]. In a batch system, the rate and extent of enzymatic conversion can be masked by rapid adsorption kinetics and large adsorbing capacity of the solid support. Such phenomena are quite evident when dye removal from liquid solution is accomplished through immobilised enzymes. It is trivial to note that a visual control can confirm occurrence of dye adsorption on the solid phase, but it is less simple to extract the extent of enzymatic conversion from the experimental data on overall dye depletion. Kandelbauer et al. (2004) addressed this issue using a direct measurement of diffusion reflectance of the solid phase. Peralta-Zamora et al. (2003), instead, followed the more usual procedure based on fed batch operation and consecutive dye feedings.

It can be concluded that, the performances of a purified enzyme immobilized on a porous carrier can be assessed provided that a detailed description of the heterogeneous enzymatic reaction embodying above mentioned features is available. The biocatalyst characterization can be accomplished using several bench-scale reactors, and the knowledge of the nature of both substrate and product(s) allows the assessment of the kinetic parameters.

The problem is made more complex if immobilization is applied to a mixture of enzymes and if the end products of the process result form complex pattern including non-enzymatic reactions. This is the case of conversion of commercially available dyes by laccases mixture.

1.2 Biofilm reactors

The recentmost developments in industrial bioremediation have been characterized by the expanding application of biofilm reactors. This success is mainly due to the numerous conversion processes accomplished by microbial consortia isolated from different environments. Many advantages are provided by microbial growth as biofilm. In particular, the ability to establish a system which embodies more than one species can lead to accelerated consumption of xenobiotic compounds thanks to the mutual beneficial interactions among different species [Singh et al., 2006]. Recalcitrant compounds converted by biofilm communities may be both organic and inorganic. The first class includes chlorinated aromatic compounds, nitroaromatic compounds and phenols, while abatement of metals (Cd, Cu, Zn, etc.)

in water and soils represents the most successful application of inorganic compound bioconversion.

In many cases the biofilm adopted is isolated from a particular environment whose characteristics concurred in the biofilm formation. That is, the selection of morphology and metabolic pathways, typical of the biofilm community, is forced by the environmental conditions (organic pollutants, metals, temperatures, mechanical stresses, etc.). Several strains of *Pseudomonas* and *Acinetobacter* are able to use aromatic compounds, such as toluene, phenol and xylene, as carbon source in aerobic degradation patterns [Foght and Westakle, 1988]. Pseudomonads species are also characterized by strong propensity to form biofilms, as demonstrated by the large research efforts directed to the investigation of the role of *Pseudomonas aeruginosa* biofilm in infection disease [O'Toole, 2003].

Waste water treatment based on biofilm reactors can be classified in different ways. It has to be mentioned that biofilm morphology and the related reactor configuration can strongly differ depending on the shape of the carrier. Referring to biofilm supported by granular solids or floating biofilm flocks a comprehensive selection of large-scale biofilm reactors is reported by Nicolella et al. [2000a]. These reactors are multi-phase systems: biofilm occurring as solid granular phase, liquid stream to be treated and gas supplied for both mixing or oxygenation or produced as bacterial grow. Typical configurations taken in consideration are: Biofilm Upflow Sludge Blanket (USB), Fluidized Bed (FB), Expanded Granular Sludge Blanket (EGSB), Biofilm Airlift Suspension (BAS) and Internal Circulation (IC) reactors. In USB, FB and EGSB reactors particles are kept fluidized by the up-flowing liquid stream. In BAS reactors air pumped into the system allows suspension of biofilm particles into the liquid phase, while in IC reactors the gas produced in the system drives the circulation and mixing of liquid and solids. A comprehensive survey of airlift reactors is reported by Chisti [1989], this reactor typology is one of the most frequently used in biotechnological applications, solid mixing is assured without moving parts and additional advantages are related to the possibility of tuning residence time and circulation rate of the liquid phase.

A detailed analysis of biofilm growing in bioreactors can be accomplished as some general information on biofilm growth in nature is available. Complex three-dimensional structures, observed on surfaces in contact with liquid streams, are the results of a cyclic process sketched in figure 1.1.

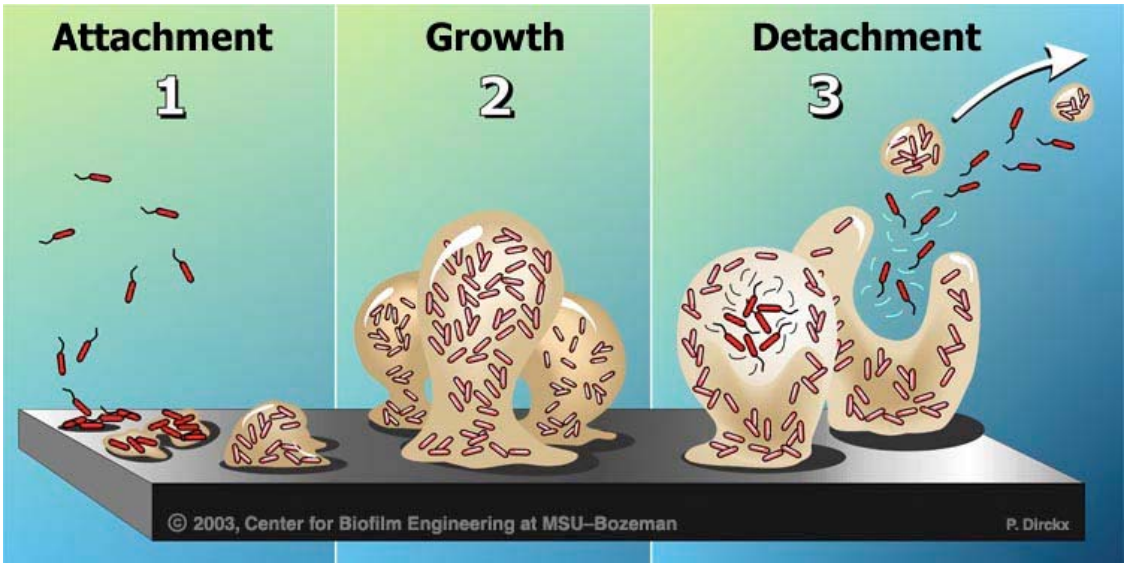

Figure 1.1: Schematic of biofilm formation on a flat surface under stagnant conditions. Available on-line on http://www.erc.montana.edu.

The three main steps are: attachment of planktonic cells, growth of cells monolayer followed by secretion of extracellular polymers towards formation of biofilm complex structure and finally detachment of biofilm fragments and single cells that return to the planktonic state giving rise to the cyclic process. The first step is strongly influenced by interaction of the cell wall with the solid surface that, in turn, is related to flow conditions in the neighbouring liquid phase (stagnant, laminar flow, turbulent flow) and with the phenotype expressed by the planktonic cells. This last feature can favourably influence adhesion of cells when appendages, as flagella or pili, are present on the external cell surface. Cell motility plays a key role even in the second stage where horizontal genetic transfer occurs [Singh et al., 2006]. Early adhesion of cells on solids surface has been widely investigated in order to identify the mechanisms involved. To this aim the knowledge of physical properties of cell wall and phenomena involved in the interaction with inert surfaces are required. Theoretical and experimental studies dealing with this issue have been reported by many authors [Rijinaarts et al., 1993-1995; Beveridge et al., 1997; Bos et al., 1999; Chen and Strevett, 2001; Strevett and Chen, 2003]. Bos et al. [1999] reviewed the techniques available to measure the cell flux in the liquid phase during the early stage (minute time scale) of adhesion and prolonged contact between the cell suspension and the solid surface (hour time scale), as well as contact angle between cell wall and substrate (solid surface or water-organic solvent interfaces) under different conditions (pH, ionic strength). Data on contact angle of bacteria cells from different strains are reviewed by van der Mei et al. [1998] who provide a reference guide for microbial cell surface hydrophobicity with respect to four solvents. Experimental data have been worked out to assess contributes of thermodynamic theory describing adhesion phenomenon. Commonly the Derjaguin-Landau-Verwey-Overbeek (DLVO) theory considers the following components acting as adhesion occurs: Lifshitz-van der Waals (non polar) component, Lewis acid-base (polar) component and electrostatic component. If parameters related to the liquid phase are known at least three parameters for cell (solid phase) need to be calculated [Strevett and Chen, 2003]. This assessment is influenced by growth conditions, physiological state and microbial surface structure. Combining three components, the total free energy (ΔG) associated with the interaction between two cells immersed in a given solvent can be obtained. Cells are classified as hydrophobic if $\Delta G<0$ or as hydrophilic if $\Delta G>0$. Similar investigations provided the components of free energy associated with bacteria deposition on solid surfaces: Lifshitz-van der Waals and Lewis acid-base components are usually negative, that is favour cell deposition, while electrostatic term is positive because usually both bacteria and the solid surface are negatively charged. On the basis of these thermodynamic analysis Chen and Strevett [2001] provided rate of cell adhesion in terms of deposition coefficients on silica gel and sand from Canadian rivers. It was concluded that all the strains investigated showed a deposition coefficient increasing with surface hydrophobicity (silica gel>sand). Results provided by Rijinaarts et al., [1993, 1995] describe adhesion, and related degree of reversibility, of pseudomonad and coryneform bacteria on Teflon and glass as a function of ionic strength, shear rate and cell concentration in the liquid phase. The flux of cells is modelled as exponential function of the free energy, the pre-exponential term is associated to cell diffusional flux under stagnant conditions. They observed that free energy ranges between 1 and 5 kt

(1kt=$4 \cdot 10^{-21}$ J at room temperature) showing lower values with respect to Teflon (adhesion favoured on hydrophobic surface). In conclusion, the information on adhesion of free cells on solid surfaces has to be taken into account to select proper support for the biofilm and to control the early stage of biofilm formation.

Steady state operation of a multi-phase biofilm reactor is moderately influenced by the adhesion process, particularly when an extended mature biofilm is present. Phenomena involved in the steady state behaviour of a granular biofilm reactor are interphase mass transfer, diffusivity of substrates into the biofilm and detachment events. Nicolella et al. [2000, b] provided a review of these subjects. Interphase mass transfer phenomena govern oxygen transfer between gas and liquid phases and oxygen and other substrates transfer between liquid and solid phase (biofilm). The volumetric gas-liquid mass transfer coefficient (commonly indicated as k_La) depends on gas hold-up (volumetric fraction of gas phase) and on the reactor configuration. Nicolella et al. [1998] found, for a BAS reactor on laboratory scale, a linear dependence between k_La and gas hold-up and reported that it is not influenced by solid hold-up. The independence of k_La on solid hold-up is also confirmed by Olivieri et al. [2003], for experiments carried out on a lab-scale internal loop airlift reactor under different solids fluidization regimes. A detailed description of relations governing mass transfer between gas and liquid phases in system characterized by submerged aeration is provided by Chisti [2000].

Mass transfer between liquid and solid phases can change, as biofilm grow on solid phase, as a consequence of changes in particles diameter and surface properties. In the case of thin biofilm, this feature does not affect the assessment of mass transfer coefficient that can be accomplished by relation provided by chemical engineering principles for heterogeneous systems [J. G. Knudsen et al., 1999; Chisti, 2000]

Diffusion of substrates (oxygen and carbon sources) into the biofilm strongly affects its morphology and amount of viable biomass formed. Tang and Fan [1987] report a reduction of oxygen and phenol diffusivities in biofilm with respect to that in water of 75 and 92% respectively. If high biofilm thickness is achieved, deep layers can be affected by substrates depletion, as a consequence, the productivity of the reactor can be reduced even for high loading of attached biomass. The effect of diffusion of substrates into the biofilm have to be analysed together with other concurrent phenomena. The simulation of biofilm morphology on flat surfaces was accomplished by Picioreanu et al. [2000]. They investigated the effect of substrate loading (growth rate), liquid flow rate (Reynolds number), biofilm physical properties (internal cohesion strength, elasticity) and extent of the colonization of the solid surface. Main results of this complex analysis are summarized in figure 1.2 from Nicolella et al. [2000-b]. It shows the simulation of biofilm morphology growing on flat plate at different substrate loading and detachment force. It can be observed that the biofilm appears smooth and thick for intermediate substrate loading and detachment force, the structure modifies forming channels and protuberances when substrate loading increases and detachment force decreases, on the contrary substrate depletion and strong mechanical stresses give rise to a smooth and thin biofilm.

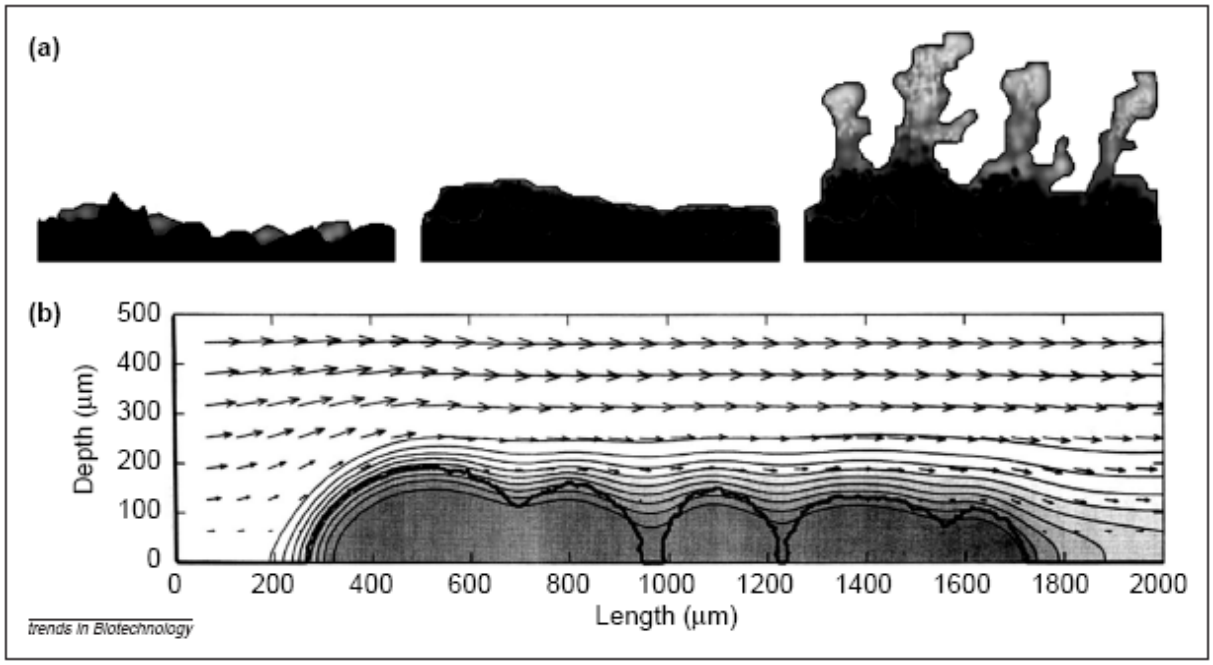

Figure 1.2: Simulation of biofilm morphology as bi-dimensional structure adhering on flat surface [Nicolella et al., 2000]. a) substrate loading increasing and detachment force decreasing form left to right, b) arrows mark liquid flow pattern, grey levels mark iso-substrate concentration plane portions.

These studies are fundamental for the investigations on detachment phenomena occurring on granular biofilm used in multi-phase reactors. The detachment can be sketched in the following steps [Characklis, 1990]: i) 'erosion' induced by shear stress, resulting in continuous loss of cells, either isolated or in small aggregates, from the carrier surface; ii) 'abrasion' of biofilm associated with particle-to-particle friction and/or collisions as effective as solid surface is rough and lacking in biofilm covering (collisions between biofilm covered particles and bare particles); iii) removal of large patches of biofilm, a random process which is usually referred to as 'sloughing'. Depending on bioreactor configuration and operating conditions, these phenomena provide an overall detachment rate that is balanced by biofilm growth (biomass produced by substrates consumption) so, a quasi-steady state biofilm amount per unit mass of solid carrier can be observed.

Heijnen and co-workers have reported on an extensive and detailed investigation on biofilm operated in airlift reactors, using handling bench-scale devices equipped with this type of reactor. In particular, Gjaltema et al. [1997] investigated formation of biofilm from *Pseudomonas putida* in airlift using supports with different properties, they found that roughness of the support is a more relevant parameter than its physical properties. They also demonstrate removal of biomass from the solid phase monitoring phenotype of cell colonies obtained plating biomass samples withdrawn from the liquid phase. Mucoid colonies show that biomass suspended in the liquid phase was constituted by biofilm debris. It has to be mentioned that the authors confirm the strong effect provided by biofilm attached on reactor wall. The relevant effect of this biomass, consuming substrate and producing detached fragments, the high surface to volume ration characterizing bench-scale reactors.

Heijnen and co-workers also investigated the operating conditions that beneficially influence biofilm formation in large scale reactors. The most important result, confirming the hypothesis formulated by Heijnen in his Ph. D. thesis [1984], was the need to operate with high dilution rate in order to achieve stable biofilm

amount in the reactor. The lower limit for the dilution rate is the maximum specific growth rate for suspended cells, in other words, to avoid competition between suspended and attached biomass, planktonic cells growth have to be prevented applying wash-out condition.

It should be mentioned the fundamental role played by experimental techniques adopted to characterize biofilm. An up to date review of these techniques is provided by Denkhouse et al. [2007]. Referring to this topic, a complete characterization of biofilm attached on solid phase should be accomplished through more than one technique. For example, the morphology of biofilm grown on solid surface can be fully characterize by different microscopy techniques and image analysis provides a quantitative assessment of biofilm thickness that can be used to obtain volumetric concentration of attached biomass. Composition of biofilm can be assessed by elemental analysis and more detailed description can be obtained by extraction procedures followed by proper liquid-chromatography and mass spectrometry investigations. The extraction procedures consist in the recovering of extracellular matrix and allows the analysis of concentration of polysaccharides, protein, etc. It is successfully accomplished if high biomass amount is available (order of grams). Impressive pictures describing aerobic granules composition through multi-staining techniques is provided by Chen et al. [2007]

Both experimental and theoretical studies have analyzed the behaviour of the biofilm reactor as operating/design variables were changed. One of the first studies addressing both modelling and experimental procedure for the study of three-phase airlift reactor loaded with biofilm of mixed cultures was accomplished by Tang and Fan [1987]. They assessed multiplicity of steady states as a consequence of non-linear growth rate using phenol as carbon source.

A renewed interest for comprehensive modelling of bioreactors, embodying the rich phenomenology associated with industrial bioprocesses, has grown over the last decade. The motivation was twofold: better understanding of the reactor behaviour and performance; optimal design and operation of bioreactors of novel conception. The dynamic and bifurcational analyses, extensively applied to chemical reactors in the past, have been now extended to the study of bioreactors. Biochemical processes are characterized by rich phenomenologies characterized by non linear behaviour that may generate multiplicity of steady states as well as periodic or chaotic dynamical patterns. Three case studies (production of hydrogen, production of bio-ethanol, and acetylcholine neurocycle in the brain) are provided by Elnashaie et al. [2006]. They highlighted the practical implications of bifurcation and chaos and the most common phenomena driving chemical and biochemical systems toward chaotic behaviour. Pavlou [1999] demonstrated the usefulness of steady state solution diagrams for a continuous bioreactor operated with microrganism characterized by substrate inhibited growth kinetic. The author showed both single and double parameters bifurcation diagrams referring to dilution rate and substrate influent concentration. One of the first studies addressing the dynamic behaviour of a Continuous Stirred Tank Bioreactor (CSTB) was published by Agrawal et al. [1982], and further expanded by Pinehiro et al. [2004] who complemented it by adding a submodel of oxygen limitation. Both studies reported multiplicity of steady states, stability analysis and occurrence of limit cycles depending on Damköhler number. Other phenomena connected with multiple steady states and periodic or chaotic behaviours are the coexistence of more than one microbial population in continuous bioreactors and cell recycling, often adopted as in high cell density reactors. Studies

on these subjects are reported by Lenas [1995, 1998] and Ajibar [2000, 2001] respectively.

As emerged by the reported analysis, a rich and multi-disciplinary literature is available on biofilm reactors and related research fields.

1.3 Scope of the thesis

The study carried out during the present Ph.D. program aimed at investigating specific aspects of process intensification, pursued along the pathway the consists of immobilizing the biocatalyst (enzyme, microrganism) on a solid carrier. The work has been carried out at the Department of Chemical Engineering of the University of Naples 'Federico II' with the contribution of the Department of Organic Chemistry and Biochemistry of the same University. The attention was focused on two processes representative of the main roots of white biotechnology: an **Enzyme-based process** (EBP) and a **Microrganism-based process** (MBP).

Enzyme-based process: conversion of the synthetic dye Remazol Brilliant Blue R (RBBR) by means of laccase mixtures from *Pleurotus ostreatus*. The conversion process was studied with reference to both free and immobilised enzymes.

The study was aimed at the optimization of the immobilization process and at the assessment of the RBBR conversion by means of free and immobilized enzymes.

The immobilization process was optimized with reference to the covalent binding on granular supports - EUPERGIT C 250L©, an acrylic resin with epoxy functionalities. The activities were focused on the selection of the optimized conditions to maximize the immobilization yield and on the design, set-up and operation of a reactor for the assessment of the enzymatic conversion rate.

Activities regarding RBBR conversion by means of laccase mixtures (free or immobilized) included the kinetic characterization of the process. They regarded: i) the design, set-up and operation of a fixed bed reactor to characterize the dye conversion kinetics; ii) the assessment of the effectiveness of laccase immobilization. The role of mass transfer phenomena both between phases and within the granular biocatalyst during operation of fixed bed enzymatic reactor was also investigated.

The role played by immobilisation yield and deactivation of biocatalysts on the performances of both free enzyme and immobilized enzyme was investigated. Two reactors were considered in the study: i) a batch Stirred Tank Reactor (STR) operated with a homogeneous liquid phase containing both the biocatalyst (crude laccase mixture) and the substrate; ii) a Continuous Fixed Bed Reactor (CFBR) loaded with laccases immobilised on EUPERGIT© and continuously fed with the dye-bearing liquid stream.

Microrganism-based process: conversion of phenol by means of *Pseudomonas sp.* OX1 biofilm in fluidized beds.

The study regarded both experimental and theoretical aspects of the conversion of phenol by means of *Pseudomonas sp.* OX1.

An experimental campaign was directed to assess the growth of a biofilm of *P. sp OX1* on siliceous granular supports. Two types of bench-scale three-phase reactors were considered: a Three Phase Circulating (3PC) reactor and an Internal Loop Airlift (ILA) reactor. Tests with the 3PC reactor aimed at optimizing the process

conditions for biofilm growth. Tests with the ILA reactor were aimed to investigate the effect of dilution rate on performance of the system.

The theoretical study was aimed at exploring the bifurcational and dynamic behaviour of an ILA reactor operated with biofilm of *P. sp.* OX1 immobilized on granular solids. The role of the growth rate of suspended and immobilised cells using phenol as carbon source, the adhesion rate of suspended cells on carrier surface and the detachment rate of biofilm from the solid carrier were characterized. Particular attention in the model implementation was paid to the role of detachment rate and dilution rate on bifurcational patterns.

The thesis will separately address these two topics. Section 2 addresses the Enzyme-based process. Section 3 addresses the microrganism-based process. Within each section manuscripts submitted to scientific journals and pertinent to the topic are included.

2 IMMOBILISED LACCASES REACTOR

This section reports the description of experiments and theoretical study accomplished during investigation on dye conversion by crude laccases. The first subsection consists of a paper submitted for publication and concerning this research line. Subsection 2.2-3 reports additional results and remarks on this subject.

2.1 Assessment of antraquinone-dye conversion by free and immobilized crude laccase mixtures

ASSESSMENT OF ANTRAQUINONE-DYE CONVERSION BY FREE AND IMMOBILIZED CRUDE LACCASE MIXTURES

M. E. Russo[a], P. Giardina[b], A. Marzocchella[a], P. Salatino[a], G. Sannia[b]

Università degli Studi di Napoli Federico II
[a]Dip. di Ingegneria Chimica - P.le V. Tecchio, 80 – 80125 Napoli, Italy
[b]Dip. di Chimica Organica e Biochimica V. Cinthia – Complesso Universitario di Monte Sant'Angelo – 80125 Napoli, Italy

Abstract

The present paper reports on the assessment of enzyme-based processes for the conversion of synthetic dyes. A crude laccase mixture, obtained from *Pleurotus ostreatus* cultures, was covalently immobilised on granular supports - EUPERGIT C 250L©, an acrylic resin with epoxy functionalities. The resulting biocatalyst was used in the conversion of an anthraquinonic dye (RBBR). The research activity included optimization of the immobilisation protocol and kinetic characterization of both dye conversion and biocatalyst deactivation under controlled operating conditions. Two fixed bed reactors were purposely designed, set-up and operated to assay the activity of the supported biocatalyst and to

characterize the dye conversion kinetics. Kinetic data were worked out in order to compare the performance of a Continuous Fixed Bed Reactor (CFBR), operated with granular-immobilised laccases, with that of a Stirred Tank Reactor (STR), operated with free laccases. The analysis highlights the relevance of immobilisation efficiency, dye conversion kinetics and laccase deactivation kinetics on the performance of the continuous vs batch dye bioconversion.

Keywords:
immobilised laccases, kinetics, immobilised enzyme reactors, RBBR

1. INTRODUCTION

Laccases are a group of phenoloxidases, characterized by low substrate specificity, able to convert both phenolic and non-phenolic compounds [1-3]. Successful application of laccases in synthetic dyes conversion [4-6] encourages the development of laccase-activated processes for decolourisation of industrial wastewater streams. In particular, recent studies aimed at investigating dye conversion catalysed by laccases from *Pleurotus ostreatus* [7-8]. Palmieri et al. [8] observed that the extent of decolourisation depends on the laccases isoform used. They found that the conversion extent is enhanced up to 70-80% by the concerted action of POXC and POXA3 isoforms [9] when compared with data related to the conversion carried out by a single isoform at equal activity. The same decolourisation extent has also been observed using a crude laccase mixture extracted from an optimized *P. ostreatus* culture broth [8].

Even though laccases are effective in the conversion of phenolic and non-phenolic compounds, their industrial applications are still hampered by several constraints among which the non-reusability is one of the most compelling. Immobilisation of enzymes represents the most straightforward way to implement continuous enzyme-catalyzed processes, and is the subject of the present study.

Application of immobilised phenoloxidases has been extensively reviewed by Duran et al. [10]. They reported on both laccases and tyrosinases, each class being derived from more then twenty different sources. Either type of enzymes was tested against one or more substrates and immobilised following different techniques (adsorption, covalent immobilisation, etc.). Among the most successful

applications, use of immobilised phenoloxidases in biosensing was highlighted. As to the possible use of immobilised laccases and tyrosinases in bioprocessing, Duran et al. [10] reported two phenomena which frequently affect enzyme deactivation: adsorption of chromophoric compounds on biocatalyst surface and precipitation of end-products of non-enzymatic coupling reactions. The first phenomenon is of particular relevance in the context of synthetic dye conversion by immobilised laccases. The adsorption of these compounds occurs at the same time as enzymatic conversion so that, when operation is carried out batchwise, the overall extent of decolourisation is strongly affected by the physical removal of the dye from the liquid phase. Kandelbauer et al. [11] and Peralta-Zamora et al. [12] suggested two different ways to obviate this drawback. The first [11] reported on experiments carried out in a reactor operated batchwise during which both dye optical absorbance in the liquid phase and diffuse reflectance spectra of the solid phase (immobilised enzyme) were monitored. They showed that dye disappearance in the liquid phase was faster than its enzyme-catalyzed consumption, a feature that was related to rapid dye adsorption on the carrier. The second study [12] applied consecutive dye feeds to a batch system loaded with immobilised laccases. Since the enzyme is only active in presence of 1-hydroxybenzotriazole, they observed that in the absence of the mediator the decolourization extent for successive dye additions decreased as adsorption approached equilibrium, whereas in the presence of the mediator the decolourisation extent during each cycle remained constant up to eight dye additions.

Other recent investigations on immobilised laccases addressed conversion of phenolic compounds, particularly polyphenols from olive mill wastewaters [13], polyaromatic hydrocarbons such as anthracene and benzo[a]pyrene [14] and 2,6 dimethoxyphenol [15]. Different covalent immobilization techniques are used based on inert carriers to be properly activated or commercially available active supports. Among these, effective use of EUPERGIT© as active support for laccases immobilisation has been reported [13, 16]. The most beneficial effect of this technique is the stabilization of the immobilised enzyme with respect to the enzyme in solution when tested against thermal inactivation, microbial proteases degradation and long term storage stability. This is the result of the multipoint attachment which typically affects immobilisation of enzymes on epoxy activated supports [17]. As multipoint covalent attachment occurs, concurrent enzyme loss of activity can take

place. Stazi et al. [13] reported the assessment of kinetic parameters for immobilised laccases, the decreased V_{max} is due to the enzyme conformational changes as well as to diffusional limitation occurring during the reaction rate measurements.

The present study aims at investigating the conversion process of a model dye (Remazol Brilliant Blue R, RBBR) by means of crude mixture of enzymes secreted by *P. ostreatus* and immobilised on granular carriers. The study was developed along the following steps: i) kinetic characterization of the RBBR conversion by free laccases mixture; ii) selection and optimization of the immobilisation technique; iii) conversion of RBBR by immobilised laccases mixture and kinetic characterization of the biocatalyst. Special care was paid to set up an experimental procedure which could enable the separate assessment of dye adsorption on the carrier and enzymatic conversion. This goal was pursued by harvesting data during steady regimes of a continuously operated fixed bed reactor. The activities of free enzymes and of immobilised ones toward RBBR conversion have been compared. The analysis has been pursued further by assessing two alternative processes for dye bioconversion: a batch process based on free laccases and a continuous one with immobilized enzymes.

2. MATERIALS AND METHODS

2.1. Fungal culture and crude laccases extraction

Pleurotus ostreatus (strain Florida) was maintained, through periodic transfer every three weeks, at 4°C on agar plates containing 24 g/L potato dextrose and 5 g/L yeast extract. Medium components were supplied by Difco Laboratories (Detroit, MI). Mycelium growth and crude laccases mixture extraction were carried out following the procedures described by Palmieri [9]. The crude laccases mixture extract is characterized by four isoforms (POXA1b, POXA3a, POXA3b, POXC). The activity of the POXC isoform accounts for about 96% of the total mixture activity [8].

2.2. Dye

Remazol Brilliant Blue R (RBBR) (Fig. 1) (Sigma-Aldrich) was adopted as anthraquinone-dye in the present study. Powder purity was 50% and colour index was 61200. Dye concentration was

measured by recording optical absorbance at 592 nm. The extinction coefficient (ε_{592}=9,000 $M^{-1}\cdot cm^{-1}$), referred to total powder concentration [8], was corrected taking into account the purity.

2.3. Proteins and activity assays in liquid phase

Proteins concentration was measured in agreement with the Bradford procedure [18]. Laccases activity was determined at 25°C using 2,2'-azino-*bis*(3-ethyl-benzothialine-6-sulfonic acid) (ABTS) as substrate. The assay mixture contained 2 mM ABTS in 0.1 M sodium citrate buffer, pH 3.0. Oxidation of ABTS was followed by measuring the increase of absorbance at 420 nm (ε_{420} = 36000 M^{-1} cm^{-1}). Enzyme activity has been expressed in International Units (IU).

2.4. Carrier for enzymes immobilisation

Epoxy-activated acrylic beads, EUPERGIT C250 L© (Sigma), were selected as solid carriers. Enzymes immobilisation was based on the covalent binding among amino, thiol and carboxyl groups of the enzymes and the epoxy residues on the carrier surface [17]. Particle size distribution was characterized by means of a back-scattering laser granulometer (Mastersizer 2000, MALVERN Instr.). The distribution resulted of Gaussian type characterized by Sauter diameter of 180 μm, in agreement with data provided by the supplier.

2.5. Experimental apparatus

Assay of immobilised enzyme

The apparatus for the characterization of immobilised enzyme activity is sketched in Fig. 2A. It consisted of a tubular reactor equipped with a liquid recirculation pump, a mixed tank and an on-line flow cell housed into the spectrophotometer (Cary 50, Varian Inc.). The tubular fixed bed reactor consisted of a Plexiglas cylindrical column 6 mm ID and 36 mm long, whose volume was 1 mL. The mixed tank was a 200 mL bottle with IN-OUT liquid stream ports located at different levels to prevent liquid bypass. The pump head and the pipes connecting the three sections of the apparatus had a total volume of about 15 mL, nearly 20% of the overall liquid volume. The liquid was circulated by means of a gear pump (VG 1000 digit, Verder) delivering liquid flow rate in the range 5 ÷ 80 mL/min. Vessels and pipes were wrapped with aluminium paper to avoid light-catalysed substrate oxidation.

The tubular reactor was packed with a fixed amount of the enzyme solid carriers, ranging between 0.18 and 0.36 mL. The bottom and the upper sections of the reactor were packed with 200 - 250 μm glass beads.

Fixed bed enzymatic reactor

Conversion of dye-bearing water streams by immobilised enzymes was investigated in a fixed bed reactor operated continuously. A sketch of the apparatus is shown in Fig 2B. The reactor is a 15 mm ID, 300 mm long column (BIORAD). The volume of EUPERGIT C 250L© packed bed, hence the reaction volume V, changed depending on the amount of biocatalyst prepared. The liquid phase feeding unit consisted of a peristaltic pump (Miniplus Gilson) and a gear pump (VG 1000 digit, Verder) able to deliver streams at volumetric flow rate ranging between 0.2 and 80 mL/min. The dye concentration in the waste stream was measured continuously by means of a spectrophotometer (Cary 50, Varian Inc.) equipped with a flow-cell. Vessels and pipes were wrapped with aluminium paper to protect RBBR from light.

2.6. Operating conditions and procedures

Dye conversion by free laccases mixture

Two types of procedures were followed:

A) Kinetics of RBBR conversion. Kinetics of RBBR conversion was assessed by means of stagewise experiments. Dye concentration and activity were first adjusted to pre-set values in 10 mL of the selected buffer (20 mM sodium acetate pH 4.5) loaded in a 15 mL vial. The initial dye concentration was set at values as large as 75 mg/L. Typically, the initial activity was set at 12±2 IU/mL. The dye conversion was monitored during each stage of the test. After dye conversion approached a steady state, a batch of dye was added to the medium so as to restore its concentration at the level established at the beginning of the test. This procedure was iterated several times, typically three. Laccases activity was also monitored in parallel experiments using a control solution without RBBR. The time-resolved measure of dye concentration was worked out using the differential method to estimate the conversion rate.

B) Laccases inhibition. Laccases activity toward ABTS was assayed in solutions containing products from RBBR conversion. The solution was recovered at the end of batch RBBR conversion by means of laccases immobilised on EUPERGIT C 250L©. Activity of free laccases in presence of products were compared with activity assayed in the buffer solution alone (section 2.3).

Enzyme immobilisation

The protocol adopted for enzyme immobilisation was based on suggestions of the carrier manufacturer (Degussa, Germany) except that some conditions were optimized during tests. The main conditions of the protocol were:

i) the mass of dry resin for mL of solution was fixed at 167 mg_{DR};

ii) incubation took place under gentle shaking at room temperature;

iii) solids recovery was accomplished by vacuum filtration and rinsing with 0.5M sodium phosphate buffer pH 6.5, fixing the ratio of rinsing liquid volume per unit of dry resin at 300 mL/g_{DR};

iv) incubation of solids lasted overnight with 4 g/L albumin (BSA by Sigma) solution to saturate unreacted epoxy residues;

v) at the end of the test, solids were rinsed and stored at 4°C.

Optimisation regarded the following operating conditions: solids pre-treatment, buffer composition, pH, temperature, incubation time, ratio activity/(mass of dry solids) and ratio (total proteins)/(mass of dry solids). Table 1 reports the range of the operating conditions investigated. In particular: i) the conditioning of solids was carried out in the immobilisation buffer; ii) protein loading for a fixed value of activity loading was changed by adding albumin.

The total initial activity ($A_{L,0}$) and the total protein content were measured in the incubation phase. The total residual activity ($A_{L,R}$) and the total residual proteins were calculated as the sum of the values measured in the liquid phases recovered after incubation and during rinsing. The total residual values were compared with the initial values and the difference was assumed as an indication of the decrease of liquid phase laccases activity and mass of immobilised proteins.

Immobilised enzyme: activity assay and immobilisation yield

The activity of immobilised enzymes was estimated by measuring the oxidation rate of ABTS (r_{ABTS}) under the operating conditions adopted for the free laccases activity assay (section 2.3). The rate was calculated by means of the mass balance (eq. 1) on the oxidized ABTS (p) extended to the liquid phase in the facility showed in Fig. 2A. The following conditions were assumed: i) perfect mixing of the liquid phase in the buffer tank (volume V_T); ii) fixed bed reactor (volume V) operated as a differential reactor (substrate conversion less than 1% for each liquid passage); iii) conversion process controlled by enzymatic reactions. In particular, the hypothesis iii) holds under the conditions detailed in Appendix A.

Under proper operating conditions the overall behaviour of the reactor closely approaches that of a stirred tank reactor. Accordingly the mass balance on the product (p) reads:

$$V_T \cdot \frac{dp}{dt} = V \cdot r_{ABTS}(p) \qquad (1)$$

The slope of the absorbance time series, recorded during the assay, was worked out to calculate the term at LHS of eq.1. Hence, the total immobilised activity per unit volume of the packed bed could be calculated.

The efficiency of the immobilisation process has been characterized by means of two yield expressions:

1) The loss of activity in the liquid phase referred to the initial activity (Y_{lost}):

$$Y_{lost} = \frac{A_{L,0} - A_{L,R}}{A_{L,0}} \qquad (2)$$

2) The effective immobilisation yield (Y) defined as the ratio between laccases activity expressed by solids biocatalyst (A_s) and total activity available in the liquid solution at the beginning of the immobilisation processes ($A_{L,0}$):

$$Y = \frac{A_s}{A_{L,0}} \qquad (3)$$

<u>Dye conversion by immobilised laccases</u>

Two complementary types of tests were carried out:

A) Kinetics of RBBR conversion. Experiments aiming at the assessment of the kinetics of RBBR conversion by immobilized laccases included a preparation/preconditioning phase and a data harvesting/postprocessing phase:

Preparation/preconditioning: a fixed amount of biocatalyst particles, of known overall activity, was loaded in the fixed bed reactor and 5 L of dye solution at the pre-set concentration were prepared starting from a 20 mM sodium acetate pH 4.5 buffer. Eventually, the dye-bearing liquid stream was fed to the reactor at a flow rate Q of 30 mL/min. Operation of the reactor under these conditions lasted until adsorption of dye onto the biocatalyst approached equilibrium, as highlighted by the breakthrough of the time-resolved dye concentration at the outlet of the reactor [19].

Data harvesting/postprocessing: during this phase a sequence of regimes were established in the reactor by decreasing stepwise the liquid feed rate Q. Each step lasted until dye concentration in the effluent approached a steady value. Raw data, consisting of the dye conversion measured for each value of Q, were analyzed in the light of an integral reactor model to assess the parameters of the dye conversion kinetics.

B) Assessment of the effects of product-inhibition on RBBR conversion kinetics. This type of test aimed at providing further support to the hypothesis that RBBR conversion kinetics was product-inhibited and consisted of an activity assay using solutions with and without dye conversion products. The assay, similar to that adopted for the assessment of the activity of free laccases, was carried out batchwise in 2 mL vials under agitation by means of a vortex mixer. 50 μL of suspension containing about 2 μL of immobilised laccases resins were mixed with 100 μL of 20 mM ABTS solution (2 mM final concentration) and 850 μL of 20 mM sodium acetate pH 4.5 buffer. Absorbance at 420 nm (section 2.3) in liquid supernatant was measured after 24, 48, 72, 96 and 120 s.

3. RESULTS

3.1. RBBR conversion by crude laccases mixture

Figures 3 A-B report data recorded during a decolourisation test of RBBR by crude laccases mixture according to the procedure described in section 2.6. These figures refer to a stepwise

experiment during which three successive make-up's of RBBR have been fed to the reactor, each at a time when conversion of the previously charged dye was nearly complete. The initial RBBR concentration and the activity were set at 77±2 mg/L and 12±2 IU/mL, respectively. Similar experiments have been carried out with different numbers and/or sequence of steps.

Figure 3A shows the time series of RBBR concentration expressed as residual dye with respect to the initial amount. It is recalled that RBBR concentration was measured by recording the optical absorbance at 592 nm. For this reason, data reported in figure 3 have been corrected by taking into account the contribution of product absorbance assessed under conditions corresponding to complete conversion of the dye. RBBR concentration decreases monotonically within each step, and the conversion rate decreases as well. The initial slope of the dye concentration vs time profiles has been worked out to yield the initial dye conversion rate r_0 corresponding to the preset concentration of 77 mg/L. Comparison of the concentration vs time profiles relative to the various steps highlights a remarkable feature: r_0 decreases all the way from the first to the third step, despite dye concentration was restored at the same levels at the beginning of each step. Laccases deactivation and/or inhibition due to accumulation of reaction products might be responsible for this feature. To better clarify the relative importance of these phenomena, a parallel characterization of laccases activity of samples retrieved from the decolourisation vial at different stages of the test has been accomplished and compared with that of a control sample. Results of these tests are reported in Fig. 3B. Values of r_0 corresponding to the beginning of each step are also reported. Comparison of results obtained with the decolourisation and the control samples indicates that laccases activity is not affected by exposure to RBBR within the assay accuracy. Comparison of values corresponding to r_0 and laccases activity curves suggests that r_0 decays during conversion to an extent that largely exceeds the parallel decrease in laccases activity. Based on this observation, one could speculate that inhibition of reaction kinetic associated with accumulation of reaction products is at work.

A further confirmation of the product-inhibited character of the reaction kinetics has been obtained in additional tests carried out as described in section 2.6. A solution containing products was prepared by decolourisation of 19 mg/L RBBR solution up to 40% conversion by immobilised laccases. The solution, separated from the granular biocatalyst, was used as buffer to measure

oxidation rate of free laccases against the standard reagent ABTS. A 9% decrease of oxidation rate resulted with respect to the rate assessed without products. During the assay, the concentration of residual RBBR was monitored and no changes were observed (data not shown).

Based on these findings, experimental data were fitted by the following product-inhibited kinetic model:

$$r(C) = \frac{v_{max} C}{k_m + C + (C_0 - C) \cdot \frac{1}{k_p}} \qquad (4)$$

The Michaelis constant k_m was assumed equal to that assessed by Palmieri [8] for POXC, considering that most of the activity of the crude laccases mixture is due to this isoenzyme. Taking into account the purity of the dye, k_m is 16.5 mg/L. With this assumption, eq. 4 was best-fitted to experimental data yielding: v_{max}=2.43±0.19 mg/L·min; k_p= 0.35±0.12. These parameters are valid for the laccase mixtures characterized by an activity concentration of 12±2 IU/mL.

3.2. Laccase mixture immobilisation

Immobilisation of laccase mixture on EUPERGIT C 250L© has been carried out in 0.1M sodium phosphate buffer at pH 6.5. A base-case immobilisation protocol was first established, then the effect of selected variables on immobilisation yield has been systematically investigated. Table 2 summarizes the relevant variables pertaining to the immobilisation tests for the base case (run 1) and for the other tests.

At the end of run 1 about Y_{lost}=80% of the initial activity was removed from the liquid phase. Correspondingly, the activity of the immobilised enzymes was 0.25 IU, with an immobilisation yield equal to Y=4.8%. The condition that $Y_{lost} \neq Y$ is remarkable. It can be speculated that this difference could be a measure of enzyme deactivation upon immobilisation. Detailed assessment of mass transfer rate from the bulk of the liquid phase to the immobilised enzymes, reported in Appendix A, enabled to rule out this process as a possible reason for the observed loss of enzyme activity upon immobilisation.

The immobilisation yield vs initial specific activity passed through a maximum (of about 7%) for an initial specific activity of about 90 IU/g_{DR}. Values of Y_{lost}, quite scattered, averaged 45%. Both

Y and Y_{lost} were barely affected by whether pre-conditioning the solids carrier in a buffer was accomplished or not. The presence of recovered activity in liquid supernatant at the end of incubation suggests to investigate the effect of incubation time: immobilisation yields measured at 4, 24 and 72 hours were nearly the same. Hence, incubation time was fixed at 4 h in order to limit enzyme deactivation.

Immobilisation yield Y and fractional activity loss Y_{lost} have been characterized as a function of pH (Table 2). Y and Y_{lost} did not change significantly between pH=6.5 and 7.5 (run 3-4-5) whereas both values decrease at pH=5.5 (run 17). All subsequent experiments were carried out at pH=6.5. Y decreases with ionic strength (Table 2). 0.1 M sodium phosphate was adopted as optimum buffer composition.

A few immobilisation tests were carried out by adding albumin to the incubation solution, in order to decrease the ratio between laccase activity and total protein content down to 75% (run: 3-4, 9-11). For given free enzyme activity, the immobilisation yield Y moderately increases with the total protein content. The observed trend of immobilisation yield with increasing protein content offers a speculative explanation for the rather small immobilisation yields found in the present study. Bonding between proteins and epoxy groups on the carrier involves both amino- and thiol groups, hence, multipoint-attachment is likely to occur [13, 17]. Consistently with the reported findings, competition between enzymes and added proteins for common carrier binding sites might hinder multipoint attachment and result in increased activity of immobilised enzymes. Of course, this effect might be reversed at even larger loadings of added proteins as competition would prevent even single-point attachment of the enzymes to the carrier.

3.3. RBBR conversion with immobilised laccases mixture

Enzymatic conversion of dye during the continuous operation in a two-phase (liquid-solids) reactor (Fig. 2B) has been investigated following the procedures reported in section 2.6. Two mechanisms, namely adsorption and enzymatic conversion, are responsible for dye depletion from the liquid phase. Tests were specifically carried out to estimate the contribution of both.

The role of the solid biocatalyst as dye adsorbent was preliminarily verified by analyzing RBBR adsorption isotherms at 25°C (data not shown). Dye uptake by EUPERGIT C 250L©, made

inert by albumin, was measured under equilibrium conditions as dye depleted from the liquid phase. The adsorption behaviour could be described by a strongly favorable isotherm and the maximum dye concentration on the solid phase was about 10 mg_{RBBR}/g_{DR}.

Dye conversion tests were carried out using laccases immobilised according to the protocol described in section 2.6. To this aim, preparation of immobilised laccases was accomplished by setting the initial activity in liquid phase at values larger than 200 IU/g_{DR} to obtain a biocatalyst with sufficiently large activity per volume unit of the fixed bed. Correspondingly, immobilisation yields ranged between 1 and 4%, consistently with data reported in Table 2.

Figure 4 shows the time resolved profiles of the RBBR concentration (C_{out}) in the effluent from the enzymatic reactor. Data refer to V = 4 mL, total activity 32 IU and inlet RBBR concentration C_{in} = 25.5 mg/L. Vertical lines mark the times at which the volumetric flow rate (Q) was changed. Q was fixed at 30 mL/min during the first stage (a). Eventually it was reduced stepwise to 0.43 mL/min (steps 'b' to 'f'). Reactor space-time τ correspondingly increased from 0.13 to 9.3 min. During step 'a', dye adsorption on the carrier was extensive and (because of the small value of the reactor space-time) enzymatic conversion negligible. Accordingly, C_{out} approaches a steady state value $C_{out} \cong C_{in}$ after about 75min. Once step 'a' is elapsed, dye depletion measured under steady state conditions at fixed Q – steps 'b' to 'f' – could be attributed to enzymatic conversion only, and transient responses that followed each flow rate change resulted from the concurrent effects of adsorption/desorption equilibration and enzymatic conversion.

The performance of the reactor was assessed in terms of dye conversion rate under given operating conditions, by means of a steady state mass balance on dye assuming: i) plug flow pattern of the liquid phase; ii) negligible mass transfer resistance between the liquid phase and the solid phase (see Appendix A), and iii) effectiveness factor of the porous biocatalyst close to 1:

$$\varepsilon S dz \frac{dC}{dt} = -QdC - R(C)\varepsilon S dz - R_{ads}(C - C^{*}_{ads})\varepsilon S dz \qquad (5)$$

where S is the reactor cross sectional area, ε the fixed bed voidage, R(C) the dye conversion rate per unit volume of the liquid phase, R_{ads} the dye adsorption rate per unit volume of the liquid phase and C^{*}_{ads} the dye concentration in the liquid phase in equilibrium with the dye adsorbed on solids.

Equation 6 can be particularized to steps 'b' – 'f', once steady equilibrium adsorption of dye has been approached ($C \cong C^{*}_{ads}$):

$$\frac{Q}{\varepsilon} dC = -R(C) S dz \qquad (6)$$

Integration of eq. (6) over the reactor length yields:

$$\int_{C_{in}}^{C_{out}} -\frac{dC}{R(C)} = \varepsilon\tau \qquad (7)$$

A product-inhibited kinetic model similar to that used for free laccases (eq. 4) has been considered:

$$R(C) = \frac{V_{max} C}{K_m + C + (C_{in} - C)\frac{1}{K_p}} \qquad (8)$$

where K_m is taken as 16 mg/L (see section 3.1), under the hypothesis that the affinity of laccases is not appreciably influenced by immobilisation. Combining eqs (7) and (8):

$$\varepsilon\tau = \frac{K_m + C_{in} \diagup K_p}{V_{max}} \ln\left(\frac{C_{in}}{C_{out}}\right) + \frac{1 - 1 \diagup K_p}{V_{max}} (C_{in} - C_{out}) \qquad (9)$$

Reactor space-times τ and dye concentration at the outlet C_{out} corresponding to steady state regimes have been worked out following the integral method according to eq. 9 to estimate the kinetic parameters. As shown in Figure 5, eq. 9 with best-fit kinetic parameters of the product-inhibited conversion kinetics eq. 8 reproduces fairly well the experimental data.

Similarly to the case of crude laccases mixture, possible inhibition of immobilised laccases due to accumulation of decolourisation products was assessed by performing ABTS oxidation assays in presence of decolourisation products. The solution containing decolourisation products was the same used for the similar test on free laccases (section 2.6). A decrease of about 20% of the ABTS oxidation rate was observed in the presence of decolourisation products. Notably, the same result was obtained both in assays with fresh biocatalyst and in assays carried out with a biocatalyst sample previously equilibrated with solution containing end-products. Accordingly, adsorption taking place during contact between fresh biocatalyst and end-products should not affect product inhibition.

4. ASSESSMENT OF ALTERNATIVE PROCESSES FOR DYE CONVERSION

In the present section an assessment is presented of two alternative options for the abatement of dye in a wastewater:

Option a) dye conversion is accomplished in a batch Stirred Tank Reactor (STR) operated with a homogeneous liquid phase containing the biocatalyst (crude laccases mixture) and the substrate;

Option b) dye conversion is accomplished by feeding the liquid stream to a Continuous Fixed Bed Reactor (CFBR) loaded with laccases immobilised on a granular carrier.

The assessment of the alternatives must take into account advantages and drawbacks of either option, listed in Table 3. Key aspects of the comparison are represented by, on one hand, the loss of biocatalytic activity in option 'b' associated with the immobilisation yield, on the other hand, the longer operation permitted in option 'b' by the enhanced enzyme stability brought about by immobilisation. The extent to which these features balance each other is critically dependent on the enzyme deactivation time in either option. The assessment of the two options has been based on reaction kinetics data reported in sections 3.1 and 3.3. Model assumptions and equations are detailed in Appendix B. In particular, the initial dye concentration in the liquid phase and the dye conversion degree have been fixed at 100mg/L and 99% in both cases.

Results of model computations have been analyzed in terms of the total volume of the liquid stream which can be processed with either system for a given initial amount of crude laccases, as detailed in Appendix B. For both options, the total treated volumes V_a and V_b are calculated with the constraint that operation of the reactors lasts until the enzyme activity decays to 10% of the initial activity, as a consequence of the deactivation. The constraint that dye conversion equals 99% implies a variable flow rate of the liquid stream fed to the CFBR during the operation. For the purpose of computations, the deactivation coefficients have been taken as $8.2 \cdot 10^{-4}$ and $1.4 \cdot 10^{-4} min^{-1}$ for free and immobilized laccases, respectively (see Appendix B).

The total treated volume computed in the batch option is $V_a = 8 \cdot 10^{-3}$ L. Figure 6 reports the ratio V_b/V_a between the total treated volumes in either option expressed as a function of the

deactivation coefficient of immobilised laccases. A threshold value of k_{imm}*=$6.2 \cdot 10^{-4}$$min^{-1}$ is computed, corresponding to V_a/V_b=1. The key role of immobilised enzyme deactivation to the proposed assessment is clarified by the plot in Figure 6: longer enzyme stability in the immobilised form may effectively overcome the penalty of option 'b' in terms of immobilisation yield. When the actual value of the average deactivation coefficient of immobilised laccases is taken into account, the total processed volume in option 'b' turns out to be larger than V_a by a factor of 4, for the given dye conversion degree and initial dye concentration.

The proposed assessment is far from conclusive, but serves to the scope of highlighting alternative options and key variables and provides the starting point for more comprehensive techno-economic assessment embodying all the relevant costs.

5. CONCLUSIONS

The present study addresses the conversion of an antraquinone-dye by means of either free or immobilised laccases mixtures.

Aspects that have been specifically investigated concern:

- The kinetics of dye degradation catalyzed by crude enzyme mixtures;
- The optimization of an immobilisation protocol of laccases mixtures onto EUPERGIT C 250L©
- The kinetics of dye conversion by the immobilised biocatalyst.

The kinetics of dye degradation by both free and immobilised laccases turns out to be product-inhibited. Kinetic parameters of a product-inhibited kinetic equation have been inferred from data for both types of biocatalysts and demonstrate the criticality of products accumulation on the course of degradation. Immobilisation of enzymes is characterized by moderate yield, when expressed in terms of immobilised activity. Comparison of the activity of immobilised enzymes with the corresponding loss of activity in the liquid phase suggests that immobilisation, though quantitative, brings about some loss of activity of the laccases. Multipoint attachment of enzymes onto the support is speculatively offered as one explanation for this finding, an argument that finds some support from experiments carried out at given activity with variable protein contents.

A preliminary assessment of alternative options for the enzymatic degradation of dye has been made. Either batchwise homogeneous degradation of dye in a medium containing free laccases or continuous degradation in a fixed bed reactor with immobilised enzymes have been considered. The comparison of the two options suggests that the enzyme deactivation time-scale in the immobilised state together with the immobilisation yield play a key role in determining the optimum process. Based on the experimental results concerning enzyme stability and dye conversion kinetics in either the free or the immobilised forms of laccases, the option based on continuous operation of a fixed bed reactor with immobilised laccases enables the treatment of a larger amount of dye-bearing liquid stream.

Appendix A

The role of interphase mass transfer between the liquid phase and the carrier surface has been assessed. A kinetic-controlled regime is established if the substrate consumption rate at the biocatalyst surface is smaller than the mass transfer rate across the boundary layer in the liquid phase around the particle:

$$r << k_l a\, C \qquad (A.1)$$

where k_l is the mass transfer coefficient and 'a' the biocatalyst surface per unit volume of packed bed. For uniform spherical particles with diameter d_p, 'a' can be calculated as:

$$a = \frac{6(1-\varepsilon)}{d_p} \qquad (A.2)$$

where ε is the local voidage.

The interphase mass transfer coefficient k_l was calculated according to Wilson and Geankoplis [20] for liquid phase flowing across a packed bed. For Reynolds number falling in the interval [0.0016, 55] it is:

$$Sh = \frac{1.09}{\varepsilon} Re^{1/3} Sc^{1/3} \qquad (A.3)$$

where Sherwood (Sh), Reynolds (Re) and Schmidt (Sc) numbers are defined as

$$Sh = \frac{k_l D}{d_p} \qquad Re = \frac{\rho v d_p}{\mu} \qquad Sc = \frac{\mu}{\rho D} \qquad (A.4)$$

D is the substrate diffusivity in the liquid phase, ρ and μ the density and the viscosity of the liquid and v the average velocity of the liquid. Whether criterion A.1 was met was verified with reference both to activity assays using ABTS as substrate and to RBBR bioconversion in the CFBR.

Appendix B

The comparison between options 'a' (STR) and 'b' (CFBR) has been based on the following assumptions:

- Kinetics of free and immobilised laccases have been expressed by eqs. 4 and 8, respectively. v_{max} and V_{max} (section 3.1 and 3.3) are proportional to enzyme activity. Accordingly:

$$\bar{v}_{max} = \frac{v_{max}}{A_{free}} \qquad \bar{V}_{max} = \frac{V_{max}}{A_{imm}} \tag{B.1}$$

yielding (see sections 3.1 and 3.3):

$$\bar{v}_{max} = 2 \cdot 10^{-4}\, mg/(\min IU) \qquad \bar{V}_{max} = 5 \cdot 10^{-3}\, mg/(\min IU) \tag{B.2}$$

- a fixed amount of 100IU of phenoloxidases activity is available as laccases mixture. If the laccases mixture is immobilized following the procedure detailed in section 2.6 the maximum immobilization yield (eq 3) is 7%, and the corresponding loss of activity in the liquid phase is about 45%. Accordingly, the comparison between the two options is made under the assumption that the CFBR is loaded with an immobilized activity $A_{0,imm}$=7 IU= 100·Y and the STR with a free enzyme activity $A_{0,free}$=45 IU=100·Y_{lost}.
- RBBR concentration in the solution is fixed at 100 mg/L. The conversion of RBBR is fixed at 99% for both reactors.
- The deactivation of both free and immobilised laccases has been modelled as an exponential decay

$$A(t) = A_0 \exp(-k\ t) \tag{B.3}$$

with $k_{free}=(8.2\pm0.7)\cdot10^{-4}min^{-1}$ and $k_{imm}=(1.4\pm1.1)\cdot10^{-4}min^{-1}$ for free and immobilized laccases respectively. k_{free} is calculated for free laccases mixtures characterized by an initial

activity of 12±2 IU/mL (see section 3.1) and k_{imm} is the average value obtained from experimental data collected during prolonged decolourization tests with immobilised activity ranging between $4.6 \cdot 10^3$ and $11 \cdot 10^3$ IU/(L of packed bed).

The CFBR as been modelled assuming a plug flow pattern for the liquid phase; in order to keep the RBBR conversion constant at 99%, the flow rate is adjusted as enzymes deactivate.

The mass balance on dye in the STR yields:

$$\frac{dC}{dt} = -\frac{A_{free}(t) \cdot \bar{v}_{max}}{V_{STR}} \cdot \frac{C}{k_m + C + (C_0 - C)\frac{1}{k_p}} \qquad (B.4)$$

$$t = 0 \rightarrow \quad C = C_0, A_{free} = A_{0,free}$$

where V_{STR} is the reactor volume and C_p has been calculated as reported in section 3.1. Solution of eq. (B.4) for V_{STR} yields

$$V_a = V_{STR} = \frac{\bar{v}_{max} A_{0,free} (k_{free})^{-1} \left(1 - \exp(-k_{free} t)\right)}{\left(K_m + C_0 / K_p\right) \ln\left(\frac{C_0}{C_f}\right) + \left(1 - 1/K_p\right)(C_0 - C_f)} \qquad (B.5)$$

that expresses the total volume V_a treated by STR as a function of duration of the batch operation t and final concentration of substrate C_f.

Under the quasi-steady state approximation, the mass balance on substrate in the CFBR yields:

$$\tau\varepsilon = \int_{C_{in}}^{C_{out}} \left(\frac{A_{imm}(t) \cdot \bar{V}_{max}}{V_{CFBR}\varepsilon} \cdot \frac{C}{K_m + C + (C_{in} - C)\frac{1}{K_p}} \right)^{-1} dC \qquad (B.6)$$

where V_{CFBR} is the volume of the fixed bed, computed from the known amount of immobilized laccases and the activity-to-carrier mass ratio corresponding to maximum immobilization yield. Integration of eq. (B.6) yields

$$\tau\varepsilon = \frac{V_{CFBR}\varepsilon}{A_{imm}(t) \cdot \bar{V}_{max}} \left[\left(K_m + C_{in}/K_p\right) \ln\left(\frac{C_{in}}{C_{out}}\right) + \left(1 - 1/K_p\right)(C_{in} - C_{out}) \right] \qquad (B.7)$$

The liquid flow rate Q can be made explicit as a function of time t and outlet dye concentration C_{out}

$$Q(t) = \frac{A_{imm}(t)\overline{V}_{max}}{\left(K_m + C_{in}/K_p\right)\ln\left(\frac{C_{in}}{C_{out}}\right) + \left(1 - 1/K_p\right)(C_{in} - C_{out})} \quad \text{(B.8)}$$

The total volume V_b treated by CFBR can be calculated by integrating the inlet flow rate Q(t) over the time interval equal to the duration of the continuous operation

$$V_b = \int Q(t) \cdot dt = \frac{\overline{V}_{max} A_{0,imm} (k_{imm})^{-1} (1 - \exp(-k_{imm} t))}{\left(K_m + C_{in}/K_p\right)\ln\left(\frac{C_{in}}{C_{out}}\right) + \left(1 - 1/K_p\right)(C_{in} - C_{out})} \quad \text{(B.9)}$$

NOMENCLATURE

A	laccases activity	IU
$A_{L,0}$	initial activity in liquid phase	IU
$A_{L,R}$	residual activity in liquid phase	IU
A_s	activity in solids phase	IU
a	surface of biocatalyst per unit volume of packed bed	m^2/m^3
C	concentration of RBBR	mg/L
C_p	concentration of product from RBBR conversion	mg/L
d_p	particle diameter	m
k_l	external mass transfer coefficient	m/s
k_m, K_m	Michaelis constant	mg/L
k_p, K_p	product inhibition constant	-
Q	volumetric flow rate of the liquid stream	L/min
p	oxidized ABTS concentration	mM
r, R	reaction rate per unit of reactor volume	mg/L min
r_{ABTS}	ABTS oxidation rate	μmol/(mL min)
S	cross section of the fixed bed	m^2
t	time	min
V_a	volume treated by system ‘a’	L

V_b	volume treated by system 'b'	L
V_{CFBR}	volume of CFBR	L
V_{STR}	volume of STR	L
V_T	tank volume	mL
V	reaction volume	mL
v_{max}, V_{max}	maximum conversion rate	mg/(L min)
Y	immobilisation yield estimated in agreement with eq. (3)	-
Y_{lost}	immobilisation yield estimated in agreement with eq. (2)	-
z	axial coordinate for fixed bed	m

Symbols

ε	packed bed void fraction	-
τ	reactor space-time	min
ρ	liquid density	kg/m^3
μ	liquid viscosity	Pa s

Subscripts

0	initial condition
ads	adsorbed state
f	final state
free	referred to free laccases
i	i^{th} step
imm	immobilised laccases
in	inlet stream
out	outlet stream

AKNOWLEDGEMENTS

This work was supported by the European Commission, Sixth Framework Program (SOPHIED contract NMP2-CT2004-505899), by grants from the Ministero dell'Università e della Ricerca

Scientifica (Progetti di Rilevante Interesse Nazionale, PRIN), and by Centro Regionale di Competenza BioTekNet. The support of Miss Alessandra Adriatico is gratefully acknowledged.

REFERENCES

1. Bollag J. M., Shuttleworth K. L., Anderson D. H., Laccases-mediated detoxification of phenolic compounds. App Environ Microbiol 1998; 54: 3086-91
2. Bourbonnais R, Paice MG. Oxidation of non-phenolic substrates.An expanded role for laccase in lignin biodegradation. FES Lett 1990; 267: 99–102.
3. Duran N., Esposito E. Potential applications of oxidative enzymes and phenoloxidase-like compounds in wastewater and soil treatment: a review. App Catal B Environ 2000;28: 83-99
4. Rodriguez E., Pickard M.A., Vazquez-Duhalt R. Industrial dye decolorization by laccases from lignolytic fungi. Curr Microbiol 1999; 38: 27-32
5. McMullan G., Meehan C., Conneely A., Kirby N., Robinson T., Nigam P., Banat I. M.,·Marchant R., Smyth W. F. Microbial decolourization and degradation of textile dyes. Appl Microbiol Biotechnol 2001; 56: 81-87
6. Claus H.,·Faber G., König H. Redox-mediated decolorization of synthetic dyes by fungal laccases. Appl Microbiol Biotech 2002; 59: 672-678
7. Palmieri, G., Cennamo G., Sannia G. Remazol Brilliant Blue R decolourization by the fungus Pleurotus ostreatus and its oxidative enzymatic system. Enz Microb Technol 2005; 36: 17-24
8. Palmieri, G., Giardina, P., Sannia, G. Laccase-Mediated Remazol Brilliant Blue R Decolorization in a Fixed-Bed Bioreactor. Biotechnol Progr 2005; 21: 1436-1441
9. Palmieri,G., Giardina P., Bianco C., Scaloni A., Papasso A., Sannia G. A Novel White Laccase from Pleurotus ostreatus. J Biol Chem 1997; 272: 31301-7
10. Duràn N., Rosa M. A., D'Annibale, A., Gianfreda, L. Application of laccases and tyrosinases (phenoloxidases) immobilized on different supports: a review. Enz Microb Technol 2002; 31:907-931

11. Kandelbauer A., Maute O., Kessler R. W., Erlacher A., Guebitz G. M. Study of dye decolorization in an immobilized laccase enzyme-reactor using online spectroscopy. Biotechnol Bioeng 2004;87: 552-563
12. Peralta-Zamora P., Pereira C. M., Tiburtius E. R. L., Moraes S. G., Rosa M. A., Minussi R. C., Duran N. Decolorization of reactive dyes by immobilized laccase. App Catal B: Environ 2003; 42(2): 131-144
13. Stazi S. R., Vinciguerra V., Giovannozzi Sermanni G. Oxirane-immobilized *Lentinula edodes* laccase: stability and phenolics removal efficiency in olive mill wastewater. J Biotechnol 2000; 77: 265 – 273
14. Dodor, D. E., Hwang H.M., Ekunwe S. I. N. Oxidation of anthracene and benzo[a]pyrene by immobilized laccase from Trametes versicolor. Enz Microb Technol 2004; 35: 210-217
15. Davis S., Burns R.G. Covalent immobilization of laccase on activated carbon for phenolic effluent treatment. Appl Microbiol Biotechnol 1992;37:474–479
16. Hublik G., Schinner F. Characterization and immobilization of the laccase from Pleurotus ostreatus and its use for the continuous elimination of phenolic pollutants. Enz Microb Technol 2000; 27: 330-336
17. Katchalski-Katzir E., Kraemer D. M. Eupergit C, a carrier for immobilization of enzymes of industrial potential. J Mol Catal B Enz 2000; 1-3: 157-176
18. Bradford M.M. A rapid and sensitive method for the quantification of microgram quantities of protein utilizing the principle of protein-dye binding. Analytical Biochemistry 1976; 72: 248–254
19. McCabe W. L., Smith J., Harriott P. Unit Operations of Chemical Engineering, McGraw-Hill, 1985.
20. Geankoplis C. J. Transport Processes and Unit Operations, 3d ed., Prentice Hall, 1993

TABLES

Table 1: Operating conditions of the laccases immobilisation processes.

Solids pre-treatment	None (dry resin), Conditioning in immobilisation buffer
Buffers	0.1 ÷ 1.5 M sodium phosphate
pH	5.5 ÷ 7.5
Incubation time, h	4, 24, 72
Activity loading, IU/g_{DR}	11 ÷ 8800
Protein loading, mg/g_{DR}	0.9 ÷ 35

Table 2: Operating conditions and main results of immobilization tests. Room temperature. Buffer: A 0.1 M sodium phosphate; B 1.5 M sodium phosphate.

# Run	Initial activity IU/g_{DS}	Initial total protein mg/g_{DS}	Support conditioning	Immobilised activity IU/g_{DS}	Recovered activity (liquid phase) IU/g_{DS}	Y* %	Y_{lost}* %	pH	Buffer
1	11	n. a.	Dry	0.5	2	4.8	81	7.5	A
2	28	n. a.	Dry	2.1	6	7.4	79	7.5	A
3	84	2.1	Buffer	6.2	70	7.4	17	6.5	A
4	84	5.2	Buffer	5.2	54	6.2	36	6.5	A
5	96	n. a.	Buffer	6	23	6.3	76	6.5	A
6	124	n. a.	Dry	9	70	7.2	44	7.5	A
7	174	7.2	Buffer	5.4	87	3.1	50	6.5	A
8	187	n. a.	Dry	6.8	63	3.6	66	7.5	A
9	198	0.9	Buffer	5.2	74	2.6	63	6.5	A
10	198	2.3	Buffer	7.6	52	3.8	74	6.5	A
11	198	3.8	Buffer	8.8	92	4.4	54	6.5	A
12	390	n. a.	Dry	16.8	153	4.3	61	7.5	A
13	624	n. a.	Dry	20.4	325	3.3	48	7.5	A
14	864	n. a.	Dry	18.2	262	2.1	70	7.5	A
15	1962	35.4	Buffer	46.8	1214	2.4	38	6.5	A
16	8825	31.6	Buffer	52	4036	0.6	54	6.5	A
17	78	n. a.	Buffer	2.8	n. a.	3.6	39	5.5	A
18	90	n. a.	Buffer	2.8	n. a.	3.1	n. a.	6.5	B
19	210	n. a.	Buffer	13.4	n. a.	6.4	n. a.	6.5	B
20	510	n. a.	Buffer	32.4	n. a.	6.3	n. a.	6.5	B

*defined in eqs. 2-3

Table 3: Assessment of batch vs continuous processes for dye conversion: advantages (+) and drawbacks (-) of either option.

	Option A: batch	Option B: continuous
+	– No immobilisation required – Easiness of reactor operation	– Confinement of the biocatalyst – Enhanced stability of biocatalyst in the immobilised form – Optimization of reactor configuration with respect to biocatalyst kinetic
-	– Separation of biocatalyst required – Re-use of biocatalyst impossible (continuous operations prevented) – Dead time associated with cyclic operation of the batch reactor	– Immobilisation required – Immobilisation yield < 100% – Complexity of design and operation of two phase reactor

CAPTIONS TO FIGURES

Figure 1: Remazol Brilliant Blue R

Figure 2: The experimental test rigs.
A) Test rig for activity assay of immobilised laccases. 1) fixed bed reactor, 2) gear pump, 3) stirred vessel, 4) flow cell – spectrophotometer, 5) data acquisition unit.
B) Continuous fixed bed reactor. 1) fixed bed reactor, 2) pumping unit, 3) feeding vessel, 4) flow cell-spectrophotometer, 5) data acquisition unit, 6) waste water vessel.

Figure 3: Decolourisation of RBBR by crude laccases mixture. **A** residual RBBR. **B** activity of control sample (●, dashed line), activity of decolourisation sample (○, solid line), RBBR conversion rate (▲, dotted line) as percentage of the initial value. Initial activity 12±2 IU/mL, initial dye concentration 77±2 mg/L, room temperature.

Figure 4: Time resolved profile of the RBBR concentration in the reactor effluent. C_{in}=25.5 mg/L (dashed line). Total activity 32 IU. Active packed bed volume 4 mL.

Figure 5: Steady state data related to the RBBR conversion by immobilised laccases in the packed bed reactor. Lines refer to eq. (10), activity loaded per unit volume of packed bed are (▲) 8000 IU/L, (●)10000 IU/L.

Figure 6: Ratio between volume treated by option 'b' (continuous) and option 'a' (batch) (V_b/V_a) as a function of enzyme deactivation coefficient (k). k_{imm}*=$6.2\cdot10^{-4}$ min^{-1}, k_{imm}=$(1.4\pm1.1)\cdot10^{-4}$$min^{-1}$

FIGURES

Figure 1: Remazol Brilliant Blue R

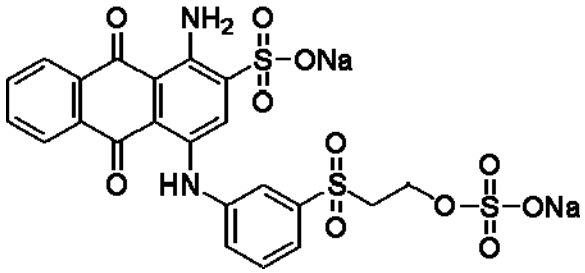

Figure 2: The experimental test rigs.
A) Test rig for activity assay of immobilised laccases. 1) fixed bed reactor, 2) gear pump, 3) stirred vessel, 4) flow cell – spectrophotometer, 5) data acquisition unit.
B) Continuous fixed bed reactor. 1) fixed bed reactor, 2) pumping unit, 3) feeding vessel, 4) flow cell-spectrophotometer, 5) data acquisition unit, 6) waste water vessel.

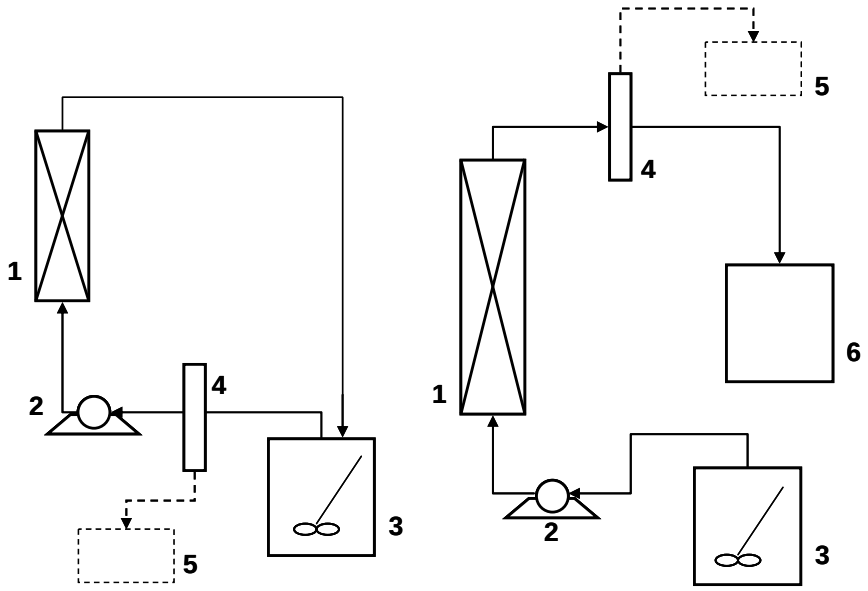

Figure 3: Decolourisation of RBBR by crude laccases mixture. A residual RBBR. B activity of control sample (●, dashed line), activity of decolourisation sample (○, solid line), RBBR conversion rate (▲, dotted line) as percentage of the initial value. Initial activity 12±2 IU/mL, initial dye concentration 77±2 mg/L, room temperature

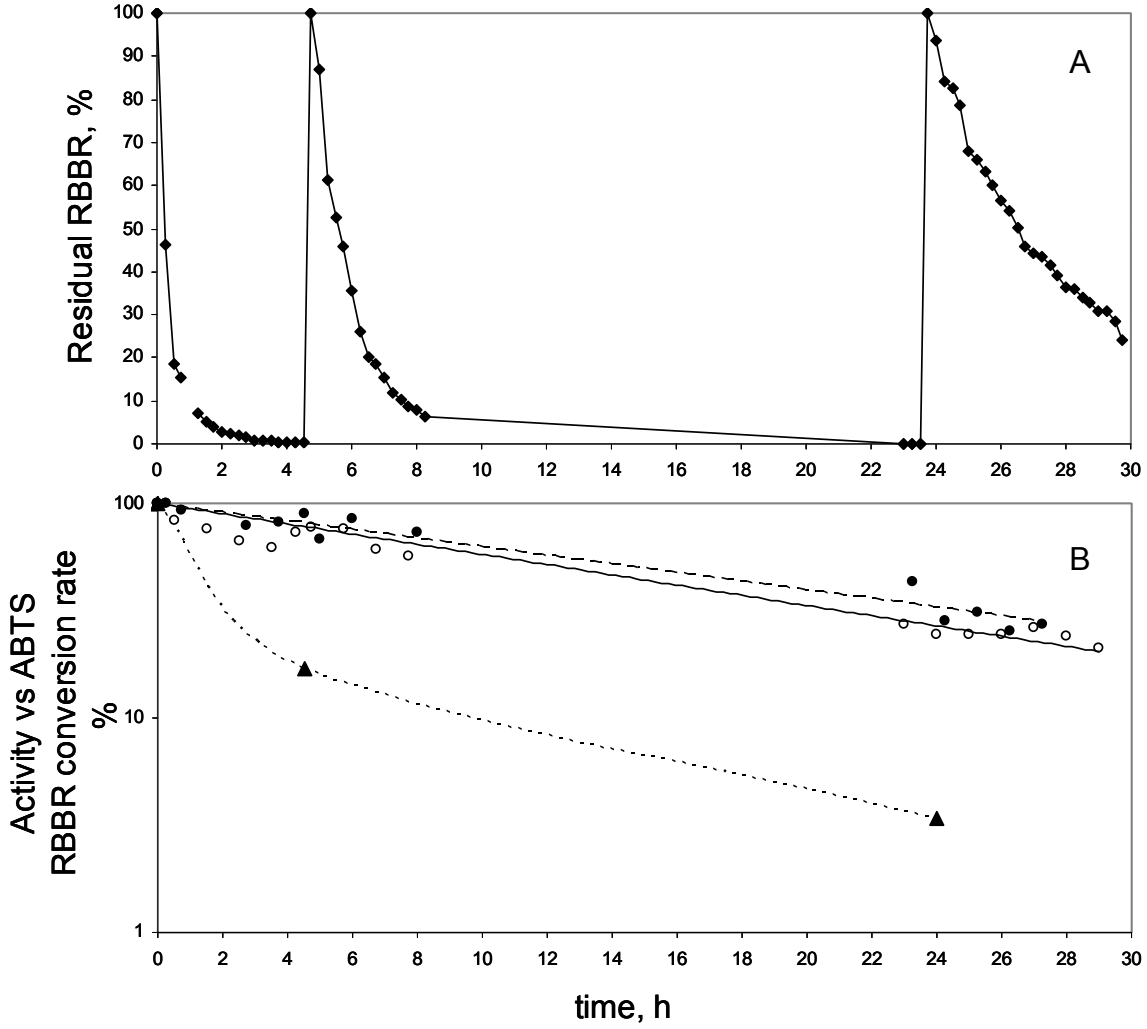

Figure 4: Time resolved profile of the RBBR concentration in the reactor effluent. C_{in}=25.5 mg/L (dashed line). Total activity 32 IU. Active packed bed volume 4 mL.

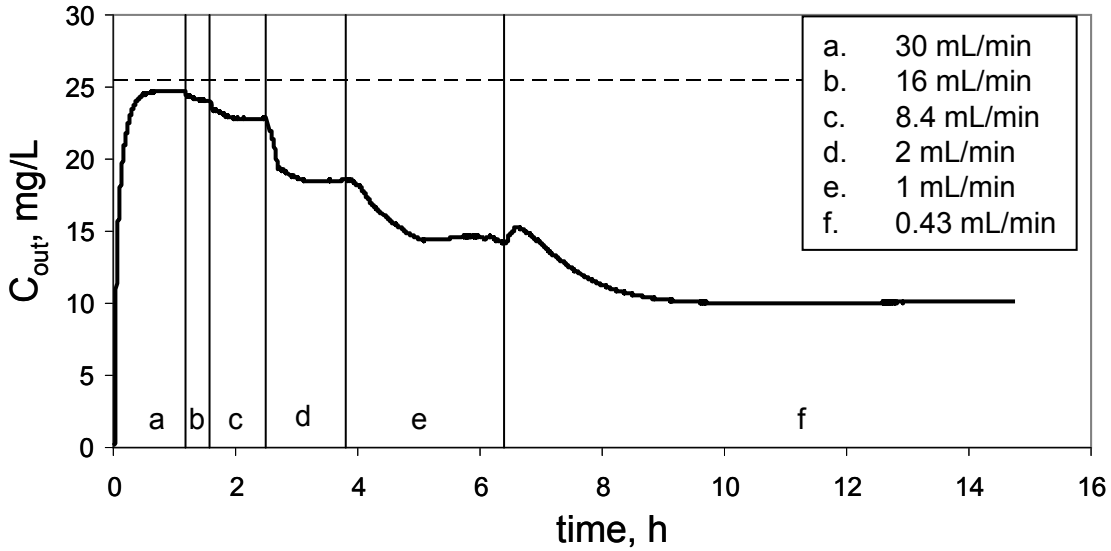

Figure 5: Steady state data related to the RBBR conversion by immobilised laccases in the packed bed reactor. Lines refer to eq. (10), activity loaded per unit volume of packed bed are (▲) 8000 IU/L, (●)10000 IU/L.

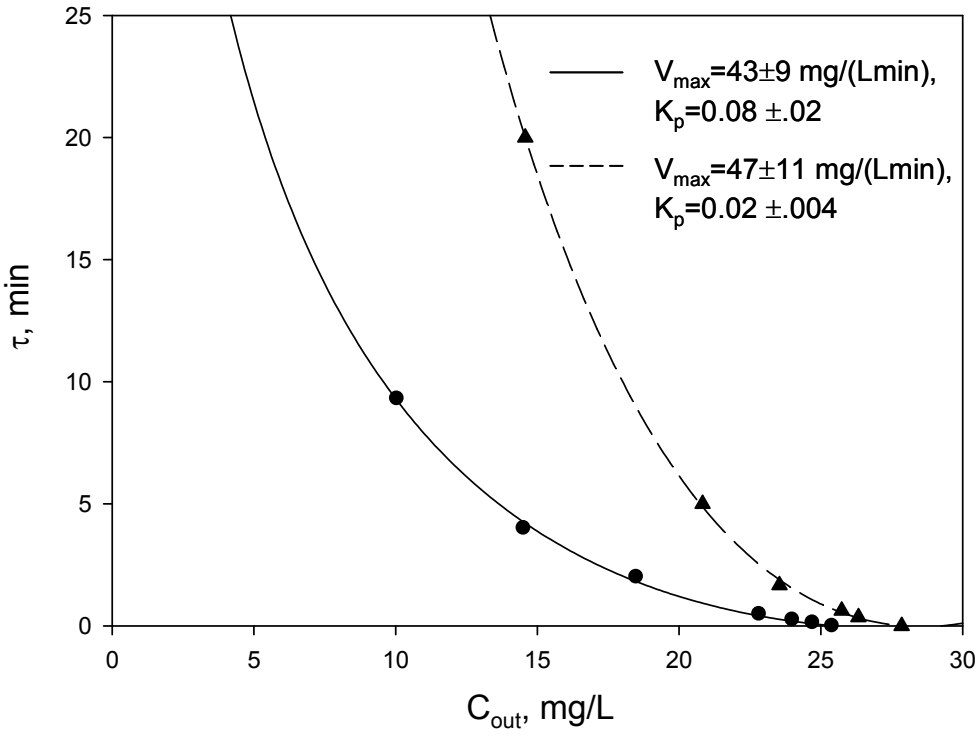

Figure 6: Ratio between volume treated by option 'b' (continuous) and option 'a' (batch) (V_b/V_a) as a function of enzyme deactivation coefficient (k). k_{imm}*=6.2·10^{-4} min^{-1}, k_{imm}=(1.4±1.1)·10^{-4}min^{-1}

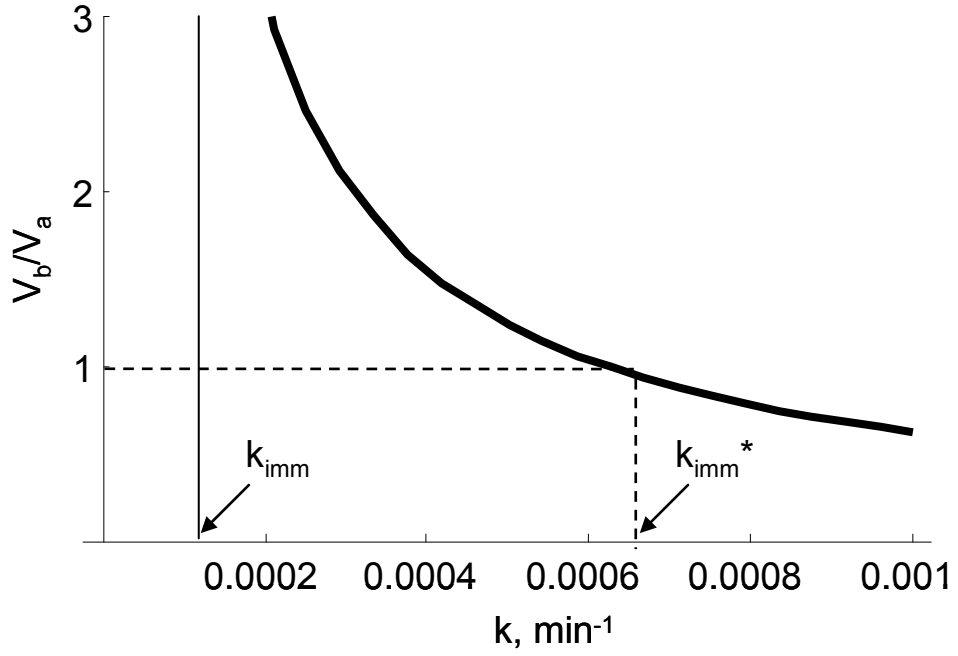

2.2 Selection of enzyme immobilisation technique

The immobilisation of laccases on a solid carrier was undertaken with the goal of achieving a highly intensified continuous enzymatic reactor, i.e. a continuous reactor characterized by a high concentration of enzymatic activity. Arguments reported in section 1 on advantages and drawbacks of enzyme immobilization have been used as guidelines during the selection of the proper immobilization technique.
The selection of the immobilisation technique was carried out taking into account the wide spectrum of characteristics of industrial waste waters containing dyes. Immobilisation techniques based on enzyme adsorption on solid surfaces was excluded because it is strongly affected by activity release during operations, in particular under the fluctuations of properties of the wastewater treated. Covalent immobilisation techniques looked more promising and attractive. Among these, two basic options were identified: techniques based on the use of inert carriers to be activated and techniques based on commercially available pre-activated carriers. The former shows some advantages because immobilization can be directed in such a way so as to involve a prescribed functional group of the enzyme. It should be recalled that a crude mixture of laccases consisting of several isoforms was used for dye conversion [Palmieri et al. 2005 a]. Hence, any immobilisation techniques that enables the control of enzyme site involved in the reaction with the support have been excluded. On the basis of these considerations a pre-activated support was selected, EUPERGIT C 250L©. It is a granular acrylic carrier activated with epoxy groups. This type of functional group allows high stabilization performances due to the occurrence of bonds with different residues of the enzyme [Katchalski-Katzir and Kraemer, 2000]. For the same reason, extensive deactivation can be showed by the enzyme in the immobilised form as a consequence of multipoint-attachment (see section 2.1).

An attempt has been carried out to immobilise laccases on purposely activated inert support. Siliceous supports activated through silanization and subsequent glutaraldheyde covalent bonding was used [Park S. W. et al., 2002; Park D. et al., 2005]. A first characterization was strongly affected by the high adsorption capacity of the silanized carrier, the activity showed by the immobilised laccases after solid phases saturation was halved. Provided that the adsorption capacity is reduced, the biocatalyst will be characterized following the guidelines provided by the results of the present work.

2.3 Remarks on kinetic assessment of immobilised laccases

The paper reported in section 2.1 addresses, among the other topics, on the kinetic assessment of immobilised laccases mixture. This investigation has been driven by the information on kinetics of free laccases mixtures collected in the first part of the work. It has been shown that RBBR conversion catalysed by laccases is affected by inhibition due to products accumulation. Reasonably, the same phenomenon have been assumed to be at work during conversion of RBBR by immobilised laccases. This assumption led to fair regression of experimental data collected during decolourization tests by immobilised laccases.

In this section some qualitative remarks are reported on the effect of kinetics

and mass transfer phenomena on the behaviour of an enzymatic fixed bed reactor. The decolourisation tests by immobilized laccases have been accomplished in a fixed bed reactor operated continuously with respect to the liquid stream containing the dye. Each test was characterized, provided that steady state regimes of the reactor were established, in terms of space-time and the corresponding dye concentration in the outlet stream. Data can be worked out to obtain dye conversion rates observed at any steady state approached during the test. As first attempt, the kinetic analysis can be performed assuming a first order model (eq. 2.1) for the rate of the reaction catalysed by immobilised laccases

$$R_1(C) = K_1 C \tag{2.1}$$

where C is the dye concentration in the liquid phase, R_1 the reaction rate per unit volume of liquid phase and K_1 the first order kinetic coefficient.

Under this hypothesis the steady state mass balance for a plug flow reactor yields:

$$\varepsilon\tau = \frac{1}{K_1}\ln\left(\frac{C_{in}}{C_{out}}\right) \tag{2.2}$$

where τ is the reactor space-time, e the voidage fraction in the fixed bed and C_{in} and C_{out} are the dye concentrations in the inlet and outlet stream respectively. This equation holds if the reactor have been operated under kinetic controlled regime, that is, if limitation by interphase mass transfer phenomena have been ruled out. In this case, working out data (τ, C_{out}) by eq. 2.2, a constant value for K_1 should be obtained for either steady regime. Figure 2.1 reports K_1, calculated for experimental data measured during decolourisation tests as function of liquid space-time. It appears that K_1 decreases with increasing space-times. This behaviour can be due to two phenomena: i) interphase mass transfer phenomenon that provides a decreasing observed rate as space-time (mass transfer rate) is increased (decreased); ii) non linear kinetics governing the enzymatic conversion. First issue has been theoretically assessed as reported in section 2.1, and it has been demonstrated that the decolourisation tests have been accomplished under kinetic controlled regimes. Hence, the effect of non linear kinetics on the behaviour of the reactor at steady state have been further investigated. To this aim, the reaction rate associated to Michaelis-Menten and product inhibited kinetics were compared. Models reported in equations 2.3 and 2.4 were used to describe these kinetics.

$$R_{MM}(C) = \frac{V_{max} C}{K_m + C} \tag{2.3}$$

$$R_{PI}(C) = \frac{V_{max} C}{K_m + C + \left(C_0 - C\right)/K_p} \tag{2.4}$$

where C_0 is the initial concentration of substrate. The effect of product inhibition has been modelled through parameter K_p that depends on the nature of the product. Figure 2.2 reports the plot of equations 2.3-4 assuming the same K_m and V_{max} values for both Michaelis-Menten and product inhibited kinetic and K_p<1. Both Michaelis-

Menten and product inhibited kinetics can be roughly described through first order Taylor polynomial of $R_{MM}(C)$ and $R_{PI}(C)$ at C=0. The plot of the first order polynomial is showed by dashed lines in figure 2.2, slopes of these straight lines is:

$$\left.\frac{dR_{MM}}{dC}\right|_{C=0} = \frac{V_{max}}{K_m} \tag{2.5}$$

$$\left.\frac{dR_{PI}}{dC}\right|_{C=0} = \frac{V_{max}}{K_m + C_0/K_p} \tag{2.6}$$

Right terms of eq. 2.5-6 can be calculated provided that the reaction rate is known at a given substrate concentration. As shown in figure 2.2, the slope of straight lines increases with increasing C referring to product inhibited kinetic while shows the opposite trend for Michaelis-Menten kinetic.

Data points in figure 2.1 have been obtained applying first order kinetic model to the enzymatic conversion of dye in the fixed bed reactor (eq. 2.2). Figure 2.1 shows that K_1 increases with decreasing space-times that is with increasing dye concentration in the effluent stream. Referring to different steady states of the fixed bed reactor, the slope of the straight lines characteristic of the point (C_{out}, $R(C_{out})$) appears to increase with C_{out}. This behaviour reflects the trend described in fig 2.2 for product inhibited kinetic.

The analysis reported can be extended to substrate inhibited kinetics, in this case the effect observed by a first order approximation should lead to the same behaviour observed for Michaelis-Menten kinetic because of the same concavity shown by the curves $R(C)$.

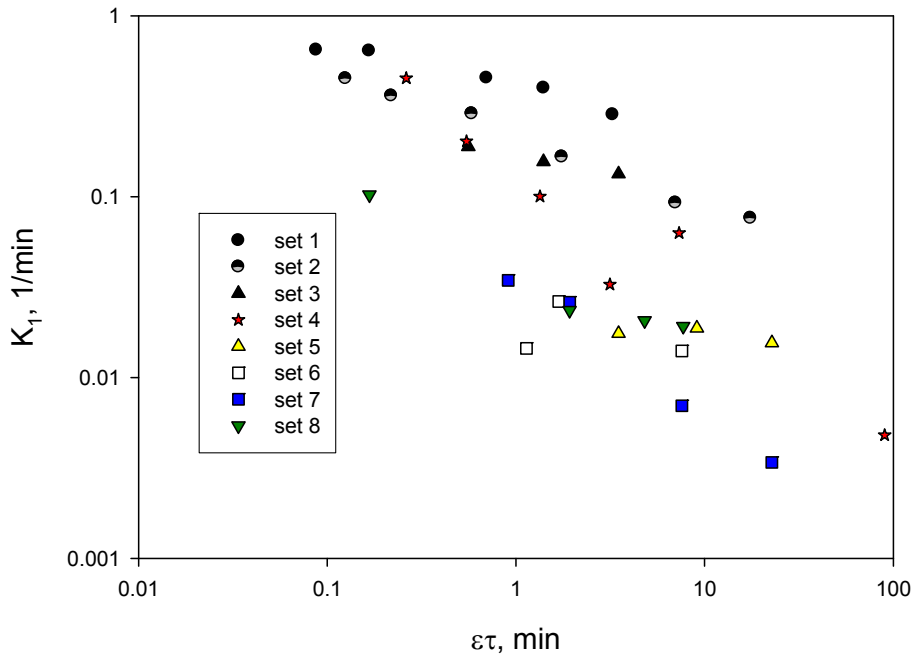

Figure 2.1: First order coefficient K_1 defined in eq. 2.1 assessed for steady regimes of fixed bed reactor during decolourization tests as function of liquid phase space-time $\varepsilon\tau$.

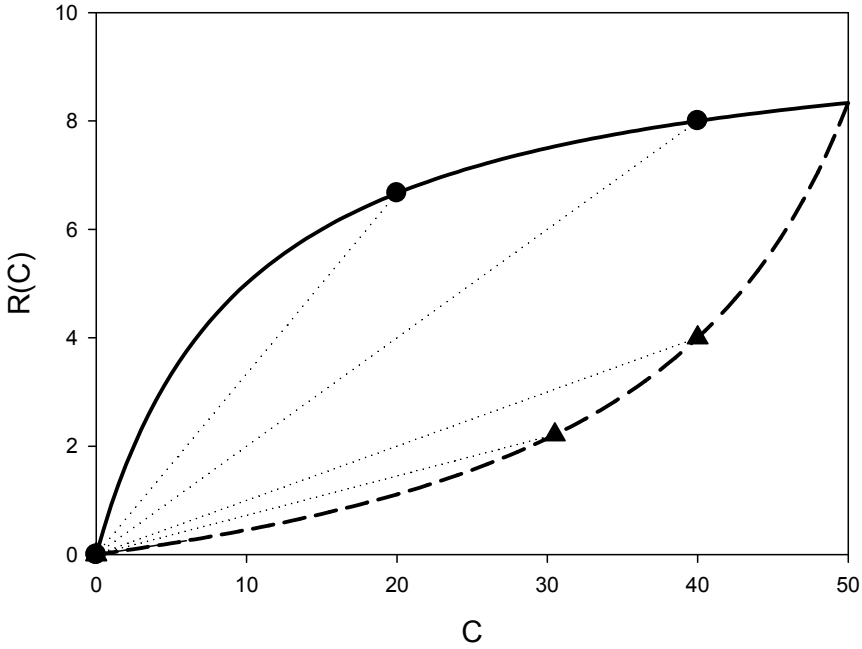

Figure 2.2: Continuous line: plot of eq. 2.3 (Michaelis-Menten), dashed line: plot of eq. 2.7 (product inhibition), straight dotted lines: first order kinetic.

3 BIOFILM REACTOR

This section reports on the experimental and theoretical study that has addressed the performance of a biofilm reactor where a biofilm of *Pseudomonas sp.* OX1 was established on a granular carrier. The first subsection consists of a paper submitted to publication to a scientific journal and concerning the theoretical model of the ILA reactor, the charecterization of the bifurcational and dynamical patterns of the biofilm reactor. The subsection 3.2-3 reports on the experimental study regarding operation of 3PC and ILA reactors.

3.1 Bifurcational and dynamical analysis of a continuous biofilm reactor

BIFURCATIONAL AND DYNAMICAL ANALYSIS
OF A CONTINUOUS BIOFILM REACTOR

M. E. Russo, P. L. Maffettone, A. Marzocchella, P. Salatino

Dipartimento di Ingegneria Chimica
Università degli Studi di Napoli Federico II
P.le V. Tecchio, 80 – 80125 Napoli, Italy

1. ABSTRACT

A dynamical model of a continuous biofilm reactor is presented. The reactor consists of a three-phase internal loop airlift operated continuously with respect to the liquid and gaseous phases, and batchwise with respect to the immobilized cells. The model has been applied to the conversion of phenol by means of immobilized cells of *Pseudomonas sp.* OX1 whose metabolic activity was previously characterized (Alfieri 2006; Viggiani et al. 2006). The model embodies the key processes relevant to the reactor performance, with a particular emphasis on the role of biofilm detachment due to combined shear, friction and interfacial phenomena promoted by the fluidized state. Results indicate that a finite loading of free cells establishes even under operating conditions that would promote wash-out of the suspended biophase. The co-operative/competitive effects of free cells and immobilized biofilm result in rich bifurcational patterns of the steady state solutions of the governing equations, which have been investigated in the phase plane of the process parameters (dilution rate and detachment coefficient). Direct simulation under selected operating conditions confirms the

importance of the dynamical equilibrium establishing between the immobilized and the suspended biophase and highlight the effect of the initial value of the biofilm loading on the dynamical pattern.

Keywords: Bifurcation, biofilm, detachment rate, dynamics

2. INTRODUCTION

The study of microbial cell aggregates has long been stimulated by issues related to the formation of biofilm in medical devices, prevention and control of infection diseases and bio-fouling in process plants. More recently, the potential of microbial aggregates as an effective route to enhanced productivity in bioprocesses has triggered additional research effort.

The natural response of microbial cells to harsh environments is the development of three-dimensional structures. Secretion of polysaccharide matrices further contributes to generate a less aggressive environment around cell colonies, compared to that experienced by freely suspended cells. Both for bacteria and fungi, growth of microbial cell aggregates occurs either as surface-adhering layers or as unsupported flocs, depending on the nature of the microrganism and on the process conditions. Formation of aggregates makes it possible to obtain cultures characterized by cell densities (biomass per unit volume) much larger than those commonly harvested in liquid broths (Nicolella et al. 2000; Qureshi 2005). The possibility of achieving large cell densities is an attractive feature which can be exploited in a number of applications of fermentation to improve process intensification. Currently, immobilization of cells and membrane reactor technology are the two common pathways to achieve high-density confined cell cultures in either discontinuous or flow reactors. Immobilization of cells by adhesion on natural, typically inexpensive, supports is the first step for the production of biofilm. Proper choice of granular supports, together with careful selection of the microbial strain, are the keys to the successful design of multi-phase biofilm reactors. Among the most common reactor configurations we list: Continuous Stirred Tank Reactors (CSTRs), Packed Bed Reactors (PBRs), Fluidized Bed Reactors (FBRs), Airlift Reactors (ALRs). For selected processes and bacterial strains, multiphase biofilm reactors have demonstrated superior reliability and availability of operation – weeks to months of continuous operation - at large biophase loadings (up to 74 g/L), even at the

industrial scale (Nicolella et al. 2000; Qureshi 2005). Biofilm reactors based on single species biofilms are generally employed to control the formation of the product along with the maximization of the productivity in the production of chemicals (Nicolella et al. 2000; Branyik et al. 2004; Qureshi 2005). On the other hand, production of biofilms from multi-species consortia is far more extensive than formation from a single strain, and is one key to successful application of immobilized cell reactors to bioremediation of waste water and waste gas.

The establishment of solid-supported biomass loading in continuous biofilm reactors results from the competition between cells adhesion/growth on the granular carrier and detachment of biofilm fragments from the granules. These phenomena have been the subject of extensive investigation with the aim of identifying the controlling parameters (Gjaltema et al. 1997; Horn et al. 2003; Branyik et al. 2004). The build-up of the biofilm results from the simultaneous progress of the following processes: i) cells adhesion on the carrier surface, an event that is strongly influenced by the nature of the interactions between the cell wall and the carrier surface; ii) adhered biomass growth and simultaneous production of extracellular matrix; iii) detachment of biomass fragments and/or individual cells from the growing biofilm. This last step, i.e. biofilm detachment, is related, in turn, to the following mechanisms: i) shear-induced 'erosion', resulting in continuous loss of cells, either isolated or in small aggregates, from the carrier surface; ii) removal of large patches of biofilm, a random process which is usually referred to as "sloughing"; iii) "abrasion" of biofilm associated with particle-to-particle friction and/or collisions (Nicolella et al. 1997). Experimental studies referred to multiphase reactors highlighted the key role of the detachment kinetic (Gjaltema et al. 1997 a,b, Branyik et al. 2004) as a consequence of erosion and abrasion. Moreover and regardless of the reactor configuration, the development of the biofilm turns out to be strongly influenced by the dilution rate, because of the competition between immobilized and free cells. Only thin biofilms can be grown with hydraulic residence times larger than the time-scale of substrate consumption (Tang and Fan 1987; Tijhuis et al. 1994) due to the continuous subtraction of the substrate by suspended cells. Operating conditions corresponding to wash-out of the free cells enhance biofilm growth by reducing the chance that immobilized cells are exposed to substrate-starving conditions and by improving the competition between the rates of biofilm production and detachment.

A mathematical model of a multiphase continuous biofilm reactor is hereby presented, aimed at characterizing the basic bifurcational patterns and dynamical behavior of the system. Though a few studies have been published on the bifurcational/dynamical behavior of chemostats (Pavlou 1999; Zhang and Henson 2001; Pinheiro et al. 2004), none has specifically addressed the complex interaction between free and immobilized biophases in biofilm reactors, which is the focus of the present study. The proposed model embodies the key features of the phenomenology of the granular-supported biofilm: adhesion of cells onto the carrier surface, growth of attached cells, biofilm detachment. Adhesion and detachment rates are modeled as linear functions of the suspended cells and biofilm volumetric concentrations, respectively (Rijnaarts et al. 1995; Gjaltema et al. 1997 a,b; Branyik et al. 2004; Telgmann et al. 2004). The kinetic of cell growth is assumed to be substrate-inhibited (Alfieri 2006; Viggiani et al. 2006).

3. THEORY

3.1 General description of the model.

A mathematical model was developed to analyse the dynamic and bifurcational behaviour of a continuous multiphase biofilm reactor. The model was specifically applied to the growth of *Pseudomonas sp.* OX1 on phenol. The growth kinetics was characterized by (Viggiani et al. 2006) and expressed by a Haldane-Andrews model (substrate inhibition). It has been shown (Viggiani et al., 2006; Alfieri 2006) that *P. sp.* OX1 effectively grows on granular materials of different nature (silica sand, pumice stone...).

The reactor flow pattern assumed in the model was that of an internal loop airlift with pneumatic mixing of both the liquid and the solids phases (Chisti 1989), the last consisting in biofilm particles supported by granular solids. The phenol-bearing liquid stream was fed continuously to the reactor at pre-fixed volumetric flow rate (Q) and phenol concentration (S_{in}).

Model assumptions

The model relies on the following assumptions:

1) the reactor was assumed well-mixed with respect to liquid, gas and solids phases as a consequence of the typical flow pattern established in airlift reactors (Chisti 1989);

2) phenol was the rate-limiting substrate for both free and immobilized cells. Aeration of the medium in the airlift reactor was large enough to make oxygen not a limiting substrate. Metabolism of nitrogen was not considered in the model.

3) both free and immobilized cells were characterized by substrate-inhibited growth kinetics. The kinetics of biofilm cells growth was assumed equal to that measured for planktonic cells. The biomass yields of planktonic cells (Z_x) and of biofilm cells (Z_y) were both set equal to 0.7 $g_{DM}/g_{substrate}$ (Alfieri 2006; Viggiani et al. 2006);

4) adhesion of suspended cells onto the carrier surface was modelled as a first order kinetics with respect to the cells concentration in the liquid phase. The adhesion coefficient (K_a) was estimated from studies available in literature (Rijnaarts et al. 1993, 1995) as described in the next section.

5) the biofilm detachment rate (r_d) was modelled as a first order kinetics with respect to the biofilm volumetric concentration (Y). The analysis was carried out by looking at the detachment coefficient (K_d) as a bifurcational parameter;

6) the biofilm detached fragments were assumed to be composed of free cells, in agreement with assumption 3);

7) resistance to mass transfer in the boundary layer around single cells and biofilm pellets was neglected when compared with intrinsic reaction kinetics;

8) the solid carrier was impervious and, accordingly, biofilm attachment could only take place at the external surface of the carrier particles. The diffusional resistance to substrate mass transfer across the biofilm was neglected when compared with intrinsic reaction kinetics. The validity of this hypothesis was checked by an order-of-magnitude assessment of substrate mass transfer rate across the biofilm. The assessment was referred to biofilm loadings of 10g/L and smaller with a biofilm apparent density of ≅1000 kg/m^3. The solid carrier consists of particles of about 250 μm size dispersed at a volumetric concentration of about 3% v/v in the liquid phase. With these figures, the biofilm thickness turns out to be of the order of 10μm or less, thin enough to ensure even distribution of the substrate across the biofilm.

Model equations

Mass balance equations on the substrate, the biofilm and the free cells extended to the volume of the liquid phase (V_l) are reported in Table I together with the relevant constitutive equations. The meaning of the symbols is reported in the Nomenclature section.

Modelling of adhesion was based on studies due to Rijnaarts and co-workers (Rijnaarts et al. 1993, 1995) and (Chen and Strevett 2001, 2003). Rijnaarts et al. (1995) indicated that, for different *Pseudomonas* strains interacting with either hydrophobic or hydrophilic surfaces, the adhesion flux can be taken equal to the diffusional flux of cells (under stagnant conditions) toward the carrier surface, neglecting activation energy barriers. Accordingly, the rate of cells adhesion (r_a) can be assumed equal to the rate of cells transfer (r_c):

$$r_a = r_c = K_c \frac{6}{d} \frac{V_s}{V_l} X \qquad (1)$$

where K_c is the mass transfer coefficient between the bulk of the liquid phase and the carrier particle and X is the volumetric concentration of suspended cells. K_c can be calculated as

$$K_c = \frac{ShD_c}{d} \qquad (2)$$

where Sh is the Sherwood number (Knudsen et al. 1999) and D_c is the diffusivity of cells in the liquid phase. From eq. 1, an adhesion rate constant K_a of a first-order kinetics can be defined as

$$K_a = K_c \frac{6}{d} \frac{V_s}{V_l} \qquad (3)$$

The biofilm detachment rate is assumed first order with respect to Y, a functional form typical of bioprocessing in ALRs and FBRs (Gjaltema et al. 1997 a, b; Branyik et al. 2004; Telgmann et al. 2004). The detachment rate constant K_d embodies the effect of all relevant detachment processes (abrasion, erosion, sloughing).

Equations T.I.1-T.I.3 (Table I) are a set of ODEs whose initial conditions are reported in Table I. Equation T.I.5 describes the substrate inhibited model $\mu(S)$ for phenol specific consumption rate, providing a maximum rate of about 0.17 h^{-1} at S=0.2 g/L. Equations and initial conditions can be re-written in dimensionless form by introducing the following variables:

$$s = S/S_{in} \qquad x = X/(S_{in} \cdot Z_x) \qquad y = Y/(S_{in} \cdot Z_y) \qquad \tau = t \cdot \mu_{max}$$

$k_i = K_i/S_{in}$ $\quad k_m = K_m/S_{in}$

$Da = \mu_{max}/D$ $\quad A = K_a/\mu_{max}$ $\quad G = K_d/\mu_{max}$ (4)

Table II reports the material balance equations and the initial conditions in terms of dimensionless variables.

The range of each dimensionless variable/parameter is as follows:

- The dimensionless variables s and x varies in the interval [0, 1].
- The dimensionless biofilm concentration y varies between 0 and a maximum value which depends on the mass fraction of the granular solids loaded to the reactor (Olivieri et al. 2003) and on the largest biofilm mass fraction establishing on granular solids (Alfieri 2006).
- The Damköhler number is positive and unbounded. For the specific growth kinetics of the present study, the value of Da corresponding to wash-out of free cells (D=0.17 h^{-1}) in a chemostat would be 4.1.
- The inlet phenol concentration is set at values smaller than 0.6 g/L: at larger values complete growth inhibition occurs (Viggiani et al. 2006)

For steady state conditions the set of ordinary differential equations T.II.1 through T.II.3 reduces to a set of nonlinear algebraic equations:

$$0 = \frac{1}{Da}\cdot(1-s_{ss}) + \frac{s_{ss}}{k_m + s_{ss} + s_{ss}^2/k_i}\cdot x_{ss} + -\frac{s_{ss}}{k_m + s_{ss} + s_{ss}^2/k_i}\cdot y_{ss}$$

$$0 = -\frac{1}{Da}\cdot x_{ss} + \frac{s_{ss}}{k_m + s_{ss} + s_{ss}^2/k_i}\cdot x_{ss} + G\cdot y_{ss} - A\cdot x_{ss} \qquad (5)$$

$$0 = \frac{s_{ss}}{k_m + s_{ss} + s_{ss}^2/k_i}\cdot y_{ss} - G\cdot y_{ss} + A\cdot x_{ss}$$

in the unknowns s_{ss}, y_{ss} and x_{ss}.

3.2 Computational methods

Model computations were directed to the following goals: i) identification of steady state solutions and bifurcational analysis; ii) characterization of the dynamic behaviour of the system.

Computations were performed using a continuation algorithm provided by the toolbox MATCONT associated with Matlab®. Analysis of the stability of steady solutions was carried out by evaluating the eigenvalues of the Jacobian matrix associated with the linearized form of system in eq. 5 (Hale and Koçak 1991).

4. RESULTS AND DISCUSSION

4.1 Analysis of steady-state solutions

Adhesion rate of suspended cells onto carrier surface was calculated from equations 1-3 assuming d= 250 μm and $V_s/V_l = 0.03$. Typical figures for cells diffusivity (D_c) of *Pseudomonas* strains are reported by Rijnaarts et al. (1993) to be about $4 \cdot 10^{-13}$ m^2. The Sherwood number (Sh) was taken equal to 2 (Knudsen et al. 1999). With these values:

$$K_{ad} = 0.008\ h^{-1} \qquad (6)$$

Corresponding to a dimensionless adhesion rate A=0.011.

Figure 1 reports results of computations referred to steady solutions for the dimensionless variables s_{ss}, x_{ss} and y_{ss} as the value of the dimensionless detachment coefficient G is varied. Since biofilm growth is strongly favoured by operation under conditions that promote wash-out of the suspended cells (Tang and Fan 1987; Tijhuis et al. 1994), the results for base case computations reported in figure 1 were obtained for Da=3, corresponding to a dilution rate larger than 0.17 h^{-1}. The substrate concentration in the feeding, S_{in}, was fixed at 0.6 g/L. Figure 1 shows that a multiplicity of steady states occurs, and the number of solutions is reported in the figure as roman numerals. A critical value for the parameter G limits the field of existence of non-trivial solutions, that is ($s_{ss}<1$, $x_{ss}>0$, $y_{ss}>0$,). For small values of G two solutions are physically consistent (II), namely the triplet ($s_{ss}=1$, $x_{ss}= y_{ss} =0$) and the high conversion solution (continuous line). As G is increased, a transcritical bifurcation marks the appearance of a third steady solution. This behaviour is observed for values of G falling between the transcritical bifurcation and the upper limit (III). For even higher values of G only the trivial solution is found (I).

The stability analysis of the steady states indicates that: i) high conversion solutions are stable (stable nodes, solid line) within their field of existence (II, III); ii) low conversion solutions, found for

G higher than that corresponding to the transcritical bifurcation (region III), are unstable (saddle-nodes, dashed line) and iii) the trivial solution is unstable for small values of G (II) and changes into a stable solution beyond the transcritical bifurcation (III, I).

It is worth noting that the stable high conversion solution shows a non-zero concentration of free cells (x_{ss}), despite the base case investigated refers to a dilution rate larger than the maximum $\mu(S)$. This result reflects the fact that continuous renewal of free cells in the medium supplemented by biofilm detachment, either as isolated cells or as aggregates effectively contrasts wash out of suspended cells. As a consequence, the competition for substrate between immobilized and free cells cannot be entirely ruled out by the choice of operating at large dilution rates. This feature affects the performance of the bioreactor along two paths. On one hand, the persistent establishment of a freely suspended biophase even under wash out conditions provides additional biological activity for the bioprocess to occur. On the other hand, the very same occurrence of a persistent free cell loading may hinder the build up of the immobilized biophase due to competition for the common substrate.

Direct experimental support to the observation that free cells are generated by detachment of the biofilm is provided by (Gjaltema et al. 1997 a). These authors periodically sampled free cells from the liquid phase of a bench scale airlift reactor operated under wash out conditions with *Pseudomonas putida* biofilm. Once plated, cell colonies displayed phenotype characteristic of the immobilized cells. In particular, a much enhanced polymer production was recorded.

The effect of the detachment coefficient G is clearly highlighted by operating diagrams in figure 1. For a given adhesion rate, the build up of a certain amount of biofilm approaching a constant value at the steady state is due to the equilibrium between growth of attached cells and detachment. Multiplicity of steady states clearly mirrors substrate-inhibition affecting the growth kinetics.

The analysis of the operating diagram for biofilm concentration y_{ss} deserves further comment. Within the interval of three steady solution, the stable steady state ($y_{ss}>0$) is approached only if the initial value of biofilm concentration is sufficiently large. In other words, in this range of detachment rate constant, the start-up of the biofilm reactor can not be achieved with sterile carriers, but a sufficiently large biofilm inoculum has to be supplied at the beginning, depending on the specific detachment rate. This feature will be further addressed in section 4.3.

4.2 Bifurcational analysis

In this section the effect of Da and S_{in} on the bifurcational patterns is analyzed. Figure 2 reports the operating diagrams relative to the steady-state values of the dimensionless variables s, x, and y as a function of G taking Da as a parameter. Solid lines indicate stable steady states (nodes) and dashed lines unstable (saddle-type) steady states.

All Da values considered correspond to dilution rates larger than the maximum value of the specific rate $\mu(S)$ ($D>0.17\ h^{-1}$). Observing the solution diagram in the plane (y_{ss}, G), it appears that increasing Da up to 4 (i.e. decreasing the dilution rate until it approaches the wash-out limit $0.17\ h^{-1}$) the non-trivial stable solution shows a lower biofilm concentration. Furthermore, an increase of the upper limit value of G is observed. It can be concluded that a smaller dilution rate makes it possible to stabilize a steady state as the detachment rate is increased. A correspondingly smaller biofilm loading will be established in this case.

Figure 3 reports solution diagrams y_{ss} vs G for different substrate inlet concentration S_{in}. Decreasing S_{in} from 0.5 to 0.1 g/L a smaller steady biofilm concentration can be reached for any given G. For $0.6<S_{in}<0.2$ the bifurcational pattern described in section 3.1 remains unchanged (see figure 2). If S_{in} is set at the value 0.2 g/L only two solutions appear, for any detachment coefficient. The transcritical bifurcation occurs at the maximum G. Only two steady state solutions are found also for $S_{in}<0.2$ g/L. This behaviour is related to the non linearity of the dependence of growth kinetics on 's'. It has to be recalled that 0.2 g/L is the substrate concentration corresponding to the maximum of $\mu(S)$. If the reactor is fed with a liquid stream containing $S_{in}\leq 0.2$ g/L, because $S<S_{in}$, only one value of $\mu(S)$ would be acceptable and multiplicity of non-trivial solutions would be prevented.

It is well known that continuous chemostats provide optimal solution for maximization of the productivity of substrate-inhibited cell growth processes (Villadsen 1999), as large throughputs can be ensured also when inlet substrate concentration approaches the inhibition limit. This model here proposed suggest that the same conclusion can be drawn for the attached cells, as well.

Figure 4 reports the operating diagrams of the reactor in the parameter plane ($S_{in,}$ G) for Da=2 and Da=4. Both diagrams show a horizontal line that represents the upper limiting value for G above

which only the trivial solution satisfies eq.5. The curves represent loci of point of the transcritical bifurcations. Regions of the plane limited by these curves are characterized by different number of steady solutions (roman numerals). Increasing Da the upper limit of G increases and the curve of transcritical bifurcation modifies accordingly. The effect of substrate inhibition is reflected also by this diagram as a consequence of the balance between adhesion/growth and detachment of the biofilm. Therefore, the value of G which marks the condition of transcritical bifurcation is a function of S_{in}, showing a non-monotonic trend similar to that of $\mu(S)$.

4.3 Analysis of the reactor dynamics

Model computations have been directed to the characterization of the transient response of the bioreactor to unsteady forcing. Figure 5 reports results of transient simulations of the bioreactor in terms of the dimensionless variables s, x and y vs dimensionless time τ. It must be noted that, consistently with the choice of unstructured microbial growth kinetics, the predicted transient effects are only those associated with the reactor dynamics and they are not due the dynamics of microbial metabolism in response to a change of the environment.

A typical start-up operation of the biofilm reactor was first simulated. To this end, values of Da and S_{in} have been fixed at, respectively, 3 and 0.6g/L. Two values of G have been considered for these computations, corresponding to different bifurcational features in the maps in figure 1: the first (G=0.14) falls in region II; the second (G=0.23) falls between the transcritical bifurcation and the maximum value of G (region III). The initial conditions set for G=0.14 reproduce start-up of the reactor as s_0=1, x_0=0.05, y_0=0.1, that is substrate concentration equal to that in the feeding stream and small inoculum of both free and immobilized cells. Simulation shows that the stable steady state is approached as foreseen by the operating diagrams (figure 1). By increasing G up to 0.23 and for the same initial conditions, the dynamic simulation shows that the dynamical system approaches the stable trivial solution, as reported by the dashed lines. The non trivial solution corresponding to G=0.23, which provides a stable amount of biofilm, can be reached only increasing y_0 up to 0.2. Solid lines report the time evolution of s, x and y in this latter case.

5. CONCLUSIONS

A dynamical model has been set up to analyze the transient behaviour of a three-phase biofilm reactor that belongs to the internal loop airlift typology. A specific feature of the model is represented by the close focus on biofilm detachment phenomena and their relevance to the establishment of a dynamic equilibrium between free and immobilized biophases. Substrate-inhibited bioconversion of phenol by *Pseudomonas sp.* OX1 has been considered. A linear dependence of biofilm detachment rate on biofilm loading was assumed. Adhesion of suspended cells on the surface of the carrier has been modelled using a first-order kinetics with respect to free cells concentration, consistently with findings reported in the literature on adhesion of *Pseudomonas* cells. The bifurcational patterns turned out to be negligibly affected by changes of the adhesion coefficient within its confidence interval (0.008 ± 0.002 h^{-1}).

Bifurcational analysis of the steady state solutions indicates that the only the trivial solutions are predicted for values of the detachment constant that exceed a given threshold. Below this value multiple stable steady states can be established and the bifurcational patterns depend on the value of the reactor Damköhler number and feed substrate concentration. An important feature of the steady operation of the reactor at small values of Da is that, even when wash-out is promoted by large volumetric feed rates, a freely suspended biophase is always present as free cells are continuously renewed by detachment of immobilized biophase. On one hand, the persistence of a freely suspended biophase even under wash-out conditions enhances the productivity of the bioreactor. On the other hand, this feature implies that competition of free and immobilized cells for the common substrate cannot be ruled out simply by operating at low Da. This, in turn, might negatively affect the development of the stable and extensive biofilm loading that would be required for highly intensified operation of the bioreactor. These two features have to be carefully balanced by proper selection of operating conditions, and more specifically by tuning the biofilm detachment rate.

Dynamical simulations of the transient behaviour of the bioreactor confirm the basic features of the steady operation. The dynamical evolution of the freely suspended and of the immobilized biophases are linked to each other by the process of biofilm detachment. Results of simulations

performed at different sets of model parameters indicate that the dynamical patterns are dominated by the initial value of the biofilm loading.

ACKNOWLEDGEMENTS

The support of Mr. Domenico Saldalamacchia e Mr. Luca Bifulco is gratefully acknowledged. Financial support from both Centro Regionale di Competenza in Biotecnologie Industriali Bioteknet and MIUR Programmi di Ricerca Scientifica di Rilevante Interesse Nazionale is also acknowledged.

NOMENCLATURE

A	dimensionless adhesion coefficient	-
d	particle diameter	μm
D=Q/V	dilution rate	1/h
Da	Damköhler number	-
D_c	diffusivity of suspended cells	m^2/s
G	dimensionless biofilm detachment coefficient	-
K_a	adhesion coefficient	1/s, 1/h
K_c	adhesion coefficient	m/s
K_d	biofilm detachment coefficient	1/h
k_i, k_m	dimensionless growth kinetic parameters	-
K_i, K_m	parameters of cells growth kinetics	g/L
Q	liquid volumetric flow rate	L/h
r_a	suspended cells adhesion rate	$kg/(m^3s)$, g/(Lh)
r_c	suspended cells transfer rate	$kg/(m^3s)$
r_d	biofilm detachment rate	g/(Lh)
s	dimensionless substrate concentration	-
S	substrate concentration	g/L
S_{in}	substrate feeding concentration	g/L
Sh	Sherwood number	-
t	time	h
V_s	solid phase volume	L
V_l	liquid phase volume	L
x	dimensionless suspended cells concentration	-

X	suspended cells concentration	g/L, kg/m^3
y	dimensionless biofilm concentration	-
Y	biofilm concentration	g/L
$Z_x=Z_y= Z$	biomass yield	g/g
V	reaction volume	L

Symbols

μ	specific growth rate	1/h
μ_{max}	growth kinetic parameter	1/h
τ	dimensionless time	-
ω	dimensionless specific growth rate	-

Subscripts

0	initial value
ss	steady state

REFERENCES

Alfieri, F. (2006). Bioconversione di composti aromatici mediante microrganismi liberi o immobilizzati [Ph.D.]. Napoli: Università di Napoli 'Federico II'.

Branyik, T., Vincente, A.A., kuncova, G., Podrazky, O., Dostalek, P., Teixeira J.A. (2004). Growth Model and Matebolic Activity of Brewing Yeast Biofilm on the Surface of Spent Grains: A Biocatalystfor Continuous Beer Fermentation. Biotechnol Prog 20, 1733-1740.

Chen, G. and Strevett, K.A. (2001). Impact of surface thermodynamic on bacterial transport. Environ Microbiol 3(4), 237-245.

Chisti, M.Y. (1989). Airlift Bioreactors. Elsevier.

Gjaltema, A., van der Marel, N., van Loosdrecht, M.C.M. and Heijnen, J.J. (1997). Adhesion and biofilm development on suspended carriers in airlift reactors: hydrodinamic conditions versus surface characteristics. Biotech and Bioeng 55(6),880-889.

Gjaltema, A., Vinke, J.L., van Loosdrecht M.C.M. and Heijnen, J.J. (1997). Biofilm abrasion by particle collisions in airlift reactors. Water Sci Tech 36, 221-228.

Hale, J.K. and Koçak, H. (1991). Dynamics and bifurcations. Springer Verlag.

Horn, H., Reiff, H. and Morgenroth, E. (2003). Simulation of Growth and Detachment in Biofilm Systems Under Defined Hydrodynamic Conditions. Biotec Bioeng 81(5), 608-617.

Knudsen, J.G., Hottel, H.C., Sarofim, A.F., Wankat, P.C. and Knaebel, K.S. (1999). Heat and Mass Transfer. In: Perry R.H., Green D.W., Maloney J.O., editors. Perry's Chemical Enginners' Handbook. 7th ed: McGraw Hill.

Nicolella, C., Chiarle, S., Di Felice, R. and Rovatti, M. (1997). Mechanisms of biofilm detachment in fluidized bed reactors. Water Sci Tech 36, 229-235.

Nicolella, C., van Loosdrecht, M.C.M. and Heijnen, J.J. (2000). Wastewater treatment with particulate biofilm reactors. J Biotech 80, 1 - 33.

Olivieri, G., Marzocchella, A. and Salatino, P. (2003). Hydrodinamics and mass transfer in lab-scale three-phase internal loop airlift. Chem Eng J 96, 45-54.

Pavlou, S. (1999). Computing operating diagrams of bioreactors. J Biotech 71, 7-16.

Pinheiro, I.O., De Souza Jr, M.B. and Lopes, C.E. (2004). The dynamic behaviour of aerated continuous flow stirred tank bioreactor. Mat Comp Mod 31, 541-566.

Qureshi, N., Annous, B.A., Ezeji, T.C., Karcher, P. and Maddox, I.S. (2005). Biofilm reactors for industrial bioconversion processes: employing potential of enhanced reaction rates. Microb Cell Fact 4(24).

Rijnaarts, H.H.M., Norde, W., Bouwer, E.J., Lyklema, J. and Zehnder, A.J.B. (1995). Reversibility and mechanism of bacterial adhesion. Coll Surf B 4, 5-22.

Rijnaarts, H.H.M., Norde, W., Bouwer, E. J., Lyklema, J. and Zehnder, A. J. B. (1993). Bacterial Adhesion under Static and Dynamic Conditions. Appl Environ Microbiol 59, 3255-65.

Strevett, K.A. and Chen, G. (2003). Microbial surface thermodynamics and applications. Res Microbiol 154, 329-335.

Tang, W.T. and Fan, L.S. (1987). Steady state phenol degradation in a draft-tube, gas-iquid-solid fluidized-bed bioreactor. AIChe J 33(2), 239-249.

Telgmann, U., Horn, H. and Morgenroth, E. (2004). Influence of growth history on sloughing and erosion from biofilms. Water Res 38, 3671-3684.

Tijhuis, L., van Loosdrecht, M.C.M. and Heijnen, J.J. (1994). Formation and growth of heterotrophic aerobic biofilms on small suspended particles in airlift reactors. Biotech Bioeng 28, 595-608.

Viggiani, A., Olivieri, G., Siani, L., Di Donato, A., Marzocchella, A., Salatino, P., Barbieri, P. and Galli, E. (2006). An airlift biofilm reactor for the biodegradation of phenol by *Pseudomonas stutzeri* OX1. J Biotech 123, 464-477.

Villadsen, J. (1999). On the Optimal Design and Control of a Biodegradation Process with Substrate Inhibition Kinetics. Ind. Eng. Chem. Res. 38(3), 660-666.

Zhang, Y. and Henson, M.A. (2001). Bifurcation Analysis of Continuous Biochemical Reactor Models. Biotech Progr 17(4), 647.

Table I. Model equations: material balance, boundary conditions and constitutive equations.

Material balance

Substrate	$\frac{dS}{dt} = D \cdot (S_{in} - S) - \mu(S) \cdot \frac{X}{Z_x} - \mu(S) \cdot \frac{Y}{Z_y}$	T.I.1
Free cells	$\frac{dX}{dt} = -D \cdot X + \mu(S) \cdot X + r_d - r_a$	T.I.2
Immobilized cells (biofilm)	$\frac{dY}{dt} = \mu(S) \cdot Y - r_d + r_a$	T.I.3

Initial conditions

	$t = t_0 \rightarrow \begin{cases} X = X_0 \geq 0 \\ S = S_0 \geq 0 \\ Y = Y_0 \geq 0 \end{cases}$	T.I.4

Constitutive equations

cell growth	$\mu(S) = \frac{\mu_{max} \cdot S}{K_m + S + S^2 / K_i}$ μ_{max} = 0.71 1/h K_m=0.31 g/L K_i=0.13 g/L*	T.I.5
Suspended cells adhesion rate	$r_a(X) = K_a \cdot X$	T.I.6
Biofilm detachment rate	$r_d(Y) = K_d \cdot Y$	T.I.7

*(Viggiani et al., 2006)

Table II. Dimensionless model equations: material balance and boundary conditions.

Material balance

Substrate	$\frac{ds}{d\tau} = \frac{1}{Da} \cdot (1 - s) - \omega \cdot x - \omega \cdot y$	T.II.1
Free cells	$\frac{dx}{d\tau} = -\frac{1}{Da} \cdot x + \omega \cdot x + G \cdot y - A \cdot x$	T.II.2
Immobilized cells (biofilm)	$\frac{dy}{d\tau} = \omega \cdot y - G \cdot y + A \cdot x$	T.II.3

Initial conditions

	$\tau = \tau_0 \rightarrow \begin{cases} x = x_0 \geq 0 \\ s = s_0 \geq 0 \\ y = y_0 \geq 0 \end{cases}$	T.II.4

Constitutive equations

Cell growth	$\omega = \frac{s}{k_m + s + s^2 / k_i}$	T.II.5
Cell adhesion rate	$A \cdot x$	T.II.6
Biofilm detachment rate	$G \cdot y$	T.II.7

LIST OF FIGURE LEGENDS

Figure 1: Steady states as a function of the detachment coefficient G for Da = 3, S_{in}=0.6 g/L, A=0.011. Stable nodes and saddle-nodes are described by solid and dashed lines, respectively. Roman numerals indicate the number of steady solutions.

Figure 2: Steady states as a function of the detachment coefficient G for S_{in} = 0.6 g/L, A=0.011 for different values of Da. Stable nodes and saddle-nodes are described by solid and dashed lines, respectively.

Figure 3: Steady states of biofilm concentration y_{ss} as a function of the detachment coefficient G for Da=2, A=0.011 for different values of S_{in}. Stable nodes and saddle-nodes are described by solid and dashed lines, respectively.

Figure 4: Bifurcation diagrams in the phase-plane (S_{in}, G). A=0.011. Roman numerals indicate the number of steady solutions.

Figure 5: Transient behaviour of the reactor (plots of Eqs. T.II) for different initial conditions and different values of the detachment coefficient G. Da=3, S_{in}=0. 6 g/L, A=0.011. Initial conditions for G=0.14 are s_0=1, x_0=0.05, y_0=0.1. Initial conditions for G=0.23, are s_0=1, x_0=0.05, y_0=0.1 dashed lines, y_0=0.2 solid lines.

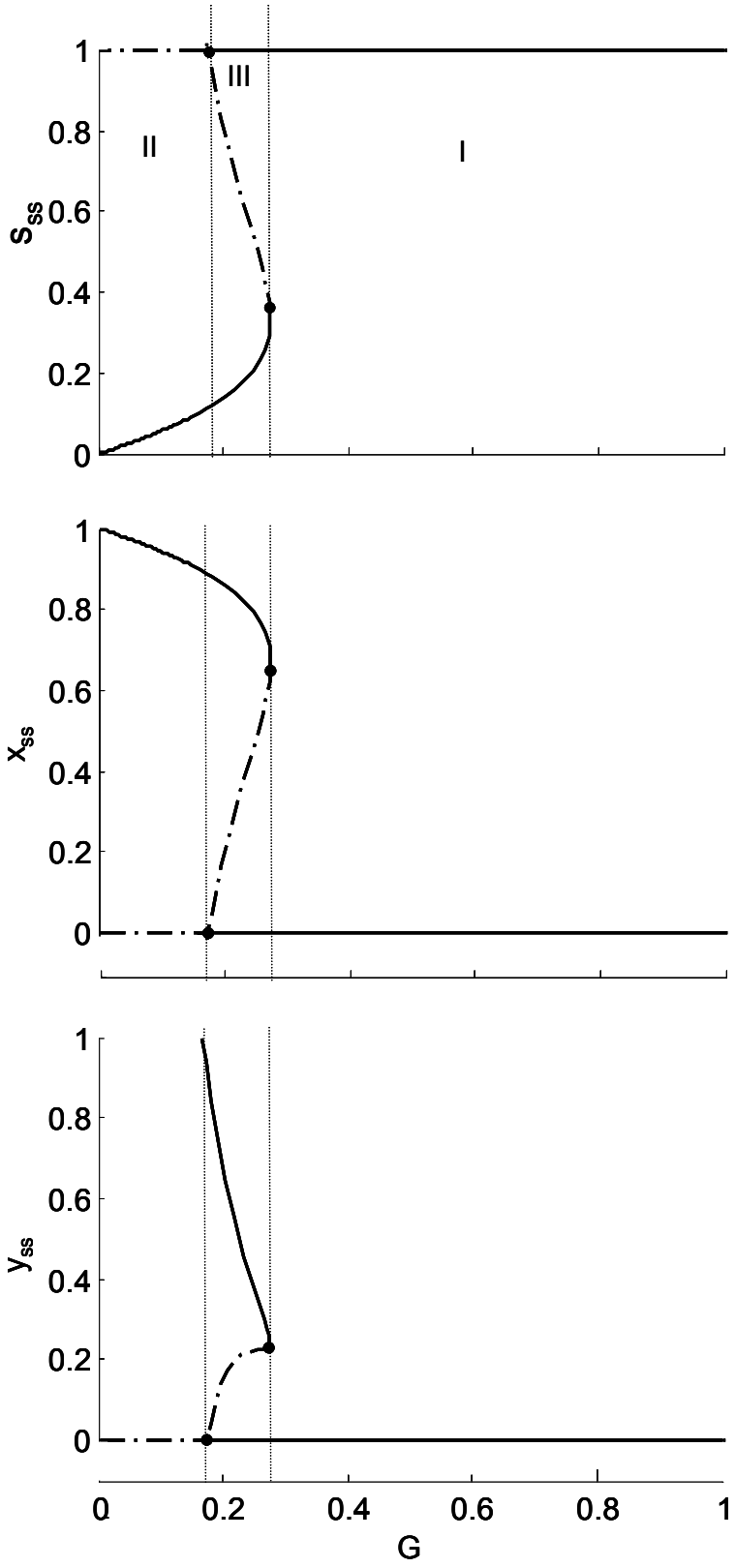

Figure 1: Steady states as a function of the detachment coefficient G for Da = 3, S_{in}=0.6 g/L, A=0.011. Stable nodes and saddle-nodes are described by solid and dashed lines, respectively. Roman numerals indicate the number of steady solutions.

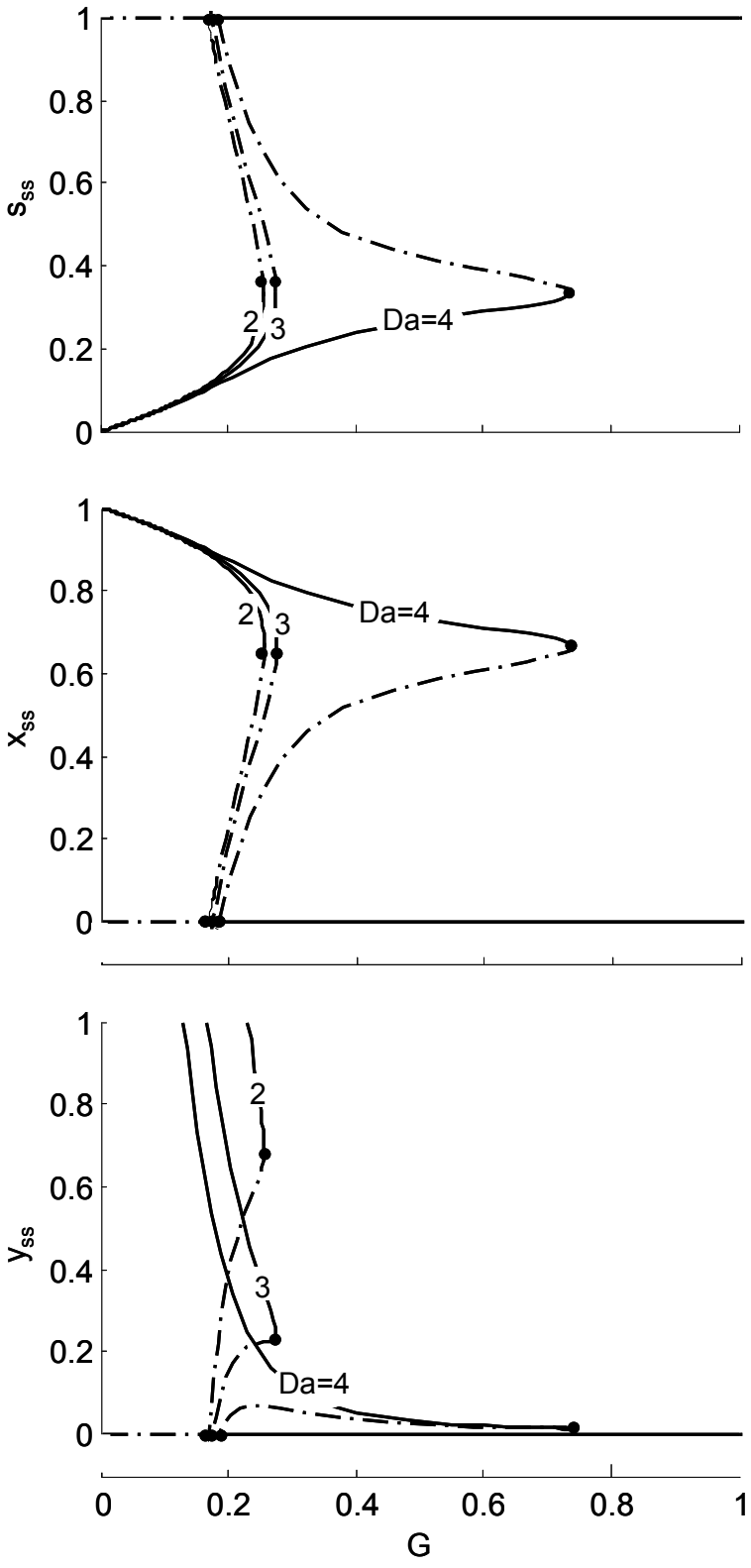

Figure 2: Steady states as a function of the detachment coefficient G for S_{in} = 0.6 g/L, A=0.011 for different values of Da. Stable nodes and saddle-nodes are described by solid and dashed lines, respectively.

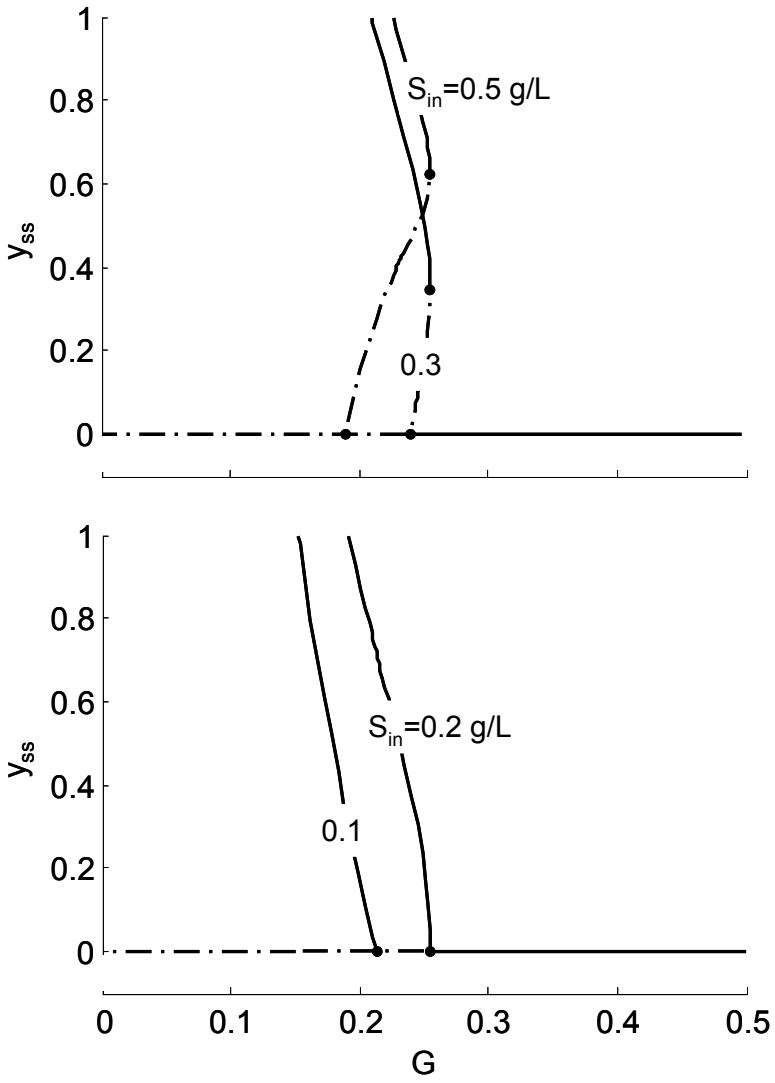

Figure 3: Steady states of biofilm concentration y_{ss} as a function of the detachment coefficient G for Da=2, A=0.011 for different values of S_{in}. Stable nodes and saddle-nodes are described by solid and dashed lines, respectively.

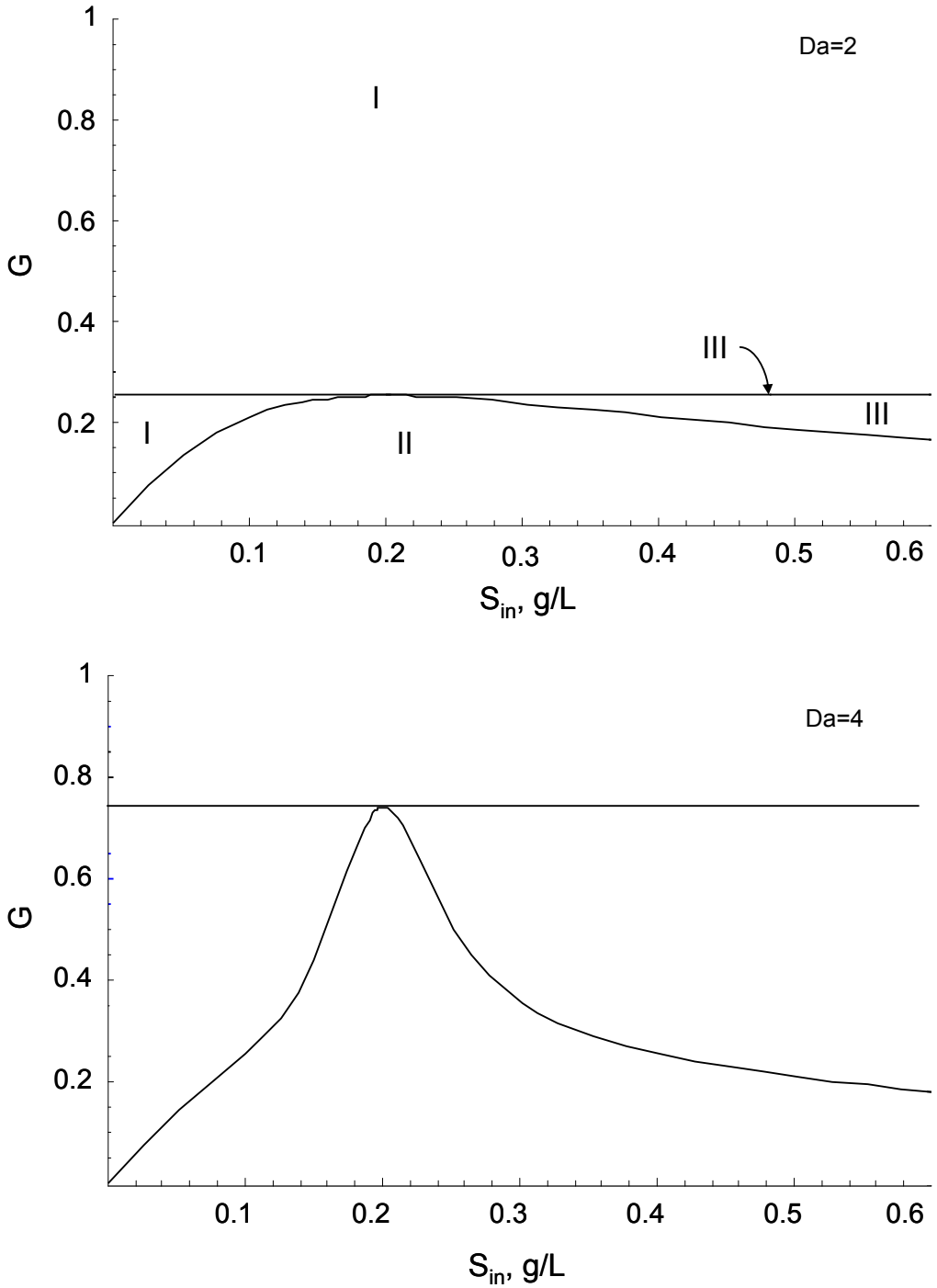

Figure 4: Bifurcation diagrams in the phase-plane (S_{in}, G). A=0.011. Roman numerals indicate the number of steady solutions.

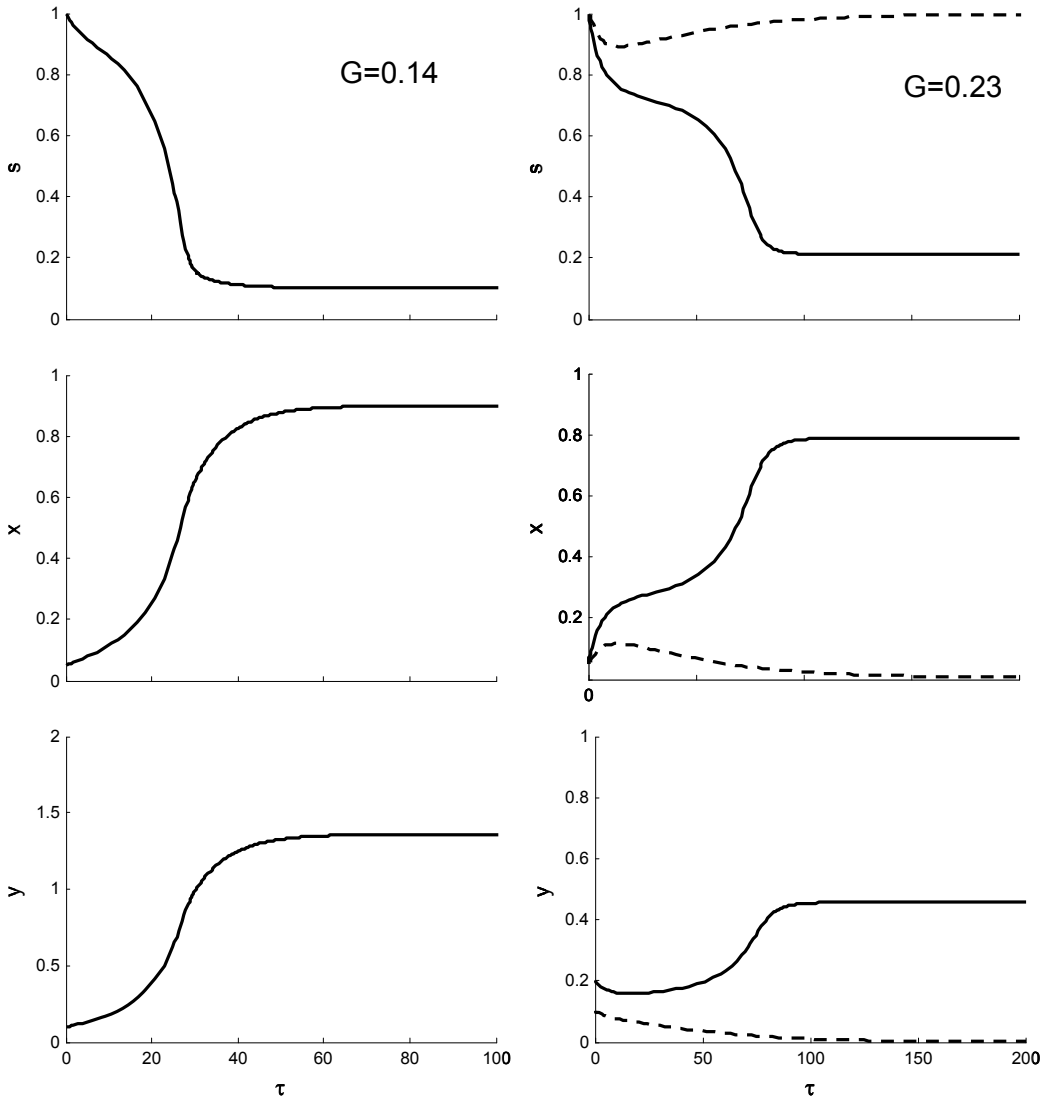

Figure 5: Transient behaviour of the reactor (plots of Eqs. T.II) for different initial conditions and different values of the detachment coefficient G. Da=3, S_{in}=0. 6 g/L, A=0.011. Initial conditions for G=0.14 are s_0=1, x_0=0.05, y_0=0.1. Initial conditions for G=0.23, are s_0=1, x_0=0.05, y_0=0.1 dashed lines, y_0=0.2 solid lines.

3.2 Growth of Pseudomonas sp. OX1 biofilm in three-phase reactors

In this section the experimental work addressing biofilm characterization is described. Experiments concerned the operation of two different three phase reactors: Three Phase Circulating (3PC) reactor and an Internal Loop Airlift (ILA) reactor. Both systems were operated with a solid phase consisting in the *P. sp.* OX1 biofilm supported by granular solids, the liquid phase was the culture medium and the gas phase was air. The experiments were focused on two main aspects: i) assessment of the extent of biofilm growth in the 3PC reactor; ii) study of influence of operating conditions (dilution rate) on ILA reactor behaviour. The results obtained were compared with those reported by Alfieri [2006] and regarding the extent of biofilm growth in ILA reactors. Furthermore, the experimental data referring to operation of ILA reactor were compared with theoretical results provided by the model of biofilm reactor reported in the paper included in section 3.1. In the following subsections experimental procedures and information on bacterial strain and materials adopted are reported.

3.2.1 Materials and Culture conditions

Pseudomonas sp. OX1 was isolated from active sludge of industrial wastes (Baggi et al.,1987). It was kindly supplied by Prof. Alberto Di Donato (Dipartimento di Biologia Strutturale e Funzionale, Università Federico II di Napoli, Italia). Stock culture was stored at -80°C. When required it was transferred on solid medium (LB/agar plates) and subsequently the operation was repeated weekly (M9/agar plates). Cultures growing on solid medium were stored at 4°C.

The composition of culture media was the following:

M9. Minimum medium was prepared according to Kahn et al. [1979] and was sterilized by autoclaving at 121°C for 20 min.

M9/agar. Minimum solid medium has been prepared by adding agarose (Difco) to liquid medium up to a final concentration of 15 g/L.

Carbon sources. Carbon sources were filtered through sterile membranes (cut-off 0.22 μm). Glucose was added to M9/agar plates as carbon source and it was used also in liquid precultures. Experiments were always carried out by growing the microrganism on M9 supplemented with phenol as carbon source. This substrate was selected as a model compound to study biodegradation of xenobiotics. Its use provides the following advantages:

- it is easily metabolized by the microrganism;
- it is spectrophotometrically measured (see next section);
- the absence of other carbon sources gives rise to a strongly selective environment for microbial growth.

The phenol concentration was smaller than 600 mg/L because above this concentration P. sp. OX1 growth is completely inhibited [Viggiani et al., 2006]

Luria-Bertani broth. It was prepared as described by Maniatis [Sambrook et al., 1989]. It was used to prepare agar plates for the first transfer of cultures stock stored at -80°C.

Biofilm carrier. Previous experimental investigations were focused on the selection of suitable carriers for *P. sp.* OX1 immobilization [Alfieri, 2006; Viggiani et al. 2006]. On the basis of acquired results, the experiments were carried out using one of the best carrier selected, pumice particles (Carlo Erba Reagenti). This carrier showed good adhesion extent thanks to its marked porosity and superficial roughness. In previous works it was employed with a particles size distribution ranging between 1000 and 800 μm. In the present investigation the selected solids were characterized by reduced porosity. Accordingly, a reduced amount of biomass is expected.

Solids were ground and sieved first, so as to obtain a size distribution ranging between 212 and 300 μm. Pumice stone was then washed to remove fine particles, dried at 80°C, weighted and sterilized by autoclaving for 20 min at 121°C.

3.2.2 Apparatus

Three Phase Circulating reactor. Figure 3.1 shows a sketch of the plant equipped with the 3PC reactor, whose characteristics are reported in table 3.1. The column was made of autoclavable glass (Pyrex), tubes and fittings were made of silicon, Teflon or stainless steel depending on requirements. Air and liquid spargers were both housed at the bottom of the column, solid phase retainment was allowed by a stainless steel net inserted between glass column and bottom screw cap. Liquid recirculation was provided by a double channel peristaltic pump (Gilson, Miniplus 3 Highflow) arranged with silicon tubes (ID 5 mm). An overflow tube fitted at the side wall of the column avoided contamination in case of clogging of the suction tube. The upper section of the column had a larger section (see table 3.1) allowing the solid separation from the circulating liquid stream, furthermore the outlet liquid stream suction tube was protected by a stainless steel net in order to prevent solid entrainment into the tank. The air stream was supplied by a membrane pump (Hartmann & Brown, Membranepump 3N) and was sterilized through on-line filtration (cut off 0.2 μm), the air flow rate was kept constant by a needle valve.

Total volume	0.25 L
Working volume	0.15 L
Total high	32 cm
Column I.D.	3 cm
Column upper section I.D.	4 cm
Tank volume	2.25 L

Table 3.1: Three phase circulating reactor geometric parameters

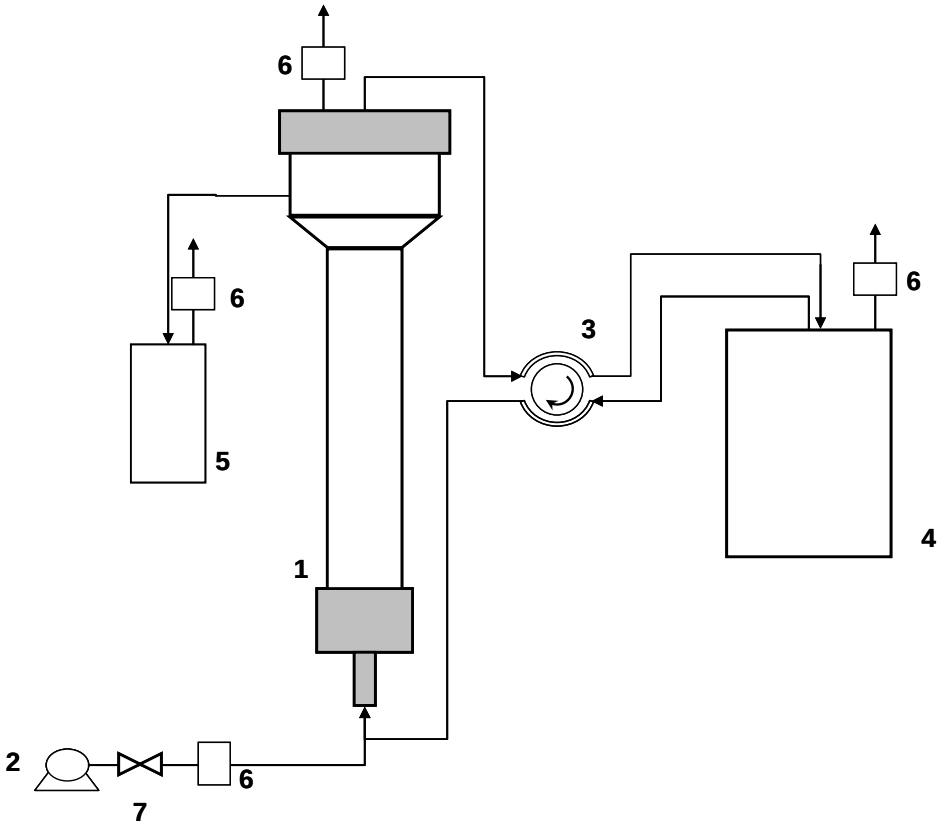

Figure 3.1: Three phase circulating reactor sketch. 1 glass column, 2 air pump, 3 perstaltic pump, 4 tank, 5 overflow collecting tank, 6 air filtering units, 7 valve.

Internal Loop Airlift reactor. Characteristics of bench scale ILAr are reported in table 3.2. Figure 3.2 shows a schematic of the complete device.

Total volume	0.15 L
Working volume	0.13 L
Total high	20 cm
Downcomer internal diameter	4 cm
Draft-tube high	10 cm
Draft-tube internal diameter	2 cm
Bottom clearance	1 cm

Table 3.2: Internal loop airlift reactor geometric parameters

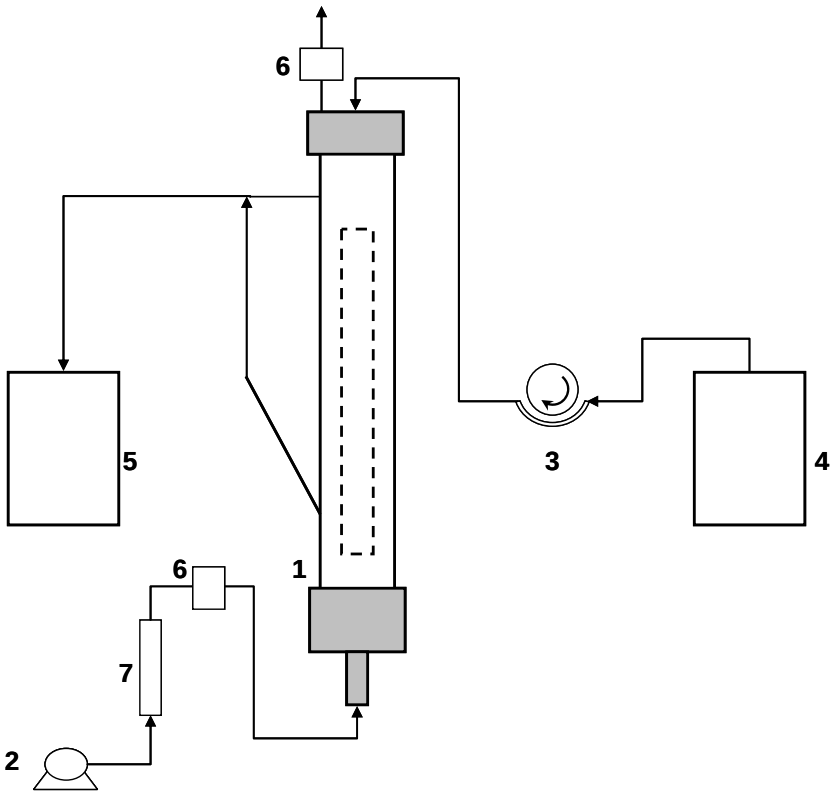

Figure 3.2: Internal loop airlift rector sketch. 1 airlift reactor (dashed draft tube), 2 air pump, 3 peristaltic pump, 4 medium tank, 5 waste tank, 6 air filtering units, 7 air flowmeter.

The ILAr was made of autoclavable glass (Pyrex), the draft-tube was kept at 1 cm form the bottom of the external vessel by means of supporting arms. Tubes and fittings were made of silicon, Teflon or stainless steel depending on requirements. Air sparger was housed at the bottom of the reactor, it consisted in a stainless steel tube plugged with a welded cap equipped with four holes (ø 1 mm).

Liquid phase was supplied by a peristaltic pump (Gilson, Miniplus 3), liquid inlet is housed at the top of the reactor. The liquid volume was kept constant through an overflow tube fitted at the side wall of the downcomer. The liquid withdrawn was collected into a sterile glass tank.

The air stream was supplied by a membrane pump (Hartmann & Brown, Membranepump 3N) and was sterilized through on-line filtration (cut off 0.2 μm), the air flow rate was kept constant at 20 NL/h by a flowmeter.

3.2.3 Analytical procedures

Liquid phase. Suspended biomass concentration and phenol concentration were measured through optical absorbance respectively at 600 and 271 nm. Optical density, related to turbidity of cell suspension, was worked out through the extinction coefficient assessed at 1.5 L/(g_{DM} cm) to obtain volumetric concentration of suspended biomass [Alfieri, 2006]. After removing biomass by centrifugation, phenol concentration was calculated reading absorbance at 271 nm, extinction coefficient was assessed at 1.65 L/(mmol cm).

Glucose concentration was measured by enzymatic assay based on Trinder reaction (Linear Chemicals) [Trinder, 1969].

Immobilised biomass

Elemental analysis. Immobilised biomass on pumice stone was measured through elemental analysis of samples withdrawn form reactors. Sample was rinsed with 9 g/L NaCl solution pH 7 to remove liquid phase carrying residual substrate, metabolites, suspended cell and biofilm debris. Then, it was dried under vacuum in a centrifugal evaporator (RC1010 Thermo Electron Corporation). Composition of the anhydrous sample was obtained with an elemental analyzer (Leyco C-H-N 2000) that provides weight percentages of carbon hydrogen and nitrogen (CHN composition). The results for every sample is compared with the CHN composition of sterile pumice stones. The amount of carbon associated with immobilized biomass was calculated by subtracting carbon percentage characteristic of pumice stones to the carbon percentage of the sample. The elemental composition of dry pellet of suspended cultures of *Pseudomonas sp.* OX1 was reported as measured by Viggiani et al [2006]: carbon 44%, nitrogen 12%, hydrogen 7%. In order to obtain volumetric concentration of the biofilm, it was assumed the same composition for immobilized biomass and elemental analysis data were worked out. In spite of extracellular substances composition was unknown, this approximation allow to apply mass balance equations to experimental data. Furthermore, the carbon percentage measured provided an effective measure to study dynamics of biofilm growth and its dependence on reactor configuration and operating conditions.

Optical microscopy. Biofilm particle withdrawn from reactors during experiments run were observed through optical microscope (Axiovert 200 Carl Zeiss). After a gentle rinsing with physiological solution, biofilm on the external surface was monitored. This procedure provided qualitative information useful for control of reactor operation.

Scanning electron microscopy. Characterization of biofilm particles by SEM was carried out after pre-treatment of samples following the procedure described by Stewart et al., 1995. Particles were rinsed repeatedly with 9 g/L NaCl solution pH 7, subsequently they were incubated for 1h with 2.5% vol glutaraldehyde at room temperature under gentle shaking. After rinsing, samples were dehydrated through extraction with ethanol aqueous solutions. The procedure needs 30 min incubation for every ethanol solution starting with 15% vol and increasing stepwise up to pure ethanol (gradient grade≥99.8%) This treatment fixes biofilm (cells and EPS) onto the support and made it resistant to SEM operating conditions (gold covering and hard vacuum). As a consequence morphology of extracellular matrix can be strongly modified, particularly thickness of large biofilm structures (higher than 100 μm). However, this modification can be considered less harsh for thin biofilms (about 10 μm depth) as in the case of *P.sp.* OX1 biofilms (Viggiani et al. 2006, Alfieri Ph. D. Th. 2006). The most relevant information withdrawn form this analysis regard the degree of covering of support surface as a dynamic variable during reactor operation.

3.2.4 Experimental procedures

Microrganism culture. Pre-cultures were obtained transferring colonies from plate to 100 mL of liquid medium (section 4.1) in 300 mL flask. Cultures were

incubated at 28°C under mixing (220 rpm). Once the steady growth phase was reached, the pre-culture was inoculated into the reactor.

Biofilm pre-culture. Two reactor configurations were adopted as described in following subsections. Biofilm pre-cultures were typically carried out in shacked flask. 150 mL of sterile M9 supplemented with glucose and phenol (3.6 and 0.2 g/L respectively) were added in 300 mL flask. Sterile pumice stones were incubated in the medium overnight, once equilibrium between solids and liquid was reached, suspension of steady culture was inoculated fixing the turbidity at 0.03 O.D. The culture was incubated at 28°C under mixing (150 rpm). Liquid was replaced with fresh medium every 24 hours, providing solids rinsing with physiological solution at each medium refreshing. Control was accomplished through a flask filled with sterile medium and pumice stones with the same carbon source concentration

Biofilm growth in 3PC reactor. Sterile parts of 3PC reactor were assembled preventing contamination. Reactor was loaded with 10÷12 g of dry sterile pumice stones (section 4.2). Solids were overnight conditioned circulating the phenol containing medium into the reactor.

The experiments were carried out operating batchwise both the liquid and solid phases. Referring to figure 4.1, the liquid medium containing phenol was circulated through reactor volume (1) and tank (4) by a multi-channel peristaltic pump. Liquid circulating flow rate (Q_r) was usually set at 56 mL/min except for over-night or over-weekend operations when it was decreased to 34 mL/min. The minimum circulating rate was calculated taking into account the respiration rate of *Pseudomonas sp.* OX1 that results 5 mg $O_2/(g_{DM}$ h) as reported by Alfieri [2006]. Considering that the tank volume was 2.25 L, assuming a maximum cell concentration of 0.5 g_{DM} and a O_2 concentration of 8 mg/L, the minimum circulating rate is 12 mL/min. Accordingly, it can be assumed that for higher values of Q_r the residence time of liquid phase into the tank is low enough to minimize cell growth in this section of the reactor. As a consequence of the oxygen supply, this operating condition allowed that cell growth mainly took place in the column as both suspended and attached biomass.

The liquid stream in the reactor vessel (1) flows through the bed of particles retained by the stainless steel wire. The tube housed at the bottom of the column supplied both liquid and air streams. Mixing of particles was accomplished by the air bubbles passing through the bed of particles. Air stream also prevented clogging of bottom wire as biofilm grew.

A sampling port in the head screw cap of the column allowed the solids and liquid sampling by a sterile pipette. Samples were analysed as described in section 4.4, solid sampling was weekly accomplished while liquid phase was withdrawn every 1-2 h. The liquid in the tank was substituted with fresh medium as the phenol concentration decreased below 0.1 g/L.

Operation of ILA reactor. The ILA reactor was assembled preventing contamination of sterile parts. Reactor was loaded with 5÷7 g of pumice stones previously operated into the 3PC reactor and carrying a finite amount of biofilm measured by elemental analysis (section 4.4), the solid concentration resulted about 46 g/L with respect to sterile pumice. The air flow rate was fixed at 20 NL/h. Under the these operating conditions, the ILA reactor was operated under solids circulating regimes [Olivieri et al, 2006].

The liquid stream was supplied at flow rate ranging between 0.03 and 0.1 L/h. Accordingly, dilution rates resulted higher than the maximum specific growth rate (0.17 h^{-1}) as reported by Viggiani et al. (2006). This operating condition was selected on the basis of results reported by Tang and Fan (1987) and … that described how wash-out condition for suspended cells favoured biofilm growth. As in the case of 3PC reactor, the liquid and solids sampling was carried out through the sampling port housed into the head screw cap of the reactor. Solid samples were recovered when necessary and liquid sampling was accomplished every 1-2 h.

3.3 Experimental Results

In this section results of experiments carried out with 3PC and ILA reactors are reported.

3.3.1 Biofilm growth in 3PC reactor

Figure 3.3 shows data measured during operation of the 3PC reactor aimed to the growth of *Pseudomonas sp.* OX1 biofilm on pumice stones. The measured values of phenol and suspended cells concentrations are reported in figure 3.3 A and B respectively. Figure 3.3 C shows the carbon percentage measured on solids sampled from the reactor vessel. Solids loaded into the reactor were previously incubated in batch conditions in shacked flask (data not reported), accordingly the biofilm content expressed as carbon percentage is about 0.2% (sterile pumice stones showed a carbon content of about 0.1%). Dashed lines in figure 3.3 A mark the time at which substrate depleted medium was replaced with fresh medium. Figures 3.3 A and B show the simultaneous consumption of phenol and suspended cells growth for each batch of fresh medium supplied. The biofilm growth can be deduced from the increasing carbon content of the solids as a function of time. The maximum carbon content, achieved after two weeks, was about 0.9%; the SEM analysis accomplished at the end of the run provided pictures reported in figure 3.7 A, an example of SEM of sterile pumice particle is reported in figure 3.5.

Some tests were carried out with sterile pumice inoculated directly into the 3PC reactor (data not reported) and operating the reactor under the same conditions described above. Results show that the biofilm established on carriers, characterized in terms of carbon percentage, was 0.5% after 10 days and 0.8% after 14 days. It can be deduced that the amount of biofilm produced over a period of 14 days in the 3PC reactor is independent on initial biofilm loaded.

Alfieri [2006] characterized biofilm growth starting from sterile pumice stone (800÷1000 μm) in shacked flasks and bench-scale ILA reactor. Biofilm concentration reported were 0.8%C (after 20 days) and 0.4%C (after 15 days) respectively. The comparison between results obtained by Alfieri and those reported in this investigation should take into account the different size of the carriers and the different typology of the reactor. The carrier adopted in the present work (212÷300 μm) is characterized by a smaller diameter with respect to that adopted by Alfieri (800÷1000 μm). From this point of view two aspects deserve consideration. The first regards the higher specific surface of the finer particles were analysed as impervious particles. The second regards the porous surface of particles that increases with the particles diameter. It appears that the two trends balance each other, therefore

biofilm growth data may be analysed neglecting possible change of available specific surface on the carriers. Particles in the 3PC reactor, adopted in the present investigation, undergo mechanical stress (shear stresses, particles collisions) weaker than those characteristic of ILA reactors. In fact mechanical stress in 3PC reactors is quite reduced with respect to ILA since the hydrodynamic pattern allows to maintain most of the solids settled at the bottom of the column while air bubbles provide mild mixing and prevent clogging. In conclusion, the phenol conversion catalysed by *P. sp.* OX1 biofilm attached on granular solid can be successfully accomplished in ILA reactor as reported by Viggiani et al. [2006] and by Alfieri [2006]. In order to obtain a useful amount of biocatalyst as rapid as possible, the 3PC reactor can be used for the build-up stage instead of starting up the ILA reactor with sterile solids.

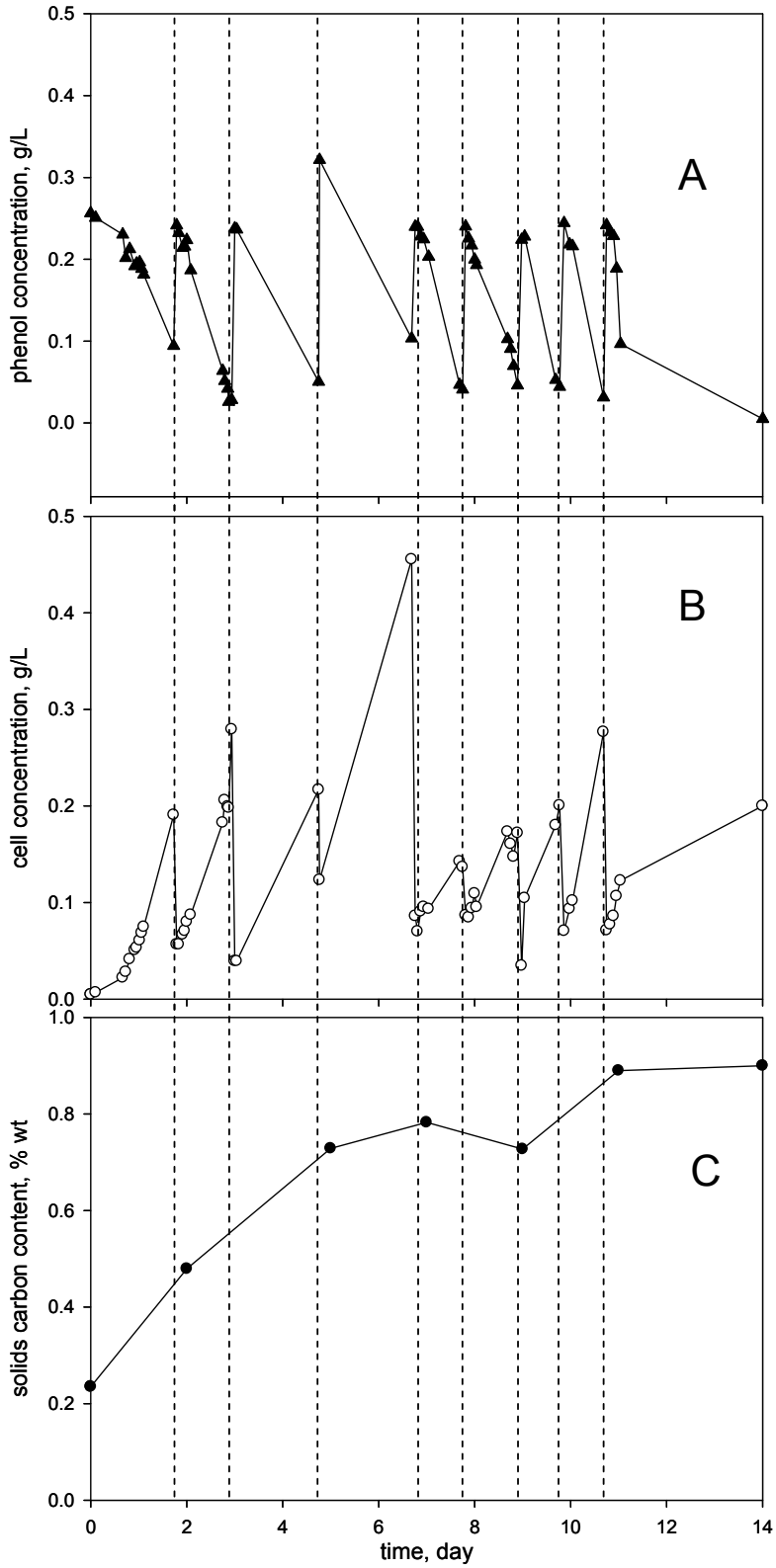

Figure 3.3: 3PC reactor operation. A) phenol concentration, B) suspended cells concentration, C) carbon content in solid phase (biofilm on pumice particles). Arrows mark replacing of liquid in the tank with fresh medium.

3.3.2 Operation of ILA reactor

The ILA reactor was operated in order to assess effect of dilution rate on biofilm growth. Variables measured were phenol and cells concentrations in the liquid phase and carbon content in the solids phase. The last is related to the biofilm concentration y, adopted in the dynamic analysis, as follows:

$$y = \frac{m_p}{x_C} \cdot \frac{1}{V_L} \qquad (5.1)$$

where m_p is the mass of dry pumice stones circulating in the reactor, x_C the carbon fraction measured through elemental analysis of sampled solids and V_L the liquid volume. This computation provides the total mass of dry biofilm per unit volume of liquid, it means that y embodies dry mass of both attached cells and extracellular biofilm matrix.

Experiments were accomplished using pumice stones inoculated and operated in the 3PC reactor for about 14 days. Run 1 was accomplished with pumice stone covered by a biofilm amount corresponding to 0.42% carbon content (fig. 3.6 A), because mass of dry pumice stones loaded was m_p=5 g, an initial amount of biofilm y=0.37 g_{DM}/L can be calculated from eq. 5.1.

Figure 3.4 reports the phenol (A) and cells (B) concentrations and carbon fraction of the solid phase (C) measured during run 1 carried out in the ILA reactor. The reactor was operated continuously with respect the liquid phase since the beginning of the test. The phenol concentration in the fed stream was set at 0.5 g/L. The liquid flow rate was set at 0.03L/h and subsequently stepwise decreased during the run. In particular, vertical dashed lines in figure 3.4 mark the instants at which the liquid flow rate is changed. The dilution rate corresponding to each flow rate is also reported in figure 3.4. it should be recalled that, with reference to suspended culture of *P. sp.* OX1, the maximum specific growth rate is 0.17 h^{-1}, when the phenol concentration is 0.2 g/L. Comparing the maximum specific growth rate with the fixed dilution rate it results that the ILA was operated always under wash-out condition with reference to suspended cells. On the contrary, a finite amount of suspended cells is detected in the liquid phase. Moreover, analysing the data of phenol and free cells concentrations measured at quasi-steady states- neglecting the increase of biofilm concentration- for each dilution rate, it results that the phenol consumption is mainly related to growth of suspended biomass. Figure 3.4 C shows a remarkable increment of carbon content in the solid phase due to biofilm growth. Working out the measured carbon fraction of the solid phase and assuming that the carbon is associated with cells, neglecting EPS and other attached biomass, it results that y increases from 0.36 up to 0.85 g/L in 18 days. Figures 3.6 B - C show the SEM view of a pumice sampled after 7 days of ILA rector operation, comparing this picture with that of pumice sampled at the beginning of the run (Figure 3.6 A), it appears that biofilm had covered a larger fraction of inner pores and appears barely thicker.

It has to be noted that the suspended cells concentration is higher than the phenol consumption calculated at steady states referring to inlet substrate concentration fixed at 0.49 g/L. This measure provides a biomass yield higher than unit (between 1 and 1.3 g_{DM}/g_{phenol}). It can be explained with production of suspended biomass through detachment of single cells or biofilm debris from solid phase.

Furthermore, this effect is emphasized because detachment phenomena affect also biofilm adhering to reactor walls, particularly on curve surfaces close to draft supporting arms and to the overflow tube fitting on the down-comer wall.

Some tests were carried out inoculating the ILA with particles operated in the 3PC reactor. The loaded solids was characterized by a biofilm amount corresponding to 0.96% carbon fraction corresponding to a patchy biofilm (figure 3.7 A). The reactor was operated for 10 days at low flow rate (dilution rate 0.23 h^{-1}), then dilution rate was stepwise increased at 0.37 and 0.69 h^{-1} (data not shown). Altogether the ILA was operated for 18 days. Biofilm concentration, in terms of carbon content, increased up to 1.2% in about 2 days from the inoculum and did not change during the entire operation, even after flow rate increase. This result can be explained assuming that the solid support is characterized by a maximum capacity in terms of biofilm loading. SEM views reported in figures 3.7 B – C show that the external surface of pumice granules is quite uniformly covered by biofilm after 16 days (carbon content 1.2%). It can be concluded that, during reactor operation biofilm grows on internal surfaces up to the maximum extent (pore filled) and on the external surfaces up to the steady value corresponding to operating conditions set. The effect of increased dilution rate (change of operating conditions) is likely masked because most of the biofilm measured by elemental analysis is that filling the pores and the expected biofilm increment affect only the external attached biomass as the internal one is limited by pore volume. In other words, the external biofilm variation due to change of dilution rate is negligible within the accuracy of elemental analysis.

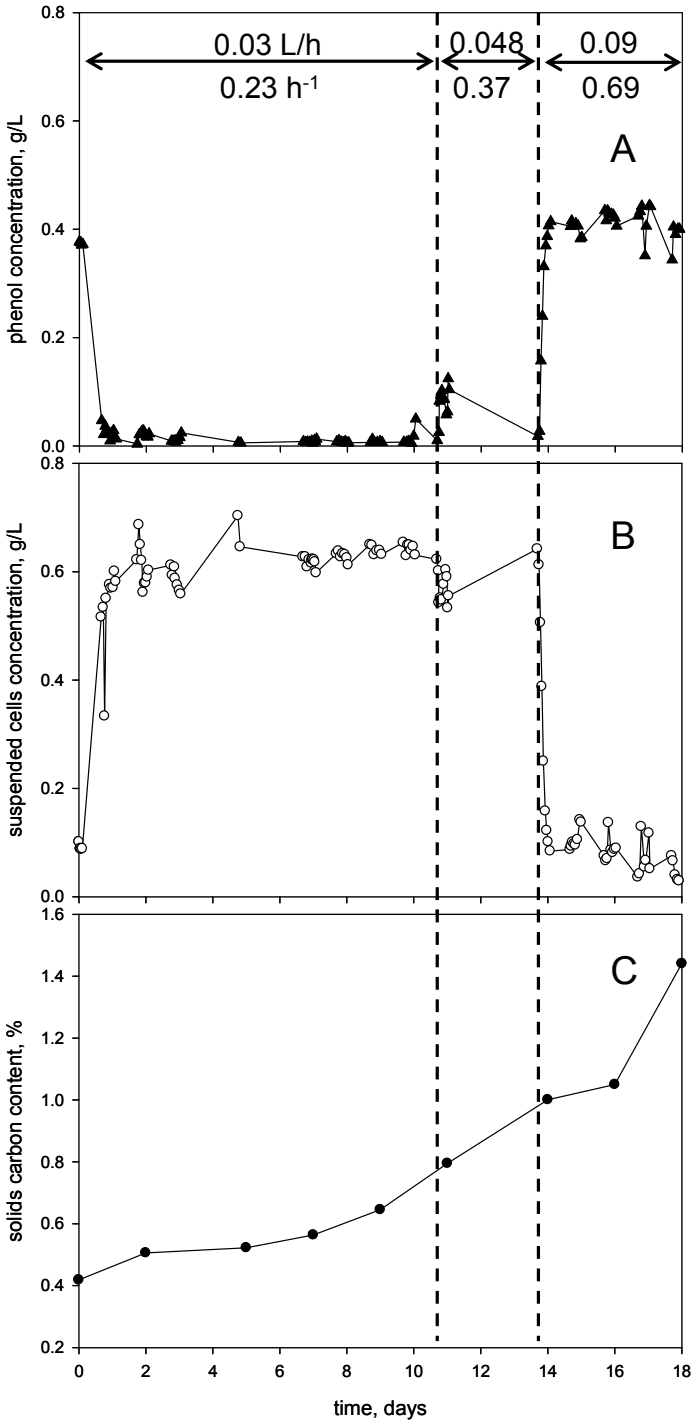

Figure 3.4: ILA reactor operation run #1. A) phenol concentration, B) suspended cells concentration, C) carbon content in solid phase. Vertical dashed lines mark changes of liquid flow rate.

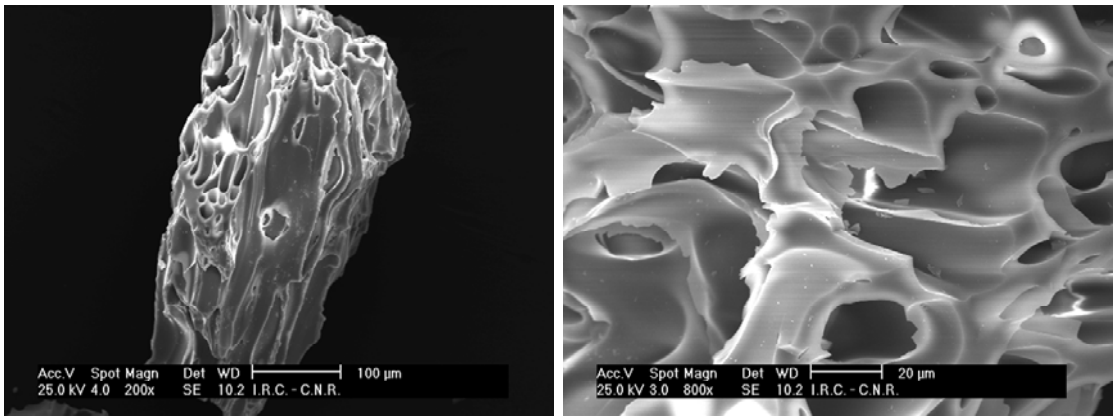

Figure 3.5: SEM of sterile pumice stone particle.

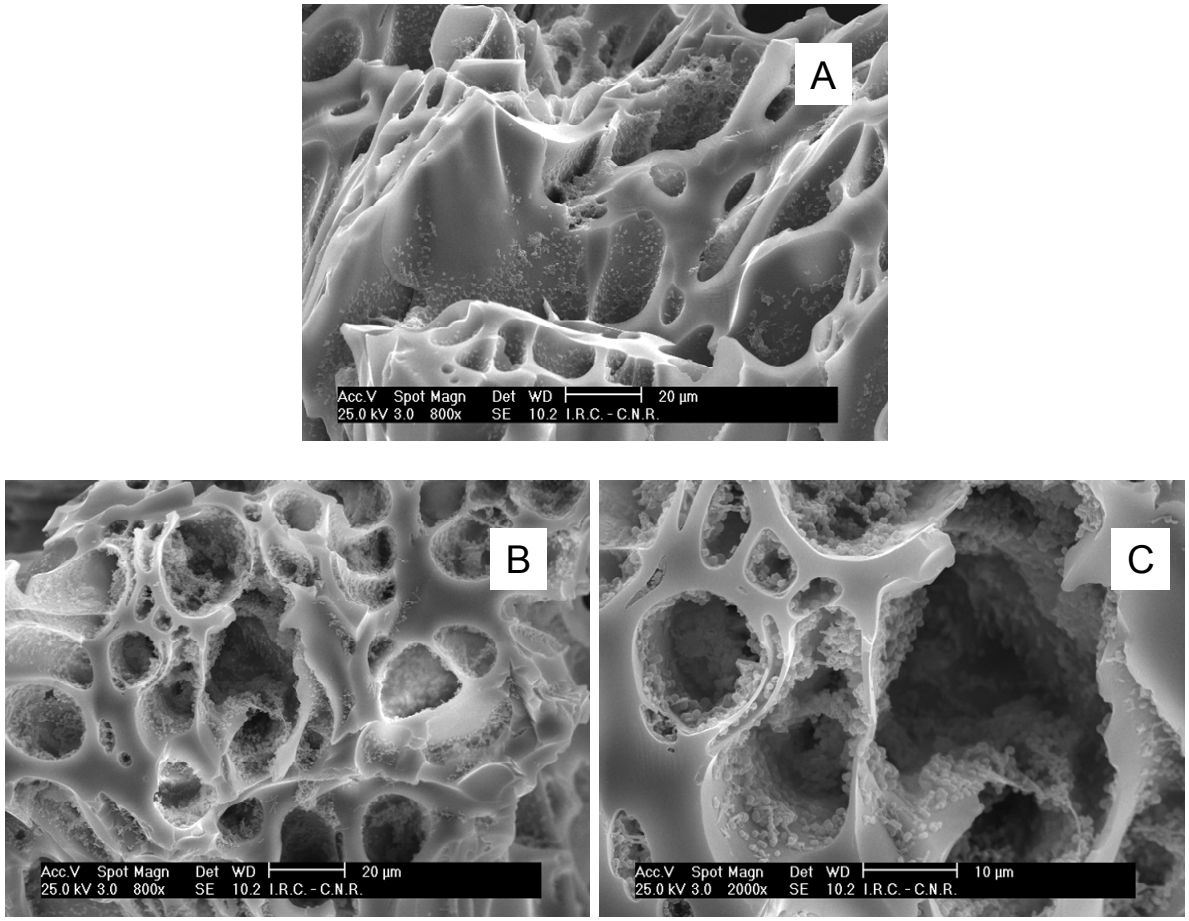

Figure 3.6: SEM analysis of pumice with biofilm of *Pseudomonas sp.* OX1 sampled in ILA reactor during run #1. A) initial condition: carbon content 0.42%, B), C) after 7 days of operation: carbon content 0.56%

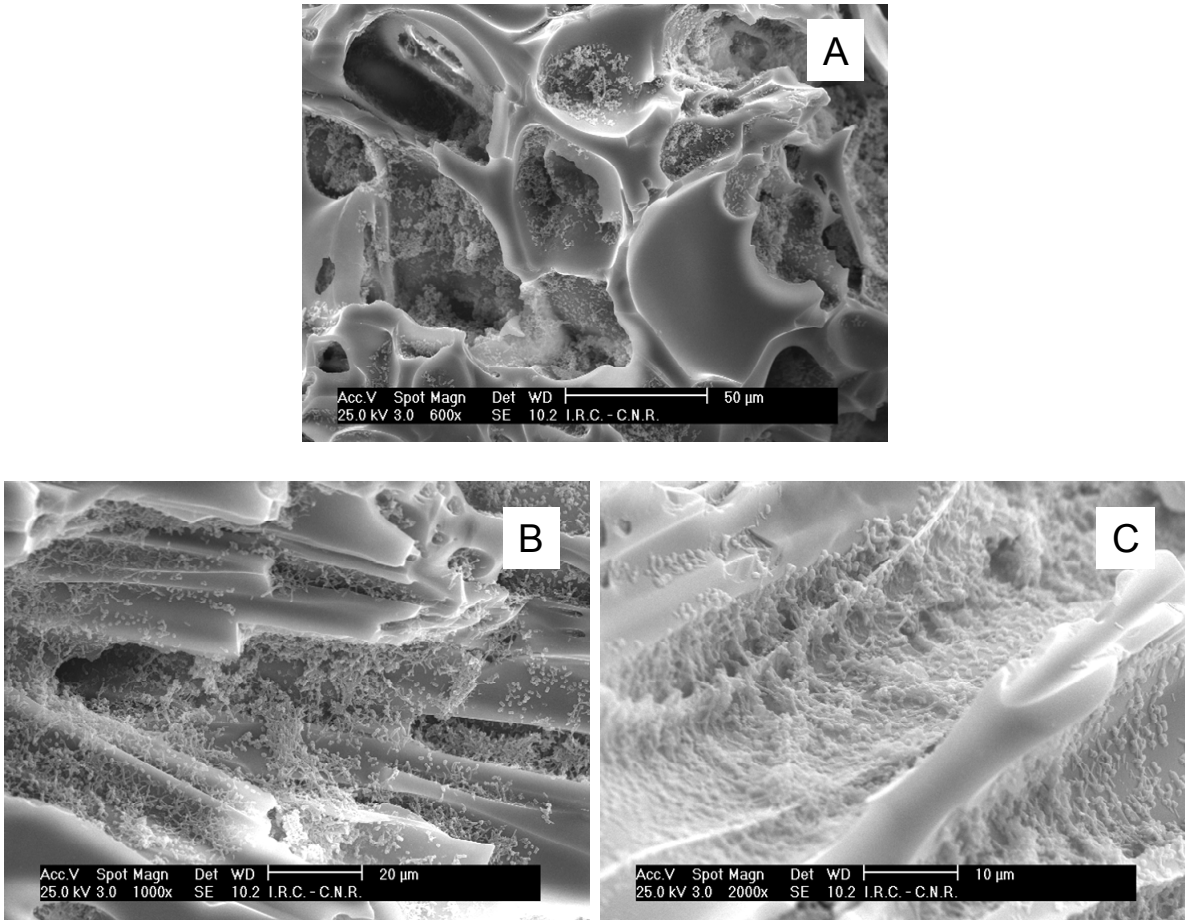

Figure 3.7: SEM analysis of pumice with biofilm of *Pseudomonas sp.* OX1 sampled in ILA reactor during run #2. A) initial condition: carbon content 0.96%, B), C) after 16 days of operation: carbon content 1.2%

3.3.3 Comparison of ILA reactor experiments with theoretical model.

Theoretical results provided by the model developed for biofilm ILA reactor are reported in figure 3.8 in the phase plane dimensionless biofilm concentration (Y) and Damköhler number (Da). In this section the results of the model reported in section 3 are compared with experimental results reported in section 3.2.

Figure 3.8 shows only the stable branches of the operating diagram, unstable steady states were not experimentally investigated.

Data points correspond to run #1 (see section 3.2) of ILA reactor. The biofilm concentrations calculated from elemental analysis of solid phase correspond to three different values of dilution rate (Damköhler number). As mentioned, it should to be taken into account that Y encloses both the mass of extracellular matter constituting biofilm and the mass of attached cells. Moreover the ILA reactor was operated with porous carrier while the model was developed assuming non porous spherical particles. As a consequence, the dependence of the biofilm concentration is expected to be more complex than the functionality adopted in the modelling (section 3). In fact the biofilm within the pores is a certain way shadowed with respect to bulk phenomena, pores stabilize microenvironment that interact with liquid phase through mass transport phenomena.

In spite of these approximations, the analysis of figure 3.8 shows that agreement between theoretical and experimental results is satisfactory. The increase of biofilm concentration with the dilution rate is reflected by the decreasing steady solution curves y vs Damköhler number. The measured increment of biofilm concentration is smaller than that foreseen by the model.

The difference between the measured and the estimated values of y may be explained by considering i) the porous nature of carriers adopted vs non-porous carriers modelled, ii) the growth kinetic of immobilised cell. As regard the porous nature of the carriers it provided that biofilm concentration approached a constant value limited by the maximum capacity of the carrier, this value is not affected by the dilution rate. The biofilm growth modelled occurs only on the external surface, hence it is not affected by any volume limitation. As regard the growth kinetics it should be recalled that the model was developed assuming the kinetic growth rate assessed for suspended cells cultures. The growth rate of immobilised cells likely deviates from these model, referring to this issue further investigation should be required.

Operating diagrams for substrate and suspended cells concentrations are not reported. Data points referred to suspended cells concentrations were affected by detachment of wall attached biomass that interfere on measurement of optical density. It has to be recalled that this effect is enhanced by the high surface to volume ratio characteristic of the bench-scale reactor. Regarding substrate concentration in the liquid phase deviation from experimental results appears at Da=1, while steady states at Da=2 and 3 fairly approach theoretical steady regimes calculated for detachment coefficient G ranging between 0.1, 0.2. It is confirmed that for high dilution rate (Da=1) the expected conversion of phenol related with biofilm growth is overestimated by the model due to deviation of growth kinetic of attached cells and to the constraint posed by the inner pores volume to the biofilm development .

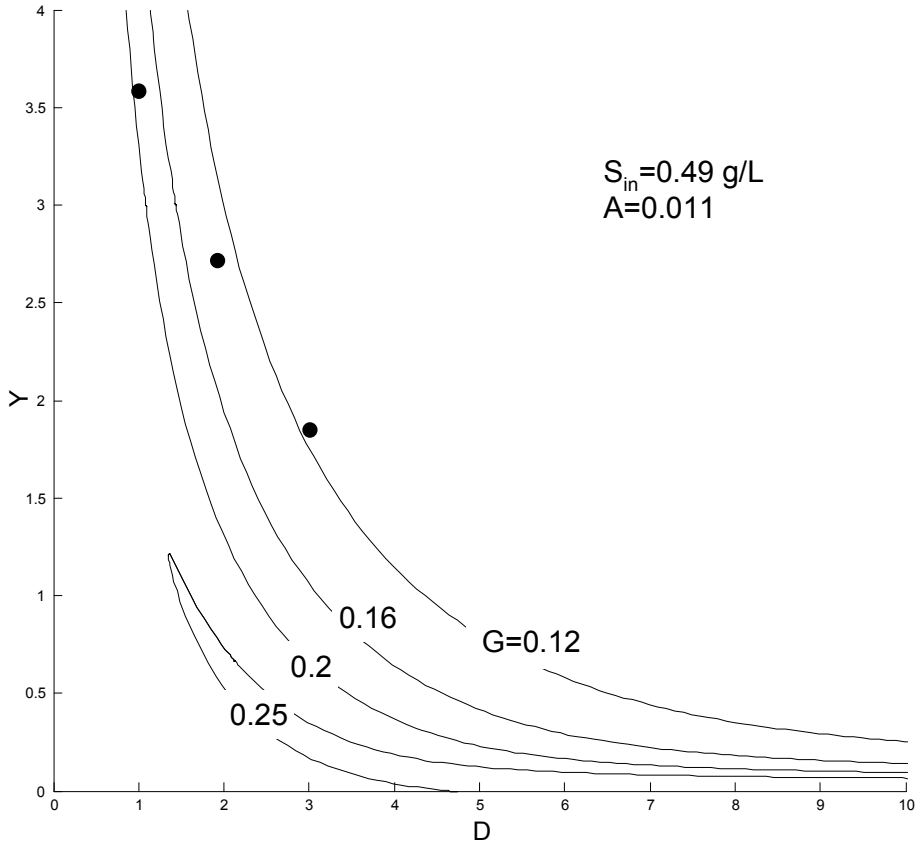

Figure 3.8: Operating diagram for ILA reactor. Dimensionless biofilm concentration vs Damköhler number. Values of inlet substrate concentration (S_{in}) and dimensionless adhesion coefficient (A) are reported. Steady states solutions of the model are plotted for different of the dimensionless detachment coefficient (G). Dots mark steady states biofilm concentration calculated form experimental measurements.

4 CONCLUSIONS

The present research program has addressed the immobilization of biological systems (enzymes, microrganisms) as a tool for bioprocess intensification. Two processes have been specifically analyzed: an **Enzyme-based process** (EBP) and a **Microrganism-based process** (MBP). The processes have been analyzed from the standpoints of reaction kinetics and pathways as well as of their potential industrial applications.

4.1 Enzyme-based process: conversion of dyes by immobilised laccases

The investigation has regarded the conversion of an antraquinonic dye, the Remazol Brilliant Blue R (RBBR), by means of laccase mixtures extracted from *Pleurotus ostreatus* cultures. The activity was carried out with either free laccases or immobilised laccases.

The immobilization of the laccase mixtures on granular solids was accomplished by covalent binding on pre-activated carriers - EUPERGIT C 250L©, an acrylic resin with epoxy functionalities. The study regarded the characterization of the immobilization efficiency and the stabilization of the enzyme. An effective system for

the activity assay of the immobilised enzymes was successful designed, set-up and operated. The system consisted of a fixed bed enzymatic reactor operated with circulation of the liquid phase. The operating conditions were purposely selected so as to prevent mass transport limitations in the conversion process and to operate the system under kinetic regime control. The activity of laccase mixtures immobilised on EUPERGIT was about 10% of the initial activity of free enzymes. The activity loss was assumed to be a consequence of multipoint attachments of the enzymes on the active solids surface. In fact, the presence of short-branched active sites on the carrier - epoxy groups spread on the metacrylate matrix - favours multipoint attachment.

The operating conditions providing the maximum immobilization efficiency with reference to the activities were assessed. The study regarded the pH and ionic strength, the initial activity per unit of mass of resin, the protein concentration and incubation time. In particular the maximum activity yield was 7% and was assessed carrying out the immobilisation under the following conditions: laccase mixture with 80 IU/g dry resin in 0.1M Sodium phosphate buffer pH 6.5, incubated for 4h at room temperature.

The kinetics of dye conversion catalyzed by free crude enzyme mixtures was successfully assessed. Purposely designed tests highlighted that the conversion rate is affected by accumulation of products. Therefore, kinetics data were interpreted by means of a kinetic model characterized by product inhibition and model parameters were assessed by regression analysis of experimental data. The lack of information on the nature of the products formed during the conversion of RBBR by free laccases calls for further characterization of the process.

The immobilised laccases were successfully applied to RBBR conversion in a fixed bed reactor continuously operated with respect to the liquid phase. The selection of this reactor configuration enabled the investigation of the kinetics of the heterogeneous conversion, ruling out the effects of the simultaneous adsorption of the dye on the protein covered solid phase. This phenomenon can strongly interfere with transient operations unless measurement of substrate accumulation on the solid phase is performed. In the present study the use of a continuous reactor operated under steady state regimes allowed to calculate the extent of dye depletion as related to the course of the enzymatic reaction. The data referring to steady states of fixed bed reactor operations confirmed that conversion rate of the reaction catalysed by immobilised laccases is product inhibited as in the case of free laccases.

The kinetic parameters inferred from experimental data were used to develop a theoretical assessment of the performances of two different reactor systems for dye conversion with laccases. The two options were: i) batch homogeneous conversion of dye in a medium containing free laccases; ii) continuous heterogeneous conversion in a fixed bed reactor with enzymes immobilised on granular carriers. The comparative analysis suggested that the total volume of dye bearing stream converted using the fixed bed reactor is larger than that converted in the homogeneous batch reactor. The analysis was carried out considering the deactivation time-scale (stability of the biocatalyst) measured in dye conversion tests by free and immobilised laccases. The obtained results reflect the balance between immobilisation yield and stabilization effect induced by the covalent immobilisation of the enzyme. In conclusion the theoretical assessment of the liquid volume treated by these two laccases-based reactors underlines the fundamental role played by the immobilisation. Further efforts are stimulated by this result with the goal of getting a better trade-off between immobilisation yield and enzyme stabilisation.

4.2 Microrganism-based process: Pseudomonas sp. OX1 biofilm reactors

The dynamics of biofilm of *Pseudomonas sp.* OX1 grown on granular solids has been studied, extending previous studies on the same subject. A Three Phase Circulating (3PC) reactor was successfully operated so that a satisfactory amount of biofilm was established on pumice particles in about 14 days. The biofilm was characterized through elemental analysis and SEM analysis of the solids covered by the biofilm. The increment of carbon fraction observed during 3PC reactor operation suggested that the controlled environmental conditions set favour biofilm formation. The tests were carried out favouring the growth of immobilized cells with respect to the free cells: oxygenation limited to the bed of particles, high substrate loading close to the inhibition limit. The SEM micrographs of the biofilm show that it grows mainly into the pores and patchy biofilm covered external surface of pumice particles developing into the channels of the pumice wall.

The biofilm-loaded carrier produced in the 3PC was used to characterize the conversion of phenol in a internal loop airlift (ILA) reactor. All tests were carried out under wash-out conditions with respect to free cells. The increase in dilution rate favours the biofilm growth when a moderate inoculum of biofilm (0.4% carbon content) was used to inoculate the ILA reactor. The results obtained are in agreement with those reported by Heijnen and co-workers [Gjaltema et al., 1997] and by Tang and Fan [1987] showing that a short hydrodynamic residence time prevents growth of suspended cells and favours the production of attached biomass. Moreover, it appears that the biofilm growth on internal surfaces is limited by the pores volume and is controlled by the detachment on the external surfaces.

The theoretical investigation regarded the dynamic and bifurcational analysis of the ILA reactor. The specific features of the model developed were: the effect of substrate-inhibited growth kinetic on steady states multiplicity; biofilm detachment phenomena and their role in the establishment of dynamic equilibrium between free and immobilized biophases; adhesion of suspended cells of particles surface in the early stage of biofilm formation; effect of the dilution rate and substrate loading on the biofilm steady concentration.

The biofilm detachment rate was assumed linear with respect to the biofilm loading. The adhesion rate was assumed linear with respect to the suspended cells concentration, in agreement with previous studies. The first order adhesion coefficient was evaluated from first principles and its value applied for model computations. The bifurcational patterns resulting form computation of continuation algorithm are not affected by changes of the adhesion coefficient within its confidence interval ($0.008 \pm 0.002\ h^{-1}$).

Bifurcational analysis of the steady state solutions indicates that the only trivial solution can be accepted at values of the detachment constant exceeding a given threshold. Below this value multiple stable steady states can establish and the bifurcational patterns depend on the value of the reactor Damköhler number and inlet substrate concentration. The multiplicity of steady state as well as the existence of a limit value for detachment coefficient allowing existence of non-trivial solution are related with the non linear kinetic describing specific growth rate of *P. sp.* OX1 over phenol.

A relevant result rising from the bifurcational analysis of the steady operation of the reactor is that, even under wash-out conditions free cells ($Da<4.09$), suspended

biomass is always present as a consequence of the continuous renewal by detachment of immobilized biophase. The effect of this phenomenon is twofold: the persistence of a freely suspended biophase even under wash-out conditions enhances the productivity of the bioreactor; competition between suspended and immobilized cells for the common substrate cannot be ruled out simply by operating under wash-out condition.

Dynamical simulations of the transient behaviour of the bioreactor show that the dynamic evolution of the suspended and of the immobilized biophases are linked to each other by the occurrence of biofilm detachment. Results of simulations performed with different sets of parameters indicate that the dynamic patterns are dominated by the initial value of the biofilm loading. This effect is related to the multiplicity of steady states, in other words the stable steady state providing finite amount of biofilm for a given detachment rate is approached only if the proper amount of biofilm is available as initial condition. The shape of the basin of attraction of the stable solutions depends on substrate feeding concentration and dilution rate. This dependence can be qualitatively described observing that the initial amount of biofilm required to approach stable solution increases with substrate loading for a given Da number, moreover it has to be as near as possible to the stable solution if the reactor is operated with Da approaching the wash-out limit (Da=4.09) and high detachment rate occurs.

The comparison between experimental data obtained from ILA reactor operation and the theoretical investigation shows a satisfactory agreement. The trend of stable biofilm concentration measured vs the dilution rate during ILA operation fairly corresponds to that provided by the model. The expected increment of biofilm concentration as a function of increasing dilution rate (decreasing Damkhöler number) is probably overestimated by the model that does not take into account the limit provided by pores volume to biofilm growth and the differences in growth kinetic of attached cells with respect to that of suspended cells.

Some update of the model would be advisable if it is to be used for parametric inference from experimental data. Furthermore, inherent limitations of bench-scale ILA reactors, with specific reference to the possibility that wall-growth phenomena become extensive and affect reliability of the measurements, should be overcome by proper revision of reactor design and experimental conditions. Additional experiments will be directed to the assessment of the actual adhesion rate of *P. sp.* OX1 cells on different carriers under either stagnant conditions or under the hydrodynamic regimes typical of ILA reactors. The ILA reactor will also be operated to assess the detachment rate under no-growth conditions. This task will require the development of mature biofilm on non-porous particles.

5 REFERENCES

Agrawal P., Lee C., et al. (1982). Theoretical investigation of dynamic behaviour of isothermal continuous stirred tank biological reactors. Chemical Engineering Science 37(3): 453-62.

Ajbar, A. (2001). Stability analysis of the biodegradation of mixed wastes in a continuous bioreactor with cell recycle. Water Research. 35: 1201-8.

Ajbar A. and Alhumaizi K. (2000). Biodegradation of Substitutable Substrates in a Continuous Bioreactor with Cell Recycle: A Study of Static Bifurcation. Mathematical and Computer Modelling. 31: 159-74.

AL-Muftah, A. E. and Abu-Reesh I. M. (2005). Effects of simultaneous internal and external mass transfer and product inhibition on immobilized enzyme-catalyzed reactor. Biochemical Engineering Journal 27: 167-78.

Alfieri F. (2006). Bioconversione di composti aromatici mediante microrganismi liberi o immobilizzati. Ph. D. Thesis. Università di Napoli 'Federico II'.

Baggi, G., P. Barbieri, et al. (1987). Isolation of a *Pseudomonas stutzeri* that degrades o-xylene. Apllied and Environmental Microbiology 53: 2129-32.

Beveridge T. J., Makin S. A., et al. (1997). Interactions between biofilms and the environment. FEMS Microbiology Reviews. 20: 291-303.

Bollag J. M., Shuttleworth K. L., et al. (1998). Laccases-mediated detoxification of phenolic compounds. Applied Environmental Microbiology 54: 3086-91.

Bos R., van der Mei H. C., et al. (1999). Physico-chemistry of initial microbial adhesive interactions - its mechanisms and methods for study. FEMS Microbiology Reviews. 23: 179-229.

Bourbonnais R. and Paice M. (1990). Oxidation of non-phenolic substrates: An expanded role for laccase in lignin biodegradation. FES Letters 267: 99–102.

Cao, L. (2005). Immobilised enzymes: science or art? Current Opinion in Chemical Biology 9: 217–26.

Characklis W. G. and Marshall K. C. (1990). Biofilms. New York, John Wiley and Co.

Chen G. and Strevett K. A. (2001). Impact of surface thermodynamic on bacterial transport. Environmental Microbiology 3(4): 237-45.

Chen M. Y., Lee D. J., et al. (2007). Distribution of extracellular polymeric substances in aerobic granules. Applied Microbiology and Biotechnology. 73: 1463-9.

Chisti, M. Y. (1989). Airlift Bioreactors, Elsevier.

Chisti, Y. (2000). Mass Transfer. Kirk-Othmer Encyclopedia of Chemical Technology, John Wiley & Sons, Inc. 15.

Claus H., Faber G., et al. (2002). Redox-mediated decolorization of synthetic dyes by fungal laccases. Applied Microbiology and Biotechnology 59: 672-8.

Denkhaus E., Meisen S., et al. (2007). Chemical and physical methods for characterisation of biofilms. Microchimica Acta. 158: 1-27.

Duràn, N., Rosa M. A., et al. (2002). Application of laccases and tyrosinases (phenoloxidases) immobilized on different supports: a review. Enzyme and Microbial Technology 31: 907-31.

Durán N. and Esposito E. (2000). Potential applications of oxidative enzymes and phenoloxidase-like compounds in wastewater and soil treatment: a review. Applied Catalysis B: Environmental 28: 83-99.

Elnashaie S.E.H. S., Chen Z., et al. (2006). Practical Implications of Bifurcation and Chaos in Chemical and Biological Reaction Engineering. International Journal of Chemical Reactor Engineering 4.
Foght, J. M. and Westlake D. W. (1988). Degradation of polyciclic aromatic hydrocarbons and aromatic heterocycles by a *Pseudomonas* species. Can J Microbiol 34: 1135-41.
Gianfreda, L. and Rao M. A. (2004). Potential of extra cellular enzymes in remediation of polluted soils: a review. Enzyme and Microbial Technology 35(4): 339-54.
Gjaltema, A., N. van der Marel, et al. (1997). Adhesion and biofilm development on suspended carriers in airlift reactors: hydrodinamic conditions versus surface characteristics. Biotechnology and Bioengineering 55(6): 880-9.
Heijnen, J. J. (1984). Biological industrial wastewater treatment minimizing biomass production and maximizing biomass concentration. Ph. D. Thesis. Delft University of Technology.
Kahn M. R., Kolter, R. et al. (1979). Plasmid cloning vehicles derived from plasmids ColE1, F, R6K, and RK2. Methods Enzymol. 68: 268-80.
Kandelbauer, A., Maute O., et al. (2004). Study of dye decolorization in an immobilized laccase enzyme-reactor using online spectroscopy. Biotechnology and Bioengineering 87(4): 552-63.
Katchalski-Katzir, E. and Kraemer D. M. (2000). Eupergit C, a carrier for immobilization of enzymes of industrial potential. Journal of Molecular Catalysis B: Enzymatic 10: 157-76.
Kobayashi T. and Moo-Young M. (1971). Backmixing and Mass-Transfer in the Design of Immobilized-Enzyme Reactor. Biotechnology and Bioengineering 3: 893-910.
Lalonde J. and Margolin A. (2002). Immobilization of enzymes. Enzyme Catalysis in Organic Synthesis (2nd Edition) 1: 163-184.
Lenas P. and Pavlou S. (1995). Coexistence of Three Competing Microbial Populations in a Chemostat with Periodically Varying Dilution Rate. Mathematical Biosciences 129: 111-42.
Lenas P., Thomopoulos N. A., et al. (1998). Oscillations of two competing microbial populations in configurations of two interconnected chemostats. Mathematical Biosciences. 148: 43-63.
Mateo C., Palomo J. M., et al. (2007). Improvement of enzyme activity, stability and selectivity via immobilization techniques. Enzyme and Microbial Technology. 40: 1451-63.
McMullan G., Meehan C., et al. (2001). Microbial decolourization and degradation of textile dyes. Applied Microbiology and Biotechnology 56: 81-7.
Michel F. C. J., Grulke E. A., et al. (1992). A kinetic model for the fungal pellet lifecycle. AIChE Journal 38(9): 1449-60.
Moreira M. T., Feijoo G., et al. (2004). Fungal bioreactors: applications to white-rot fungi. Reviews in Environmental Science and BioTechnology 2(2-4): 247-59.
Nicell, K. J. J. A. (1996). Potential Applications of Enzymes in Waste Treatment. Journal of Chemical Technology and Biotechnology 69: 141-53.
Nicolella C., van Loosdrecht M. C. M., et al. (2000). Wastewater treatment with particulate biofilm reactors. Journal of Biotechnology. 80**:** 1 - 33.
Nicolella C., van Loosdrecht M. C. M., et al. (2000). Particle-based biofilm reactor technology. Trends in Biotechnology. 18: 312-20.

Nicolella C. et. al (1998). Hydrodynamic characteristics and gas-liquid mass transfer in a biofilm airlift suspension reactor. Biotechnology and Bioengineering 60: 627-35.
Nierstrasz V. A. and Warmoeskerken M. M. C. G. (2003). Process engineering and industrial enzyme applications. Textile Processing with Enzymes: 120-57.
Olivieri G., Marzocchella A., Salatino P. (2003). Hydrodynamics and mass transfer in lab-scale three-phase internal loop airlift. Chemical Engineering Journal 96: 45-54.
O'Toole G.A. (2003). To build a biofilm. Journal of Bacteriology 185(9): 2687-9
Palmieri G., Cennamo G., Sannia G. (2005). Remazol Brilliant Blue R decolourization by the fungus *Pleurotus ostreatus* and its oxidative enzymatic system. Enzyme and Microbial technology 36: 17-24.
Palmieri G., Giardina P., et al. (2005). Laccase-Mediated Remazol Brilliant Blue R Decolorization in a Fixed-Bed Bioreactor. Biotechnology Progress 21(5): 1436-41.
Palmieri G., Giardina P., et al. (1997). A Novel White Laccase from *Pleurotus ostreatus*. The Journal of Biological Chemistry 272(12): 31301–7.
Park D., Haam S., et al. (2005). Immobilization of starch-converting enzymes on surface-modified carriers using single and co-immobilized systems: properties and application to starch hydrolysis. Process Biochemistry. 40: 53-61.
Park S. W., Yong In Kim, et al. (2002). Covalent immobilization of GL-7-ACA acylase on silica gel through silanization. Reactive and Functional Polymers. 51: 79-92.
Pavlou S. (1999). Computing operating diagrams of bioreactors. Journal of Biotechnology. 71: 7-16.
Peralta-Zamora P., Pereira C. M., et al. (2003). Decolorization of reactive dyes by immobilized laccase. Applied Catalysis, B: Environmental 42(2): 131-44.
Picioreanu C., van Loosdrecht M. C. M., Heijnen J. J. (2000). Two-Dimensional Model of Biofilm Detachment Caused by Internal Stress from Liquid Flow. Biotechnology and Bioengineering 72(2): 205-18.
Pinheiro I. O., De Souza Jr M. B., et al. (2004). The dynamic behaviour of aerated continuous flow stirred tank bioreactor. Mathematical and Computer Modelling. 39: 541-566.
Rijnaarts H. H. M., Norde W., et al. (1995). Reversibility and mechanism of bacterial adhesion. Colloids and surfaces B 4: 5-22.
Rijnaarts H. H. M., Norde W., Bouwer E. J., Lyklema J., Zehnder A. J. B. (1993). Bacterial Adhesion under Static and Dynamic Conditions. Applied Environmental Microbiology 59: 3255-65.
Rios G. M., Belleville M. P., et al. (2004). Progress in enzymatic membrane reactors a review. Journal of Membrane Science 242: 189-96.
Robinson T., McMullan G., et al. (2001). Remediation of dyes in textile effluent: a critical review on current treatment technologies with a proposed alternative. Bioresource Technology 77: 247-55.
Rodrìguez E., Pickard M. A., et al. (1999). Industrial dye decolorization by laccases from lignolytic fungi. Current Microbiology 38: 27-32.
Sambrook J., Fritsch F. E., et al. (1989). Molecular Cloning. A Laboratory Manual. New York, 2nd ed. Cold Spring Harbor Laboratory Press.
Singh R., Paul D., et al. (2006). Biofilms: implications in bioremediation. Trends in Microbiology. 14: 389-97.

Soetaert W. and Vandamme E. J. (2006). The impact of Industrial Biotechnology. Biotechnology Journal 1: 756-769.
Stewart P., Murga S., et al. (1995). Biofilm structural heterogeneity visualized by three microscopic methods. Water Research 29(8): 2006-9.
Strevett K. A. and Chen G. (2003). Microbial surface thermodynamics and applications. Research in Microbiology. 154**:** 329-35.
Swamy J. and Ramsay J. A. (1999). The evaluation of white rot fungi in the decoloration of textile dyes. Enzyme and Microbial Technology. 24: 130-7.
Tang W.-T. and Fan L.-S. (1987). Steady state phenol degradation in a draft-tube, gas-iquid-solid fluidized-bed bioreactor. AIChe Journal 33(2): 239-49.
Tisher W. and Volker K. (1999). Immobilized enzymes: crystals or carriers? Trends in Biotechnology.17(8): 326-35.
Trinder P. (1969). Determination of Glucose in Blood using Glucose Oxidase with an alternative oxygen acceptor. Ann. Clin. Biochem. 6: 24.
van der Mei H. C., Bos R., et al. (1998). A reference guide to microbial cell surface hydrophobicity based on contact angles. Colloids and Surfaces B: Biointerfaces. 11: 213-21.
Verstraete W., Wittebolle L., et al. (2007). Microbial Resource Management: The Road to Go for Environmental Biotechnology. Engineering in Life Sciences 7(2): 117-26.
Viggiani A., Olivieri G., et al. (2006). An airlift biofilm reactor for the biodegradation of phenol by *Pseudomonas stutzeri* OX1. Journal of Biotechnology.123: 464-77.
Wesenberg D., Kyriakides I., et al. (2003). White-rot fungi and their enzyme for the treatment of industrial dye effluents. Biotechnology Advances 22: 161-87.